NATIONAL ACADEMIES OF SCIENCE AND ENGINEERING

NATIONAL RESEARCH COUNCIL

of the

UNITED STATES OF AMERICA

UNITED STATES NATIONAL COMMITTEE

International Union of Radio Science

National Radio Science Meeting

5-8 November 1979

Sponsored by USNC/URSI
in cooperation with
Institute of Electrical and Electronics Engineers

University of Colorado
Boulder, Colorado
U.S.A.

Price $5.00

National Radio Science Meeting
5-8 November 1979
Condensed Technical Program

SUNDAY, 4 NOVEMBER

1600-2200		
Wave Propagation Standards Committee		UMC 230
2000-2400		
USNC/URSI Meeting		UMC 305

MONDAY, 5 NOVEMBER

0900-1200		
B-1	Scattering: Direct and Inverse	UMC West Ballroom
C-1	Evolving Approaches and Problems in Communications Networks	UMC Forum Room
J-1	Low Noise Receivers - I	UMC 235
1330-1700		
B-2	Asymptotic Methods	UMC West Ballroom
C-2	Signal Processing for Antenna Arrays	UMC Forum Room
F-1	Remote Sensing of the Earth's Surface	UMC East Ballroom
G-1	Ionospheric Predictions	UMC 159
J-2	Low Noise Receivers	UMC 235
1700		
Commission A	Business Meeting	UMC 158
Commission C	Business Meeting	UMC 156
1800-2000		
Reception		UMC West Ballroom and Glenn Miller Lounge
1830-2000		
Wave Propagation Standards Committee		UMC 230

TUESDAY, 6 NOVEMBER

0830-1200		
Combined Session		UMC Center Ballroom
1330-1700		
A-1/ E-1	EMI/EMC Measurements and Techniques	UMC 158
B3/ J3	Large Arrays and Related Techniques	UMC 305
B4	Electromagnetic Theory	UMC West Ballroom
C3	Multiple-Access Communications	UMC Forum Room
F-2	Scattering From the Clear Atmosphere	UMC East Ballroom
G-2	Recent Radio Beacon Results - I: Total Electron Contents	UMC 159
H-1	Active Experiments From the Space Shuttle	UMC 157
1700		
Commission F	Business Meeting	UMC East Ballroom
Commission H	Business Meeting	UMC 157
1800-2400		
IEEE AP-S AdCom Meeting		Broker Inn

United States National Committee

INTERNATIONAL UNION OF RADIO SCIENCE

PROGRAM AND ABSTRACTS

National Radio Science Meeting
5-8 November 1979

Sponsored by USNC/URSI in cooperation
with IEEE groups and societies:

Antennas and Propagation
Circuits and Systems
Communications
Electromagnetic Compatibility
Geoscience Electronics
Information Theory
Instrumentation and Measurement
Microwave Theory and Techniques
Nuclear and Plasma Sciences
Quantum Electronics and Applications

Hosted by:

National Oceanic and Atmospheric Administration
National Bureau of Standards
Institute for Telecommunication Sciences
National Telecommunications and Information Administration
University of Colorado, Boulder
and
The Denver-Boulder Chapter, IEEE/APS

NOTE:

Programs and Abstracts of the USNC/URSI Meetings are available from:

USNC/URSI
National Academy of Sciences
2101 Constitution Avenue, N.W.
Washington, DC 20418

at $2 for meetings prior to 1970, $3 for 1971-75 meetings, and $5 for 1976-79 meetings.

The full papers are not published in any collected format; requests for them should be addressed to the authors who may have them published on their own initiative. Please note that these meetings are national and they are not organized by international URSI, nor are the programs available from the international Secretariat.

MEMBERSHIP

United States National Committee
INTERNATIONAL UNION OF RADIO SCIENCE

Chairman:
Dr. C. Gordon Little, Environmental Research Labs, NOAA **
Vice Chairman:
Mr. George H. Hagn, SRI International**
Secretary:
Dr. Thomas B.A. Senior, University of Michigan**
Editor and Secretary Designate:
A. Ishimaru, University of Washington **
Immediate Past Chairman:
Dr. John V. Evans, Lincoln Laboratory, M.I.T.**

Members Representing Societies, Groups and Institutes:

American Geophysical Union	Dr. Christopher T. Russell
Institute of Electrical & Electronic Engineering	Dr. Ernst Weber
IEEE Antennas & Propagation Society	Dr. Robert C. Hansen
IEEE Circuits & Systems Society	Dr. Mohammed S. Ghausi
IEEE Communications Society	Mr. Amos Joel
IEEE Information Theory Group	Dr. Aaron D. Wyner
IEEE Microwave Theory & Techniques	Dr. Ken J. Button
IEEE Quantum Electronics Society	Dr. Robert A. Bartolini
Optical Society of America	Dr. Steven F. Clifford

Liaison Representatives from Government Agencies:

National Telecommunications & Information Administration	Mr. Samuel E. Probst
National Science Foundation	Dr. W. Klemperper
Department of Commerce	vacant
National Aeronautics & Space Administration	Dr. Erwin R. Schmerling
Federal Communications Commission	vacant
Department of Defense	Mr. Emil Paroulek
Department of the Army	Mr. Allan W. Anderson
Department of the Navy	Dr. Leo Young
Department of the Air Force	Mr. Allan C. Schell

Members-At-Large:

Mr. D.E. Barrick
Mr. L.S. Taylor
Mr. A.W. Guy

Chairmen of the USNC-URSI Commissions:

Commission A	Dr. Raymond C. Baird
Commission B	Prof. George A. Deschamps
Commission C	Prof. Mischa Schwartz
Commission D	Dr. Kenneth J. Button
Commission E	Dr. Arthur D. Spaulding
Commission F	Dr. Robert K. Crane
Commission G	Dr. Jules Aarons
Commission H	Dr. Robert W. Fredricks
Commission J	Dr. Alan T. Moffet

Officers of URSI resident in the United States:
(including Honorary Presidents)

Vice President	Prof. William E. Gordon **
Honorary President	Prof. Henry G. Booker**

Chairmen and Vice Chairmen of
Commissions of URSI resident
in the United States:

Chairman of Commission B	Prof. Leopold B. Felsen
Chairman of Commission C	Prof. Jack K. Wolf
Chairman of Commission E	Mr. George H. Hagn
Chairman of Commission F	Prof. Alan T. Waterman, Jr.
Chairman of Commission H	Dr. Frederick W. Crawford
Foreign Secretary of the U.S. National Academy of Sciences	Dr. Thomas F. Malone
Chairman, Office of Physical Sciences-NRC	Dr. Ralph O. Simmons
NRC Staff Officer	Richard Y. Dow
Honorary Members:	Dr. Harold H. Beverage
	Prof. Arthur H. Waynick

** Member of USNC-URSI Executive Committee

DESCRIPTION OF

INTERNATIONAL UNION OF RADIO SCIENCE

The International Union of Radio Science is one of 18 world scientific unions organized under the International Council of Scientific Unions (ICSU). It is commonly designated as URSI (from its French name, Union Radio Scientifique Internationale). Its aims are (1) to promote the scientific study of radio communications, (2) to aid and organize radio research requiring cooperation on an international scale and to encourage the discussion and publication of the results, (3) to facilitate agreement upon common methods of measurement and the standardization of measuring instruments, and (4) to stimulate and to coordinate studies of the scientific aspects of telecommunications using electromagnetic waves, guided and unguided. The International Union itself is an organizational framework to aid in promoting these objectives. The actual technical work is largely done by the National Committees in the various countries.

The officers of the International Union are:

President	W.N. Christiansen (Australia)
Past President:	M.J. Voge (France
Vice Presidents:	W.E. Gordon (USA)
	A.P. Mitra (India)
	A. Smolinski (Poland)
	F.L.H.M. Stumpers (Netherlands)
Secretary General:	P. Hontoy (Belgium)
Honorary Presidents:	H.G. Booker (USA)
	B. Decaux (France)
	W. Dieminger (West Germany)
	J.A. Ratcliffe (UK)
	R.L. Smith-Rose (UK)

The Secretary's office and the headquarters of the organization are locared at Rue de Nieuwenhove, 81, B-1180 Brussels, Belgium. The Union is supported by contributions (dues) from 36 member countries. Additional funds for symposia and other scientific activities of the Union are provided by ICSU from contributions received for this purpose from UNESCO.

The International Union, as of the XVIII General Assembly held in Helsinki, Finland, August, 1978, has nine bodies called Commissions for centralizing studies in the principal technical fields. The names of the Commissions and the chairmen follow.

A. Electromagnetic Metrology
Okamura (Japan)

B. Fields and Waves
Felsen (USA)

C. Signals and Systems
Zima (Czechoslovakia)

D. Physical Electronics
Farnell (Canada)

E. Interference Environment
G. Hagn (USA)

F. Wave Phenomena in Nonionized Media
Waterman (USA)

G. Ionospheric Radio
Hultquist (Sweden)

H. Waves in Plasmas
Crawford (USA)

J. Radio Astronomy
Tanaka (Japan)

Every three years, the International Union holds a meeting called the General Assembly. The next General Assembly, the XX, will be held in Washington, D.C., in August, 1981. The Secretariat prepares and distributes the Proceedings of these General Assemblies. The International Union arranges international symposia on specific subjects pertaining to the work of one Commission or to several Commissions. The International Union also cooperates with other Unions in international symposia on subjects of joint interest.

Radio is unique among the fields of scientific work in having a specific adaptability to large-scale international research programs, for many of the phenomena that must be studied are worldwide in extent and yet are in a measure subject to control by experimenters. Exploration of space and the extension of scientific observations to the space environment is dependent on radio for its research. One of its branches, radio astronomy, involves cosmos-wide phenomena. URSI has in all this a distinct field of usefulness in furnishing a meeting ground for the numerous workers in the manifold aspects of radio research; its meetings and committee activities furnish valuable means of promoting research through exchange of ideas.

NATIONAL RADIO SCIENCE MEETING COMMITTEE MEMBERS:

Steering Committee:

S.W. Maley, Steering Committee Chairman
T.B.A. Senior, Technical Program Committee Chairman
R.H. Ott, Assistant Chairman, Technical Program Committee
L.N. Christiansen, Registration & Facilities Committee Chairman
P.L. Jensen, Publications Chairwoman

S.W. Maley
R.C. Baird
D.C. Chang
L.N. Christiansen
R.Y. Dow
W.L. Flock
P.L. Jensen
C.T. Johnk
E.F. Kuester
C.G. Little
R.H. Ott
T.B.A. Senior
A.D. Spaulding
W.F. Utlaut
T.E. VanZandt
J.R. Wait

Technical Program Committee:

T.B.A. Senior, Chairman
R.H. Ott
J. Aarons
R.C. Baird
R.F. Benson
C.M. Butler
K.J. Button
D.C. Chang
R.K. Crane
K. Davies
G.A. Deschamps
R.W. Fredricks
E. Gossard
J.L. Massey
A.T. Moffet
M. Nesenbergs
A.D. Spaulding
J.R. Wait
M. Kindgren, Secretary to the Committee

SCATTERING: DIRECT AND INVERSE

Commission B, Session 1, UMC West Ballroom
Chairman: G. A. Deschamps, Department of Electrical Engineering, University of Illinois, Urbana, IL 61801

B1-1 0900 FORWARD SCATTERING FROM A ROUGH INTERFACE: A MULTIPLE SCATTERING THEORY

J.A. DeSanto, Ocean Sciences Division, Naval Research Laboratory, Washington, DC 20375

We consider scattering from a rough interface separating two semi-infinite media V_1 and V_2. For simplicity we treat the scalar problem where the media are fluids having different densities. Using the equations satisfied by the Green's functions G_j ($j = 1,2$) in the two media, with a source in V_1, we derive via Green's theorem in V_1 an integral relation for the field value of G_1 in terms of surface values of G_1 and its normal derivative, and an integral equation relating the surface values. Green's theorem is also used in V_2 with the field point in V_1. Continuity conditions at the interface then yield a non-local impedance-type boundary condition from V_2. It is also called an extended boundary condition or extinction coefficient. The results of the two applications of Green's theorem can be combined into a single integral equation for the surface value of G_1. The derivation follows for an arbitrary deterministic surface.

In Fourier transform space it is shown that the T-matrix for the scattered field satisfies a Lippmann-Schwinger (LS) integral equation analogous to the quantum mechanical result. However, the "quantum potential" analogue here is both complex and non-central.

For a Gaussian distributed random surface with homogeneous statistics, the LS equation reduces to a one-dimensional integral equation for the coherent field (Dyson equation). An approximation of this latter equation whose Born term is originally due to Ament can be solved. The result is thus a multiple scatter theory for the coherent field. Comparison of the result with experimental data for plane wave incidence and specular return demonstrates the improvement over single scatter theories for large roughness. Higher order multiple scatter theories and the effect of non-Gaussian statistics are also discussed.

B1-2
0920 SHADOWING OF RANDOM COMPOSITE SURFACES:
Gary S. Brown, Applied Science Associates,
105 E. Chatham, Apex, NC 27502

In an earlier analysis [G. S. Brown, IEEE Trans. Ant. & Propg., AP-26, 472-482, 1978] of backscattering from a perfectly conducting Gaussian distributed composite surface, shadowing was properly included in the formal results. However, due to the use of an incorrect form for the shadowing function, its effect was erroneously evaluated. This paper incorporates the correct shadowing function into the above analysis and determines its impact upon the large angle of incidence scattering. Two consequences of shadowing are found to significantly reduce the surface scattering cross section per unit area or σ° near grazing incidence. These result from the nonzero variance of the large scale slopes and the total shadowing (with probability one) of points on the surface with unfavorably oriented slopes. Of these two effects, the former is the most important since it causes σ° to approach zero near grazing incidence. The maximum impact of the latter effect is a reduction in σ° by 3 dB very near grazing incidence. In this paper, particular attention is given to the physical reasoning behind the causes and effects of shadowing for a composite surface.

B1-3
0940 ANTENNA-MODE RADAR CROSS-SECTION ESTIMATION OF A TACAN ANTENNA:
M. S. Sohel, General Dynamics, Fort Worth, TX 76101

An antenna radar cross-section (RCS) is composed of two components, the structural-mode RCS, and the antenna-mode RCS. While designing aircraft antennas from an RCS standpoint, it is essential to know accurately the magnitude and the phase of the antenna-mode RCS component. In this study, an L-band TACAN annular-slot antenna is investigated, and the antenna-mode RCS is determined at the in-band and out-of-band frequencies. Antenna gain and voltage-standing-wave-ratio were recorded at 1, 7, and 16 GHz to get in-band and out-of-band antenna characteristics. It is shown that at the in-band frequencies the antenna-mode RCS is negligible; however, at the out-of-band frequencies it can vary over a wide range of values. The results of this study will be very useful to an aircraft-antenna design and application engineer.

B1-4
1000

PSEUDO-ANALYTICAL ANALYSIS OF COUPLED, TM-ILLUMINATES NARROW CONDUCTING STRIPS

W.A. Walker and C.M Butler, Department of Electrical Engineering, University of Mississippi, University, MS 38677

The problem of determining the surface current induced on coupled conducting strips that are narrow relative to the wavelength is investigated by a method which is essentially analytical. The parallel strips reside in a homogeneous medium of infinite extent and are excited by an incident field which is transverse magnetic to the strip axes. From the equations for coupled strips of any width, narrow-strip equations are deduced and are solved for the strip current. Aside from the use of numerical integration to determine coupling coefficients (constants), the solution procedure is entirely analytical, and the results are indeed presented in analytical form. For selected cases of interest, the strip current and the associated scattered fields are presented.

B1-5
1040

AN INVERSE SCATTERING APPROACH TO ANTENNA AND OPTICAL SYSTEM SYNTHESIS PROBLEMS:

W. Ross Stone, Megatek Corporation, 1055 Shafter Street, San Diego, CA 92106

The classical synthesis problem of inverse scattering theory can be briefly summarized as follows: Given a desired field which is a solution to the inhomogenous wave equation, determine the source term in that wave equation. The system designer specifies the field he wants produced and solves for the distribution of sources which will produce it. The Exact Inverse Scattering Theory, developed by N.N. Bojarski, provides a solution to this inverse source problem. However, when the system design includes the specification of inhomogeneous (conducting and/or dielectric) media, the problem is more complex. Mathematically, the source term in the inhomogeneous wave equation then includes both a "real" source term and a term due to induced sources (which depends on both the total field and the generalized refractive index). Such synthesis problems arise in the design of antenna systems, microwave lenses, radomes, and in optical system design.

It is shown that in applying the Exact Inverse Scattering Theory to synthesis problems involving inhomogeneous media, the presence of both the refractive index and the field in the source term requires an extra, non-trivial step in the solution. The author has taken the application of this theory to the synthesis problem one step further, and has developed an inverse integral equation approach. This approach permits the system designer to directly specify the desired scattered (or transmitted) field as a function of the field incident on the system, and to solve for the complete distribution of the refractive index. Both of these approaches are exact, applicable to a very wide range of synthesis problems, give the designer total freedom with respect to the presence or absence of design constraints, and permit rigorous statements to be made about the uniqueness and computational effort required for a design. Both theories will be derived and explained in this paper, and a simple numerical design example will be presented. For the microwave lens, radome, and optical design applications, the classical approach has been to employ ray tracing techniques. It will be shown that because of the use of the fast Fourier transform, the inverse scattering techniques presented in this paper should be several powers of ten faster than ray tracing techniques for equivalent design problems.

B1-6 1100 DIRECT AND INVERSE SCATTERING IN CAUSAL SPACE:

Norbert N. Bojarski, 16 Pine Valley Lane, Newport Beach, CA 92660

The conventional exact time-domain formulation of the one-dimensional electromagnetic direct scattering problem is re-derived and transformed into causal space, the axies of which are defined as x±ct. In this causal space, the direct scattering solution reduces to an exceedingly simple expression, which is solvable numerically in the order of N^2 operations (where N is the number of data points in time as well as in space), vis-a-vis the conventional time domain formulation which requires of the order of N^3 operations for a numerical solution. This causal space solution yields the scattered (transmitted and reflected) fields incidentally, without computations additional to the basic solution for the current densities.

The inverse scattering problem is then solved in this causal space. This solution to the inverse problem also consists of an exceedingly simple expression, which is also numerically solvable in the order of N^2 operations. Appropriate physical reasoning greately reduces the mathematical complexity of the derivation of this inverse solution.

Numerico-experimental results for both the direct as well as the inverse causal space solutions are presented. Since simplicity is a salient feature of these solutions, the computer programs are listed and discussed. Also discussed are the preliminary results of an error analysis.

B1-7 1120 RECONSTRUCTION USING RAY BENDING:

Roger D. Radcliff and Constantine A. Balanis, Department of Electrical Engineering, West Virginia University, Morgantown, WV 26506

It is often desirable to remotely determine from measurements the electrical constitutive parameters (conductivity and permittivity) as a function of position within an object or an underground region of interest. The process of reconstructing such a three-dimensional image by transmission of radiation is known as reconstructive tomography. In the past, tomographers have always made the simplifying assumption of straight-line electromagnetic wave propagation between the source and receiver. As a consequence, previous reconstruction methods yield questionable results for applications in media where refraction effects are significant.

To account for refraction, the Eikonal equation of geometrical optics is solved by the method of characteristics, and phase paths can be traced from source to receiver in lossless media. Examining Fermat's Principle in both lossless and lossy media reveals that this ray tracing technique can be applied to find the attenuation ray paths in lossy media. As an intermediate step toward incorporating this information into the reconstruction process, the problems of remotely determining the conductivity of a two-dimensional slab and a rectangular cylinder are solved by applying the attenuation ray tracing method in an iterative manner.

B1-8
1140 TIME DOMAIN PROFILE RECONSTRUCTION FOR INHOMOGENEOUS LOSSY MEDIA:

C.Q. Lee and B.C. Phan, Communications Laboratory, Department of Information Engineering, University of Illinois at Chicago Circle, Box 4348, Chicago, IL 60680

A time domain method for the reconstruction of parameter profiles of inhomogeneous, lossy and stratified regions is presented. The problem considered is one-dimensional in which the physical characteristics of the medium are functions of the position x along which the wave propagates, but which is homogeneous in directions perpendicular to this disturbance. We assume that it can be modeled by piecewise uniform sections of lossy transmission lines. Relations between terminal voltages and currents in each section are derived by means of Largrangian approach which utilizes moving observers traveling in opposite directions. Solutions are obtained by satisfying the boundary conditions observed by these observers.

The concepts of pseudo incident and reflected waves in the time domain are introduced. Using these concepts, the time domain reflection coefficient in a lossy system is described and similarities between lossy and lossless systems are shown.

For a given driving voltage, the constitutive parameters of the regions considered can be determined by the voltage or current sampled at the sending end. The numbers of uniform sections used in the approximation is directly proportional to the sample rate. This method can be conveniently used in computer on-line analysis and is particularly useful for tissue identification by ultrasound. Using the method presented, examples of computer simulated results for some known cases are presented.

Commission C Session 1

EVOLVING APPROACHES AND PROBLEMS
IN COMMUNICATIONS NETWORKS
Monday Morning, 5 Nov., UMC Forum Room
Chairman: J. L. Massey, Department of System Science, University of California, Los Angeles, CA 90024

C1-1 0900 AN OVERVIEW OF PUBLIC KEY CRYPTOGRAPHY:
R. C. Merkle, BNR, Inc., 3174 Porter Drive, Palo Alto, CA 94304

C1-2 0952 DISTRIBUTED ALGORITHMS FOR DATA NETWORKS:
Pierre A. Humblet

A distributed algorithm in a network is a set of procedures, one at each node, that cooperate to achieve some objective, like determining the best routes between any two nodes, or insuring the correct delivery of messages at their destinations. Distributed algorithms are a necessity in communication networks, as the knowledge itself is distributed. Generally a node is (and should remain) unaware of most events occurring in distant parts of the network. This talk will present several distributed algorithms, paying particular attention to two common flaws. Sometimes the nodes exchange so many messages to accomplish their objectives that this traffic dwarfs user data. In addition, some algorithms contain subtle deadlocks, where two nodes each wait for the other to send a message.

C1-3 1044 AN OVERVIEW OF MULTIPLE USER INFORMATION THEORY:
A. El Gamal, Department of Electrical Engineering and Computer Science, University of Southern California, Los Angeles, CA 90007

C1-4
1121

CONGESTION CONTROL TECHNIQUES IN DATA NETWORKS:*

Mischa Schwartz, Department of Electrical Engineering,
Columbia University, New York, NY 10027

In this paper we discuss the problem of congestion in packet-switched data networks and techniques adopted for controlling congestion. Techniques in current use include such procedures as window (end-to-end) control, local control, input buffer limiting, and link buffer assignment.
We describe the results of an analytic study designed to provide a comparative performance evaluation of some of these techniques as well as others suggested in the literature. Specific network models and analytical approaches used to obtain these results are discussed as well. The results of the analysis coupled with results obtained by simulation provide insight into the operation of congestion control mechanisms and provide a basis for suggesting improved control procedures.

---

*The work reported here was supported by the National Science Foundation under grant ENG-78-08260.

Commission J Session 1

LOW NOISE RECEIVERS - I
Monday Morning, 5 Nov., UMC 235
Chairman: A. T. Moffet, Owens Valley Radio Observatory, Caltech, Pasadena, CA 91125

J1-1 0900 **LOW-NOISE, 5 GHZ COOLED GASFET AMPLIFIER:**

S. Weinreb, Nat'l. Radio Astronomy Obs., 2015 Ivy Rd., Charlottesville, Va. 22903

Cryogenically-cooled gallium-arsenide field-effect transistor amplifiers (GASFET'S) have the potential of replacing cooled parametric amplifiers and masers for very low noise microwave applications such as radio astronomy. The GASFET amplifiers offer simplicity (no pump), low construction cost, and wide bandwidth. However, the ultimate noise temperature for cooled GASFET'S is unknown. A comprehensive noise theory has been published (Pucel, et al., Adv. in El. and El. Phys.; vol. 38, 1975, pp. 195-265) but the results are complex with several noise generation mechanisms (thermal, hot electron, intervalley scattering, and high-field diffusion) with unknown temperature dependencies of some of the parameters describing these mechanisms.

Several measurements of the noise temperature of cooled GASFET amplifiers have been reported (i.e. Miller, et al., Elect. Let., 13, Jan 6, 1977). In general, these authors have reported results with a single transistor type and except for Liechti and Larrick (IEEE Trans. 1976 MTT-24, pp. 376-381) the source impedence presented to the transistor has not been reoptimized at the cryogenic temperature. In our work, we have tested several transistors in the same amplifier at temperatures of 300°K to 20°K with provisions for adjustment at each temperature. Typical results are shown in the figure below. The amplifier utilizes air-line construction, adjustable-impedence quarter-wave lines, and P70 or P103 packaged transistors. Problems in the design of such an amplifier include input match, high-frequency (∿ 20 GHZ) oscillations, and thermal stress; these will be discussed at the conference.

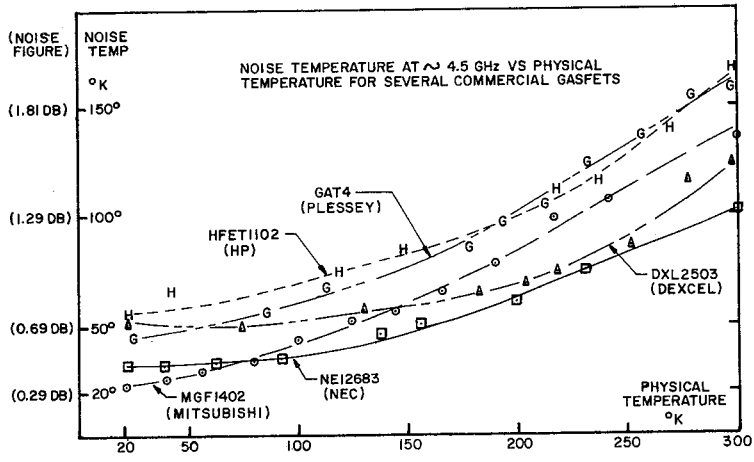

J1-2
0925 LOW NOISE PERFORMANCE OF GaAs FET AMPLIFIERS IN THE 1-2 GHZ REGION

William Tappan Lum, Development Engineer, Radio Astronomy Laboratory, University of California, Berkeley, CA 94720

A survey of the low noise performance of L-Band GaAs FET amplifiers both at room temperature and at cryogenic temperatures. Amplifiers of 15° K noise temperature at 20° K physical temperature have been built as well as 45° K noise temperature. These amplifiers employ source inductance feedback to achieve reasonable input VSWR.

The techniques of fabricating amplifiers for cryogenic operation will be discussed as well as some of the problems of materials used in amplifiers at reduced temperatures. Complete data on existing cooled and uncooled amplifiers built recently at Berkeley and put into operation on telescopes will be presented.

J1-3
0950 CRYOGENIC PARAMETRIC AMPLIFIER NOISE PERFORMANCE AT 4.2 K: W. J. Wilson, R. L. Dickman, and G. G. Berry, Electronics Research Laboratory, The Aerospace Corporation, Los Angeles, Calif. 90009.

Low noise amplifiers are required in many areas of communications, radar and radio astronomy. In millimeter-wave mixer receivers, with large conversion losses, very low-noise IF amplifiers are of prime importance. Cryogenic parametric amplifiers have been developed which have noise temperatures of 18 K when cooled to an ambient temperature of 18 K. This paper reports the results of an experiment in which a 4.5 - 5.0 GHz cryogenic paramp was operated at 4.2 K to determine how much improvement in noise temperature could be obtained. At an ambient temperature of 4.2 K, the paramp operated satisfactorily and the measured noise temperature was 12 K, which is a decrease of 6 K from its normal noise temperature. A question raised by these results is why the factor of four decrease in ambient temperature did not produce a similar drop in noise temperature. It is concluded, based on a variety of factors, that varactor heating by the pump oscillators limited the improvement in noise performance. Prospects for further improvements in paramp noise temperatures using better varactors are discussed. This work was supported by the Aerospace Corporation's Sponsored Research Program.

J1-4
1045

ULTRA-LOW-NOISE PARAMETRIC UP-CONVERTER AND MASER DEVELOPMENT AT THE JET PROPULSION LABORATORY:

R. C. CLAUSS AND S. M. PETTY, MICROWAVE ELECTRONICS GROUP, TELECOMMUNICATIONS SCIENCE AND ENGINEERING DIVISION, JET PROPULSION LABORATORY, 4800 OAK GROVE DRIVE, PASADENA, CA. 91103

The recent combination of a cooled, S-band parametric up-converter and a K-band reflected-wave maser has demonstrated an effective noise temperature of 3.5 Kelvin at 2.3 GHz. The up-converter has an instantaneous bandwidth of 500 MHz with a conversion gain of 8 dB; the unit was developed by AIL, a division of Cutler-Hammer under contract to the Jet Propulsion Laboratory (JPL). The upper-sideband up-converter is pumped at 21.7 GHz and converts 2.3 GHz input signals to 24 GHz where a reflected-wave maser is used as an intermediate frequency amplifier. The up-converter and maser are cooled to 4.5 Kelvin in a closed-cycle helium refrigerator (CCR) and the combination provides a total net gain of 40 dB.

JPL has been active in the development and use of ultra-noise masers for deep space communications in the NASA Deep Space Network for 20 years. Both open and closed-cycle cryogenics systems have been used with the many masers (more than 50 units) accumulating over 2 million hours run time at temperatures between 4.0 and 4.6 Kelvin. Effective input noise temperatures of 2,7,9, and 13 Kelvins have been achieved at 2.3 GHz, 8 GHz, 15 GHz, and 24 GHz respectively. A cooperative effort with the University of California at San Diego resulted in the development of a reflected-wave maser. Another cooperative effort (during the past few years) with the National Radio Astronomy Observatory produced a K-band reflected-wave maser with wide bandwidth and tunability (C. R. Moore and R. C. Clauss, IEEE Trans. Microwave Theory Tech. VOL. MTT-27, 249-256, 1979). Evaluation of ruby as a maser material at frequencies between 27 and 42 GHz shows that it will be possible to achieve 1000 MHz instantaneous bandwidth with masers above 40 GHz.

J1-5
1110 A NEW GENERATION OF MASER AMPLIFIERS FOR RADIO ASTRONOMY APPLICATIONS: Craig R. Moore, National Radio Astronomy Observatory, Green Bank, WV 24944

The reflected-wave maser offers wide instantaneous bandwidth and large tuning range while retaining the low noise performance typical of masers. When mounted on a closed cycle 4.6 K helium refrigerator a stable, reliable and low maintenance system is achieved. Freedom from instability induced by pump power and frequency variations and mechanical vibration is inherent in the design.

Pertinent design features will be discussed as well as the projected performance of ruby masers offering 500 to 1000 MHz of bandwidth in the 15 to 50 GHz frequency range. Experimental results in the 18 to 26 GHz and 40 to 50 GHz bands will be presented.

A four stage ruby maser employing cryogenically cooled circulators has been developed for the 18 to 26 GHz band (C. R. Moore and R. C. Clauss, IEEE Trans. MTT, 27, 249-256, 1979). Five such units have been constructed at NRAO and the design is being duplicated at several other institutions. A cryogenically cooled circulator has been developed for the 40-50 GHz band, and a single stage ruby maser has been constructed to evaluate performance and pump power requirements.

J1-6
1135 LOW NOISE K-BAND RECEIVER FOR NRAO 140-FOOT TELESCOPE: Charles J. Brockway, Electronics Engineer, National Radio Astronomy Observatory, P. O. Box 2, Green Bank, WV 24944

An 18.4-26.4 GHz reflected-wave maser receiving system has been used for several months of radio astronomy observations on the 140-foot diameter radio telescope at the National Radio Astronomy Observatory in Green Bank, WV. A total system temperature of 52°K has been attained at 20 GHz. An instantaneous 3 dB bandwidth of at least 200 MHz is obtained over the tuning range of 21-24 GHz; the bandwidth decreases to 50-80 MHz at the band edges. Net gain is 33 dB. The maser amplifier was developed in a joint program between the NRAO and the Jet Propulsion Laboratory in Pasadena, CA. Single conversion translates the sky frequency to the 50-600 MHz range for additional processing. A frequency/phase locked local oscillator system has been built to tune over 18-26.5 GHz with lock up times of 2 milliseconds for frequency steps of 30 MHz and 4 milliseconds for 100 MHz. The receiving system is used in the Cassegrain configuration. The 10.5 foot diameter secondary reflector can be nodded by the use of an electrohydraulic servomechanism at a 1 to 5 Hz rate causing a beam shift of up to 18 arc minutes. This spatial switching, or nutating, is employed to largely eliminate receiver output changes due to atmospheric fluctuations. The maser amplifier is cooled to 4.5°K by using a closed-cycle 3-stage helium refrigerator. Cool down from room temperature is about eight hours and the system has been kept cold for as long as three months without attention.

The emphasis of this paper is on the operating characteristics of the receiving system. After reviewing a block diagram of the receiver and the nutating geometry, typical system temperatures with frequency and weather conditions are discussed. Chart recordings are shown to demonstrate the value of nutating in inclement weather to locate and maximize telescope positioning on weak radio sources. Typical gain-bandpass characteristics of the receiver are presented. Major factors affecting system performance over two years of operation are mentioned. The continuing development of a low noise receiving system for the 140-foot telescope is outlined. A 500 MHz bandwidth maser has been built at NRAO and will have parametric upconverters placed in front to provide C, X, and Ku band coverage.

ASYMPTOTIC METHODS
Commission B, Session 2, UMC West Ballroom
Chairman: T. B. A. Senior, Radiation Laboratory, University of Michigan, Ann Arbor, MI 48109

B2-1
1330 Evanescent Wave Tracking -- A New Approach to the Analysis of Large Reflector and Aperture Antennas

L. B. Felsen, Electrical Engineering Department, Polytechnic Institute of New York, Farmingdale, New York 11735

The radiation characteristics of large reflector and aperture antennas are analyzed conventionally by physical optics or GTD methods. By these procedures, one may establish equivalent fields in an aperture plane on or near the antenna surface and then perform a Kirchhoff type integration to obtain the far field. Although for certain types of antenna and feed combinations, the GTD approach may be employed to pass directly from the antenna to the far field, this is not possible for tapered aperture fields (for example, Gaussian) that de-emphasize the effects of aperture truncation.

To avoid the integration over an equivalent aperture plane, a new method, based on local evanescent wave tracking, is proposed. Here, the tapered illumination from the feed is approximated by an exponential envelope of the type $\exp(-kI)$, where k is the wavenumber and I is a positive real function. From this information and the phase on an initial reference surface such as the feed aperture, one may track local evanescent plane waves along phase paths to one or more reflectors and thence to the far field without need of an intervening integration (S. Choudhary and L. B. Felsen, Proc. IEEE 62, 1530-1541, 1974). When edge illuminations (for example, on a subreflector) are important, these can be taken into account by inclusion of evanescent wave edge diffraction contributions. The determination of the phase paths, a principal difficulty in applying the evanescent wave method, can be simplified and systematized by assigning to the evanescent field at each point P on the initial or on a reflecting surface a virtual complex source point whose location in complex space is determined by the conditions at P (P. Einziger and L. B. Felsen, to be published). In real space, phase paths generated by the resulting complex caustic are hyperbolas. For the special case of a symmetrical field distribution with Gaussian amplitude taper, the caustic collapses to a complex source point and the hyperbolic phase paths are confocal.

The presentation stresses the physical implications of evanescent vs. geometric optical wave tracking for tapered illuminations, with emphasis on radiation and power flow processes.

B2-2
1350

Complex-Source-Point and Evanescent Wave Analysis of Parabolic Reflectors and Offset Gaussian Beam Feeds

F. J. V. Hasselmann and L. B. Felsen, Department of Electrical Engineering, Polytechnic Institute of New York, Farmingdale, New York 11735

Dual mode horns employed commonly as feeds for parabolic reflector antennas generate a radiation pattern that can be well approximated by a Gaussian beam. To determine the far field of the antenna, which may contain multiple subreflectors, it has been customary to perform integrations either of the physical optics currents on the reflector surfaces or of the GTD field in the antenna aperture. These integrations may be avoided if the Gaussian beam is tracked directly from the feed horn via subreflectors (if any) to the main reflector and then to the far zone. The tracking may be accomplished either by the complex-source-point method or by the evanescent wave method. Both procedures are applied here to a two-dimensional configuration comprising a parabolic reflector with offset beam feed centered at the focus. It is shown that the results so obtained agree with those deduced elsewhere by a semi-heuristic procedure (M. J. Gans and R. A. Semplak, Bell System Tech. J. 54, 1319-1340, 1975). The complex-source-point method is also readily adapted to the three-dimensional configuration and yields directly the depolarization and ellipticity of the reflected vector beam near or far from the reflector surface.

B2-3
1410 **Local-Complex-Source-Point Method for Evanescent Wave Tracking, with Application to Gaussian Beam Scattering by a Circular Cylinder**

P. Einziger and L. B. Felsen, Electrical Engineering Department, Polytechnic Institute of New York, Farmingdale, New York 11735

The propagation and scattering of highly collimated high-frequency electromagnetic fields can be described effectively by the tracking of local evanescent plane waves with complex phase $S = R + iI$, where R and I are real functions (S. Choudhary and L. B. Felsen, Proc. IEEE 62, 1530-1541, 1974). These waves are tracked along phase paths I = constant whose determination poses difficulties that may be overcome in part by associating with the local (weakly) evanescent field at each point P or an initial surface a virtual complex source point. The phase paths are then hyperbolic. This procedure improves a previous formulation where the unperturbed phase paths were taken to be the straight geometric-optical rays. Local hyperbolic matching for the phase paths can be given various but equivalent interpretations that involve caustics in complex coordinate space, construction of a local elliptic coordinate system in real space, and local approximation of a general profile function I by a circle. To examine the quality of this procedure, the problem of Gaussian beam diffraction by a circular cylinder is examined in detail. With the rigorous solution constructed by the complex-source-point method serving as a reference, numerical comparisons are presented to establish the range of validity of the local matching technique.

B2-4
1430

A SPECTRAL DOMAIN APPROACH FOR SOLVING A CLASS OF WAVEGUIDE DISCONTINUITY AND PERIODIC GRATING PROBLEMS:

R. Mittra, C.H. Tsao, V. Jamnejad and W.L. Ko,
Department of Electrical Engineering, University of Illinois, Urbana, Illinois 61801 USA

The conventional approach to solving waveguide discontinuity problems is to formulate the boundary-value problem in terms of an integral equation and derive a numerical solution using the method of moments. The same technique is also applied to the open-region problem of diffraction by a periodic grating of apertures in a conducting plane.

In this paper, we propose an alternative method based on the spectral domain concepts (Ko and Mittra, Trans. AP-S., March 1977), which allow one to derive an iterative solution to the problem of an aperture in a waveguide, or a periodic array of apertures in a conducting plane. The solution is generated using only the numerically efficient FFT algorithm, and without the need for matricizing the integral equation. The application of the spectral domain approach involves the following steps: (a) formulating the integral equation for the aperture electric field; (b) extending the range of the integral equation such that it encompasses the entire waveguide or the periodic cell rather than just the aperture. (This is accomplished by introducing an additional unknown besides the aperture field); (c) making an initial approximation for the aperture field and deriving the zero-order approximation for this new unknown; (d) solving the extended integral equation whose kernel is exactly invertible in the extended range using the FFT; (e) deriving the next order approximation for the aperture field; and (f) repeating the process until convergence is achieved.

The principal advantages of the spectral domain approach over the conventional mode-matching method are discussed in the paper, and extensive numerical results are presented.

B2-5
1510

AN APPLICATION OF THE SPECTRAL THEORY OF DIFFRACTION TO THE PROBLEMS OF FORWARD SCATTERING BY STRUTS IN REFLECTOR ANTENNAS: W.L. Ko, R. Mittra and S.W. Lee, Department of Electrical Engineering, University of Illinois, Urbana, Illinois 61801 USA

A conventional approach to evaluating the blockage effect due to the feed and the supporting struts in a reflector antenna involves two basic steps: casting optical shadows onto the reflector aperture and subtracting the radiation field from the shadow area from the antenna pattern of the unblocked reflector. Such an approach, though straightforward, is limited to angles near the main beam region. A more detailed analysis requires the computation of the induced surface currents on the struts which are then integrated to obtain the scattered field. However, the evaluation of the radiation integral can be time-consuming, particularly at high frequencies, when the diameter of the strut is not small in terms of the operating wavelength. In this paper, we describe an alternative approach which is accurate and yet numerically efficient because it bypasses the numerical computation of the integral of the strut currents. In the present approach, which is based on the spectral domain approach (Mittra and Ko, AP-TRANSACTIONS, November 1977) for solving the problem of high-frequency scattering by smooth convex surfaces, the current on the strut is replaced by an equivalent aperture distribution on a planar surface placed in juxtaposition with the strut. The aperture distribution is chosen such that it radiates the same field as the original strut current. The equivalent aperture distribution is obtained by using the quasi-optical method of shadowing. The first step in this analysis is to identify three regions in the equivalent aperture, namely, the deep shadow, the unblocked, and the transition region. The extent of these regions can be estimated from the high-frequency diffraction theory of cylinders. Essentially, the scattered field in the aperture can be approximated by the negative of the incident field in the deep-shadow region, the zero field in the well-illuminated (unblocked) region, and by a smooth interpolation function in the transition region. The scattered aperture field is then Fourier transformed to obtain the far scattered field due to the struts. The advantage in using the scattered aperture field approach is that it has a finite support, and hence, its Fourier transform is conveniently derived. To illustrate the application of the method, numerical results for a reflector antenna system are presented in the paper.

B2-6
1530

A HYBRID UTD-EIGENFUNCTION METHOD FOR SCATTERING BY A VERTEX: J. N. Sahalos, University of Thrace, Xanthi, Greece, and G. A. Thiele, Department of Electrical Engineering, The Ohio State University, Columbus, Ohio 43210

Present solutions for the electromagnetic scattering by a vertex are either approximate or difficult to use for computations. For example, GTD solutions for vertex scattering are not yet fully developed and yield approximate results of unknown accuracy. The exact eigenfunction solution is both difficult to use and computationally inefficient due to the large number of eigenfunctions that must be retained.

In this work, we obtain the scattering by a vertex (e.g., a quarter plane) by employing the exact eigenfunction solution only in a very small region close to the tip of the vertex (i.e., within 0.2λ). Thus, only a small number of eigenfunctions (e.g., two or three) are required to obtain the current in the tip region. Outside of this region, the UTD is employed to obtain the current. The changeover point is determined by finding the point where the eigenfunction current has decayed to that predicted by UTD wedge diffraction theory.

Results will be shown for both the current on the quarter plane and also for the scattered field. In addition, the field scattered by a rectangular plate using this method will be compared with that predicted by the UTD with vertex diffraction, and the results are seen to be in very close agreement, as shown below.

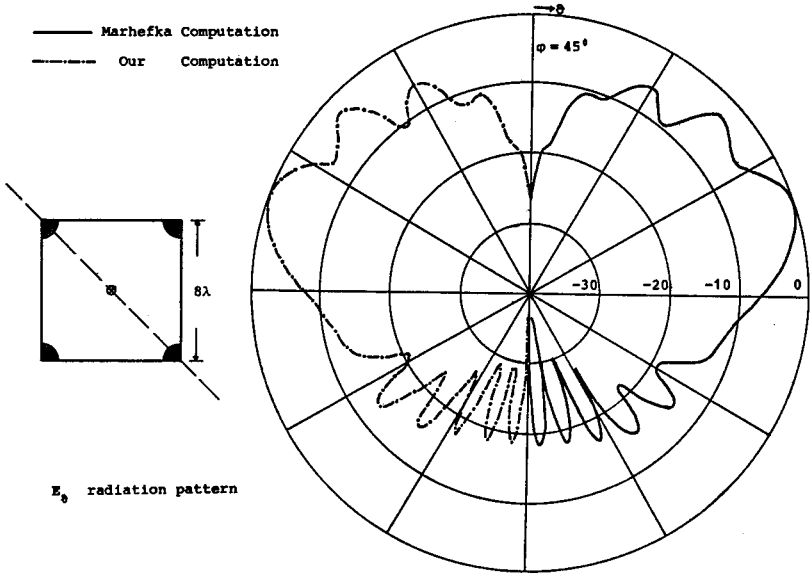

B2-7
1550 GENERALIZED GEOMETRICAL OPTICAL ANALYSIS OF ELECTROMAGNETIC REFLECTION FROM A NUMERICALLY SPECIFIED SURFACE: A.M. Rushdi and R. Mittra, Department of Electrical Engineering, University of Illinois, Urbana, Illinois 61801 USA

The work reported in this paper is an extension of two methods recently developed by the authors, viz., the Launching Method (AP Trans., 1979) and the Generalized Geometrical Optics or GGO (URSI Meeting, June 1979). We consider the problem of electromagnetic reflection from a surface that is described only numerically in terms of the coordinates and the normal directions of the surface at a set of grid points. A conventional approach to attacking this problem would entail a numerical interpolation through these grid points, followed by a search for the specular point. Even when one is willing to invest the computer time and effort to perform the numerical interpolation, one often finds that the geometrical optics (GO) analysis of the reflected field, which retains only the terms of the order of k^0, is not sufficiently accurate. Again, in the conventional approach, one then resorts to a numerical integration of the physical optics integral in order to derive a result which is more accurate than the one given by GO. However, the evaluation of the above integral can also be very time-consuming. In contrast, the method presented in this paper is numerically efficient, because it neither requires the interpolation of the surface nor a numerical evaluation of the radiation integral involving the surface current. And yet, it yields explicit expressions for the field which are accurate to within k^{-1}. These higher-order terms cannot, in general, be derived for numerically specified surfaces using the classical transport equations for GO. The accuracy and efficiency of the method have been verified by applying it to a test surface, and the results have been found to have good agreement with the PO method. Numerical results illustrating the application of the method are presented in the paper, and the scope as well as limitations of the paper are discussed.

B2-8
1610

SCATTERING BY IMPEDANCE STRIPS:

Thomas B.A. Senior, Radiation Laboratory, The University of Michigan, Ann Arbor, MI 48109

The use of resistive sheet materials is of interest for cross section reduction purposes. At the last two National Radio Science Meetings the scattering of E- and H-polarized plane waves by resistive strips was considered [1,2] and, in particular, it was shown [2] that for an E-polarized plane wave at edge-on incidence the backscattered field could be expressed in terms of the currents on the corresponding half plane at locations appropriate to the front and rear edges of the strip. This type of asymptotic expansion gives accurate results even for strip widths as small as $\lambda/10$, but does necessitate the evaluation of the half plane currents. A program is described for computing these currents as a function of position for any resistivity, real or 'complex'.

To create a viable structure the strip must be rigidized, for example by encasing it in a thin plastic layer. The effect is to make the apparent resistivity complex, and the reactive part of the resulting impedance can be either inductive or capacitative. The presence of the imaginary part not only produces a strip whose electrical properties are now frequency dependent, but also diminishes the cross section reduction that can be achieved. This is illustrated using data found by numerical solution of the corresponding integral equation for the strip. The results are also compared with those obtained from the asymptotic representation of the scattered field in conjunction with values of the half plane currents for a variety of impedances.

[1] T.B.A. Senior, 'Backscattering from resistive strips', National Radio Science Meeting, Boulder, November 1978.

[2] T.B.A. Senior, 'Scattering by resistive strips,' National Radio Science Meeting, Seattle, June 1979.

B2-9
1630

GTD ANALYSIS OF A HYPERBOLOIDAL SUB-REFLECTOR WITH CONICAL FLANGE ATTACHMENT: M. S. Narasimhan, P. Ramanujam, and K. Raghavan, C.S.D., I.I.T., Madras-600036, India

A GTD analysis of the principal plane radiation patterns of a hyperboloidal sub-reflector with a conical flange attachment, illuminated by a primary feed radiating spherical waves, based on UGTD and its modified slope diffraction version (Y. M. Hwang and R. G. Kouyoumjian, 1974), which have been shown to closely follow the most rigorous Surface Theory of Diffraction (Y. Rahmat-Samii and R. Mittra, 1978), is presented in this paper. The non-axial far-field patterns in the principal planes are derived after considering diffraction by the wedge formed between the rim of the hyperboloidal and the conical flange as well as contributions to the diffracted fields from the flange-edge, which receives illumination from the feed as well as from the rays diffracted by the wedge. Special care is taken while deriving the diffracted far-fields in the H-plane, since in this plane, E-vector of the rays diffracted by the wedge and illuminating the flange-edge will be parallel to the surface of the conical flange. The diffracted field along the bore-sight axis is obtained from the equivalent edge currents. The computed diffracted far-fields of a typical hyperboloid with conical flange attachment illuminated by a high-performance primary feed shows excellent agreement with the measured data. The GTD analysis presented can be easily extended to any other reflector geometry involving a conducting flange or shroud attachment at its rim.

SIGNAL PROCESSING FOR ANTENNA ARRAYS
Monday Afternoon, 5 Nov., UMC Forum Room
Chairman: A. Vigants, Bell Laboratories, Holmdel, NJ 07733

C2-1
1330

SIGNAL PROCESSING METHODS FOR LARGE BANDWIDTH ADAPTIVE ARRAYS

C. Jim and L. Griffiths
Department of Electrical Engineering
University of Colorado
Boulder, Colorado 80309

Spread spectrum techniques in both radar and communications involve the use of bandwidths which may be a significant fraction of the center frequency of the system. This is particularly important in modern microwave applications. Adaptive array processing offers the advantage of interference rejection through null steering but traditional approaches in the past have relied upon narrow bandwidth gain/phase adjustments.

This paper describes a signal processor which can be employed at large bandwidths in adaptive microwave receiving arrays. The beamforming system contains analog tapped delay lines in which the taps are switches which are restricted to have values of ± 1 or zero. An off-line digital processor provides adaptation by controlling the value of each switch in the system. Because of this quantization, conventional adaptive signal processing algorithms are inappropriate. In this paper, new algorithms which achieve effective interference rejection using switched tapped delay lines are presented. The performance characteristics of the resulting processor are illustrated using field-recorded data.

C2-2
1400

SOME EFFECTS OF HARD LIMITING IN ADAPTIVE ANTENNA SYSTEMS: F.W. Floyd and J.T. Mayhan, M.I.T. Lincoln Laboratory, Lexington, MA 02173

A common implementation of an adaptive antenna consists of an antenna array comprised of equal gain elements coupled with an Applebaum-Howells type adaptive processor. In this scheme, the signals from the antenna elements are weighted and linearly combined to form a single output in which the interference signals from the various elements tend to cancel one another. The weight settings are determined by the action of feedback loops controlling the weights.

In analog circuit versions of the Applebaum-Howells processor, it has been common practice to insert a hard limiter between each antenna port and its correlation mixer. There are two reasons for doing this, both relative to the convenience of circuit implementation. At first, it would appear that the dynamic range required of the correlator and subsequent circuitry could be reduced considerably. Secondly, the correlators in adaptive antenna systems are often implemented with readily available, balanced diode mixers. This type of mixer is inherently a hard limiting device because one of its inputs, the local oscillator (LO) input, saturates the diodes and drives them in a switching mode; therefore, the output is sensitive to the phase of this input, but not to its amplitude.

Brennan and Reed (IEEE Trans. Aeros. and Electron. Sys., AES-7, 68, 1971) analyzed the effects of hard limiting on the performance of Applebaum-Howells processors. Their conclusions suggest that hard limiting has no harmful effect on the fundamental principle of operation of the adaptive processor because no information is lost by amplitude limiting one input of the correlator as long as the phase dependence is retained. This conclusion about hard limiters must be applied with caution. There are adaptive antenna applications for which the performance of a hard-limited processor is much worse than one without hard limiting. The problem with hard limiting arises when the correlation matrix of array signals has two or more eigenvalues with widely different magnitudes and when the processor has a sensitivity threshold. Multiple eigenvalues might arise, for example, from separate interference sources or from a single, broad-band source coupled with the frequency dispersion of the array, or from a combination of these effects. We show in this paper that the action of the hard-limiter is to suppress the smaller eigenvalues relative to the threshold level. The degree of small-eigenvalue suppression is dependent on the operating dynamic range of the processor. Specific examples of this effect relative to both array antennas and multiple beam antennas will be presented.

C2-3
1430

GRATING LOBE EFFECTS IN LINEAR ADAPTIVE RECEIVING ARRAYS

F. Kitson and L. Griffiths
Department of Electrical Engineering
University of Colorado
Boulder, Colorado 80309

Antenna array systems which use linear, equally-spaced elements may be subject to the influence of grating lobe phenomena. The effect of these lobes on conventionally beam-steered arrays is well known and usually results in an increased sidelobe level. The purpose of this paper is to describe the effects of grating lobes on adaptive arrays and to suggest methods for minimizing these effects.

The adaptive array processor uses subarray outputs which are derived from the linear array elements. In general, the number of adaptive subarrays is much less than the number of antenna elements. Because of this, there are many different ways in which the subarrays can be formed and the effect of grating lobes can be much more pronounced than for the conventional array. In this paper, we demonstrate that the procedure used to derive the subarrays greatly influences the effect of grating lobes on adaptive array performance. Several phase-center geometries are described (including minimum redundancy) and compared. It is shown that variations in subarray geometry also impact the convergence rate of adaptation. Specific subarray geometries which minimize the effects of grating lobes while simultaneously providing good convergence properties are presented.

C2-4
1520

SIMULTANEOUS BEAM FORMATION AND RANGE COMPRESSION WITH A SINGLE CHIRP FITLER:

B. R. Jean, Remote Sensing Center,
Texas A&M University, College Station,
Texas 77843

A multiple antenna beam formation technique is presented which provides for one dimensional beam formation processing and linear FM pulse compression using a single dispersive filter. Beam formation is accomplished by time multiplexing individual antenna array element receiver outputs. As shown by Johnson (M. A. Johnson, Proc. of IEEE, Vol. 56, No. 11, 1801-1811, 1968), time multiplexed elements provide frequency multiplexed beams. Beam demultiplexing may then be implemented using the chirp Z-transform (CZT) algorithm which requires premultiplication of the input signal by a chirp (linear FM) waveform, convolution with a chirp waveform of the opposite sense, and a final chirp post multiplication to remove a residual phase factor.

For a radar system employing linear FM pulse compression, the premultiplication required for the CZT algorithm is performed in the transmitter. Upon reception, the individual antenna element outputs are time multiplexed into a single channel and applied to the input of a dispersive filter whose impulse response is a linear FM signal of opposite sense to that of the transmitted signal and whose bandwidth is equal to the product of the number of beams times the rf bandwidth of the transmitted pulse. The individual beam outputs appear at the filter output in time sequence with the linear FM pulse compression having been accomplished simultaneously with beam formation.

C2-5 1550 SIGNAL PROCESSING FOR THE SEARCH FOR EXTRATERRESTRIAL INTELLIGENCE (SETI) PROGRAM,

J. Van Cleave, Communications Engineering Department, American Electronic Laboratories, Inc., Lansdale, PA

Efforts to receive a radio signal from an extraterrestrial source have recently reached the level of serious consideration. The signal parameters of center frequency, bandwidth and modulation are of course, unknown. The principal approach being taken involves the use of large aperture, radio-astronomy-like antenna arrays, combined with spectrum analyzer equipments having a large (10^9) number of frequency bins and instantaneous bandwidths of perhaps 300 MHz (R.E. Edelson and G.S. Levy, Conference Record 1976 National Telecommunications Conference 1.5-1 to 1.5-5).

The concept of these spectrum analyzers contains one very basic and heretofore argueable assumption: that the extraterrestrial intelligence is being communicated by use of sinusoids of high purity and very narrow bandwidth. This paper presents the characteristics of orthogonal waveform sets other than that of Fourier sinusoids; for example, the sets of Walsh-Hadamard and Harr. It is shown that Walsh Functions are by far the easiest orthogonal function set to recognize, in terms of hardware complexity; for example, a Fast Walsh Transform (FWT) equipment is at least ten times less complex than that of a Fast Fourier Transform (FFT), for the same analysis bandwidth and number of bins. Furthermore, the FWT technology is particularly well adapted to detect pulses of unknown time of arrival and width. Recent Walsh based developments in signal processing technology used for electronic warfare surveillance of unfriendly radars are potentially applicable for SETI. (J. Van Cleave, Defense Electronics, March 1979 p-77-84). We cannot afford to be prejudiced toward sinewaves for SETI.

It would appear that if another civilization is intelligent enough to beam out a signal advertising their technology, then they would choose a signal format that would be as easy as possible to detect from light years away, using equipment that is as uncomplicated as possible. This assumption seems to fit our earthborne problem of finding a SETI program that is affordable, hopefully being something lower in cost than the multibillion dollar Cyclops concept.

C2-6
1620

SIGNAL DESIGN FOR PULSE COMPRESSION RADAR:

M.C. Chandra Mouly and R.C. Pande, Centre for Systems and Devices, Indian Institute of Technology, Madras 600 036, INDIA

It is possible, at least in theory, to synthesize radar signals from a given ambiguity function. In practice, the phase structure of the ambiguity function is unimportant and thus is never specified. In general, a given ambiguity function will not correspond to realizable signals. A simpler and most-often sufficient method of radar signal design is that of synthesizing signals from specified autocorrelation functions, which are the cross-sections of the ambiguity function along the time axis. The specified autocorrelation functions, in most cases, will not yield realizable signals. In such cases, they must be approximated by realizable autocorrelation functions. In particular, synthesis from optimal autocorrelation functions results in unrealizable signal formats. The quasi-optimal autocorrelation functions, based on the Dolph-Chebyshev polynomials, however, yield realizable signals.

The design philosophy here is to start with an autocorrelation function with a specified side-lobe level and to use the quasi-optimal autocorrelation functions for its approximation. In this approach, either the amplitude envelope or the frequency law of the signal can be chosen and the other determined using the synthesis method. It is established that the "quasi-optimal autocorrelation function" approach yields a linear FM law for the Gaussian envelope case and a non-linear FM law for the rectangular pulse case, the former representing the "best" optimum (very low side-lobe level) and the latter the "worst" optimum (high side-lobe level). Hence it is concluded that for pulse compression radar, which incorporates the practical advantages of a wide pulse with the good resolution of a narrow pulse, the "optimum" signal is a linear FM pulse with a Gaussian envelope.

REMOTE SENSING OF THE EARTH'S SURFACE
Monday Afternoon, 5 Nov., UMC East Ballroom
Chairman: J. A. Kong, Department of Electrical Engineering and Computer Science and Research, Laboratory of Electronics, M.I.T., Cambridge, MA 02139

F1-1
1330 EMPIRICAL MODELS FOR SCATTERING AND EMISSION FROM SNOWPACK

Fawwaz T. Ulaby and William H. Stiles
University of Kansas Center for Research, Inc.
Remote Sensing Laboratory
Lawrence, Kansas 66045

Experimental measurements of the variation of the radar backscattering coefficient and microwave emissivity with snow wetness and snow water equivalent over a winter season are presented, and compared with predictions of semi-empirical scattering and emission models.

Through these models, the sensor penetration depths are evaluated as a function of snow wetness. Also, the effective contributions of the snowpack and underlying ground are examined as a function of the snow and ground parameters.

F1-2
1355

RADIATIVE TRANSFER THEORY FOR ACTIVE REMOTE SENSING OF HOMOGENEOUS LAYER CONTAINING RAYLEIGH SCATTERERS:

R. Shin, J. A. Kong, and L. Tsang,
Department of Electrical Engineering and Computer Science and Research Laboratory of Electronics,
Massachusetts Institute of Technology,
Cambridge, MA 02139

In the active remote sensing of low-loss and scattering dominant areas, the effect of volume scattering can be modelled by a homogeneous layer containing spherical scatterers. The radiative transfer theory with a Rayleigh scattering model is used to study the effect of volume scattering by obtaining backscattering cross sections through an iterative and a numerical approach. The iterative approach gives a closed form solution which is valid when the effect of scattering is small. The radiative transfer equations and the boundary conditions are first cast in the form of integral equations. Then an iterative process is applied to solve the integral equations to both first and second orders in albedo. The depolarization of the backscattered intensity is shown to be a second order effect. The numerical approach gives a solution which is valid for both small and large albedos. A Fourier series expansion in the aximuthal direction is used to eliminate the ϕ-dependence from the radiative transfer equations. Then, the set of equations without the ϕ-dependence is solved using the method of gaussian quadrature. The results have been used to match experimental data collected in snow fields as functions of frequency and incident angles.

F1-3
1420 RANDOM MEDIUM MODEL APPLIED TO ACTIVE AND PASSIVE MICROWAVE REMOTE SENSING OF EARTH TERRAIN:

J. A. Kong, M. Zuniga, T. Habashy, L. Tsang, R. Shin, and B. Djermakoye, Department of Electrical Engineering and Computer Science and Research Laboratory of Electronics, Massachusetts Institute of Technology, Cambridge, MA 02139

In active and passive microwave remote sensing of earth terrain, volume scattering effects due to terrain media can be accounted for with the model of a random medium characterized by a correlation function with a variance and vertical and horizontal correlation lengths. In applying the theoretical results to match experimental data, it is found that for snow-ice fields, the horizontal correlation length is usually larger than the vertical correlation length whereas for vegetation fields their relative sizes depend on the types of vegetation. In some snow fields when the horizontal correlation length is much larger than the vertical correlation length, the passive remote sensing data can also be matched with a laminar random-medium model where closed form analytical solutions for the brightness temperatures are available for easy computation. To account for diurnal change in snow-fields and different vegetation structures, three-layer random-media models are also used where the double resonance phenomenon can be identified. In the data matching exercise it is essential to characterize the same terrain field with one single set of parameters which can be used to match all remote sensing data plotted as functions of frequency, observation angle, and polarization. We illustrate such a match with both the active and passive data from a snow field by using the theoretical model of a three-layer random medium.

F1-4
1505 MEASUREMENT OF THE RADAR BACKSCATTER RESPONSE OF SEA ICE IN THE BEAUFORT SEA:

C.V. Delker, R.G. Onstott, R.K. Moore, J. Patel,
Remote Sensing Laboratory, University of Kansas,
Lawrence, KS 66045

The radar backscatter properties of sea ice were investigated by a team from the University of Kansas Remote Sensing Laboratory during the month of March 1979, off the Canadian coast near Tuktoyaktuk, N.W.T., Canada. Their investigation was part of the Beaufort Sea Ice Experiment segment of the Surveillance Satellite Project (SURSAT). Backscatter measurements were made using both a surface-based and a helicopter-borne scatterometer system. Thick first-year sea ice, thin first-year sea ice, brackish sea ice, and a fresh-water inland lake were investigated.

Results for the above categories of ice at microwave frequencies in the 8-18 GHz region indicate a strong correlation between radar scattering cross-section and the salinity of ice. The ice with the highest salt content, thin first-year sea ice, produced the greatest backscatter return. The ice with the lowest salt content, fresh inland lake ice, produced the lowest backscatter return.

Significant changes in the level of backscatter return were measured when significant modifications were made to the roughness of the snow cover of lake ice. Radar return was dramatically reduced when the snow surface was removed from the ice and significant increases in radar return were measured when the snow surface was roughened.

Support of the U.S. Office of Naval Research under Contract N00014-76-C-1105 is gratefully acknowledged.

F1-5
1530

DUAL FREQUENCY CORRELATION RADAR MEASUREMENTS OF THE ROUGHNESS AND SLOPE CHARACTERISTICS OF ICE PRESSURE RIDGES: J. W. Johnson and W. L. Jones, NASA Langley Research Center, Hampton, VA 23665; and D. E. Weissman, Hofstra University, Hempstead, NY 11550

A dual frequency radar scattering technique for detecting and measuring the surface characteristics of ice pressure ridges is being studied. This two frequency correlation technique has been applied successfully to the measurement of ocean wave height statistics and is currently being used to measure the height statistics and slope characteristics of ice ridges off the north slope of Alaska. Airborne dual frequency microwave scatterometer measurements at 13.9 GHz and 13.9 $-\Delta f$ GHz, where Δf_{max} = 15 mHz, were made during the Sea Ice Ridge Experiment (SIRE) of 1978. Measurements were made versus Δf with a 1.5^{o} pencil beam at both nadir and 50^{o} viewing angles. Scatterometer data taken over both isolated ridges and shear ridges is presented along with laser profilometer and photographic surface truth. The scatterometer response to both the small scale roughness properties and the large scale slope characteristics of ice ridges is demonstrated.

F1-6
1555

DEPOLARIZATION EFFECTS IN RADAR BACKSCATTER FROM VEGETATION LAYERS: A. J. Blanchard, Remote Sensing Center, Texas A&M University, College Station, TX 77483

The quantitative radar response from vegetation system has become one important factor in the application use of active microwave systems. In some applications, vegetation acts as a confusion factor in masking radar response to the soil interface. In other applications the vegetation/energy interaction is the principle response in vegetation discrimination using radar backscatter. Both polarized and depolarized response of EM energy from vegetation targets will be a function of system parameters (i.e., wavelength, polarization, incident angle, etc.) and vegetation parameters (i.e., density, geometric orientation, depth, etc.). Several attempts have been made to model radar backscatter from such inhomogenous volume targets. Very little work, however, has been done on the effects of finite vegetation layers and their overall contribution to backscatter measurements.

Some questions which still need to be answered are: 1) At what point does the vegetation layer mask the response due to the subsurface? and 2) What effect does the air/soil interface play in the electromagnetic response of a vegetation system. This paper presents the characteristics of an analytical model of radar backscatter from a simplified vegetation system shown in the accompanying figure. The scattering effects of the vegetation and the influence on the backscattering from the soil interface are taken into account.

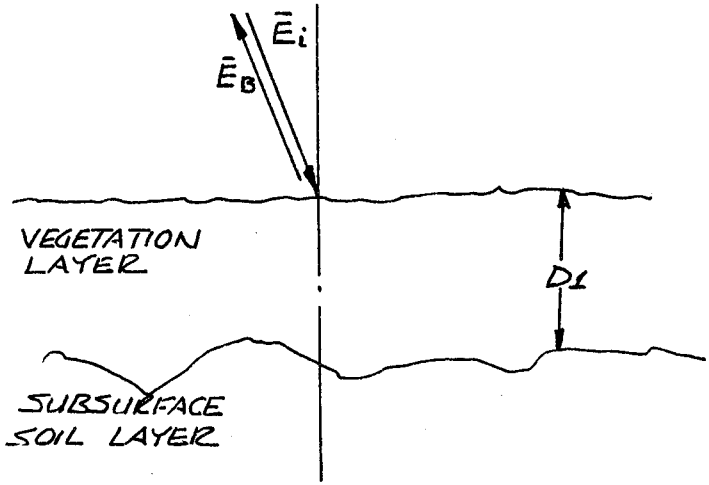

F1-7
1620

ANISOTROPIC EARTH TERRAIN FEATURES IN ACTIVE AND PASSIVE MICROWAVE REMOTE SENSING:

S. L. Chuang, Department of Electrical Engineering and Computer Science and Research Laboratory of Electronics, Massachusetts Institute of Technology, Cambridge, MA 02139;
R. Hevenor, US Army Engineer Topographic Laboratory, Ft. Belvoir, VA 22060;
J. A. Kong, Department of Electrical Engineering and Computer Science and Research Laboratory of Electronics, Massachusetts Institute of Technology, Cambridge, MA 02139

In both active and passive remote sensing of vegetation and soil moisture where the fields are plowed in row structures, experimental data exhibit anisotropic behavior as measured from different azimuthal directions. We model such earth terrain features with a random medium possessing different horizontal correlation lengths ℓ_x and ℓ_y with ℓ_z denoting the vertical correlation length. The radar backscattering cross-sections from active sensing are calculated with a Born series approximation and a first order renormalization method. The theoretical results for a correlation function which is exponential in z-direction and Gaussian in x and y directions, give rise, in addition to other anisotropic factors, the exponential factor $\exp[-k^2\ell_x^2\sin^2\theta\cos^2\phi]\exp[-k^2\ell_y^2\sin^2\theta\sin^2\phi]$, where k is the wavenumber and θ and ϕ are the polar and azimuthal angles in spherical coordinates. For passive remote sensing we calculate the brightness temperatures by solving the radiative transfer equations with an iterative approach. The theoretical results with various correlation functions are applied to matching the experimental data from vegetation fields.

IONOSPHERIC PREDICTIONS
Monday Afternoon, 5 Nov., UMC 159
Chairman: R. F. Donnelly, Space Environment Laboratory, NOAA, Boulder, CO 80303

G1-2 SOLAR-TERRESTRIAL PREDICTIONS
1330 R. F. Donnelly, Space Environment Lab., ERL
NOAA, Boulder, Colorado 80303

The major results of the International Solar-Terrestrial Predictions Workshop, held April 23-27, 1979, in Boulder, are reviewed. Predictions of the rest of a sunspot cycle, once the cycle is two years or more in progress, are fairly good. Such predictions have not improved greatly in the past decade. The main advance in long-term solar-activity predictions involves the work of Ohl in the U.S.S.R. and Brown in the U.K., who use geomagnetic activity during the decay of a sunspot cycle to predict the following sunspot cycle, i.e. predictions made just before or at the cycle minimum have improved. Unfortunately, longer term predictions, which are of great interest to system designers, are quite poor and have not improved much in the past decade. Short-term warnings of major geomagnetic storms have improved through technological advances in monitoring solar activity.

Solar-terrestrial predictions are now made not only for applications for ionosphere radio propagation but also for radiation hazards to manned space flight or high-altitude, high-latitude aircraft flights for satellite lifetime predictions, and for warnings of geomagnetic-activity induced disruptions to long-line electric power systems and geomagnetic survey programs. This broader scope of applications helps maintain solar-terrestrial disturbance monitoring and forecast services. On the other hand, these other applications do not share a direct interest in the radio propagation or ionospheric effects.

G1-2 THE STATUS OF SCINTILLATION MODELING
1400

E. J. Fremouw
Physical Dynamics, Inc.
Bellevue, WA 98009

Among the modern objectives of ionospheric prediction is a desired capability to provide prior assessment of transionospheric propagation conditions. For transionospheric systems susceptible to group delay and dispersion, TEC predictions are of prime interest. For other communication systems, the main need is for assessment of scintillation conditions. A true predictive capability for scintillation has not yet been achieved, but descriptive scintillation models can provide a vehicle for implementing predictions on the basis of either large data bases or fundamental understanding of mechanisms (or, most likely, a combination of the two). Such models provide both signal-statistical characterization of complex-signal (both phase and intensity) scintillation and information on temporal and spatial occurrence trends (morphology). Scintillation models currently available, and being improved, are based on three data types: (1) past scintillation observations, (2) spread-F and other ground-based ionospheric records, and (3) in-situ measurements of electron-density irregularity. This paper will summarize the present status of scintillation models based on the foregoing three types of data base and on current understanding of scintillation production mechanisms.

G1-3
1430 Review of Low- and Mid-Latitude E and F Region Predictions: Charles M. Rush, NTIA/ITS, Department of Commerce, Boulder, CO 80303

At the Solar-Terrestrial Predictions Workshop held in April, 1979, Working Group C3 addressed the issue of predicting and specifying the ionization structure in the low- and mid-latitude E and F regions. These regions have been the subject of intense study for over 50 years and their influence on the propagation of radio waves that are reflected from the ionosphere has been addressed for over 35 years. A level of sophistication has emerged in the ability to understand, specify, and predict the effects of the low- and mid-latitude E and F regions on radio propagation. Ionospheric physicists, propagation system operators and telecommunication policy-makers, however, are demanding an increased knowledge of the effects of these regions on propagation system performance. This results primarily from the fact that the level of current understanding with regard to the formation and variation of the ionosphere permits those individuals who must deal with the ionosphere to ask the right questions to ensure further understanding and exploitation of the ionosphere.

This paper reviews the current status of our ability to predict the low- and mid-latitude E and F regions as discussed in the Workshop.

G1-4 1530 PRESENT STATE OF IONOSPHERIC TIME DELAY PREDICTION

J. A. Klobuchar, Air Force Geophysics Laboratory, Hanscom AFB, MA 01731

This is a report on the conclusions of the working group on trans-ionospheric propagation predictions held at the STP workshop in Boulder in April 1979. Present capability to predict trans-ionospheric time delay, proportional to total electron content (TEC), is based largely on the ITS-78 empirical model of f0F2 developed over a decade ago by the Institute for Telecommunications Sciences (ITS-78, May 1969). Long term predictions, those significantly longer than 30 days in advance, suffer from inaccuracy in solar flux prediction, while short term, day to day, predictions suffer from unknown changes from the mean TEC behavior, which are mainly due to magnetic storms. While progress has been made in understanding how magnetic storms affect the F region, day to day improvements to monthly median TEC model predictions taking into account the effects of magnetic storms, have come about thus far, using empirical data on average storm behavior, rather than from physical theory.

The substantial majority of available TEC data is from the Faraday effect, where the contribution to total time delay from heights greater than $\approx$ 2000 km is not measureable. The few measurements of electron content above $\approx$ 2000 km come from ATS-6 beacon transmitter monitoring, mostly during solar minimum conditions, and show a $\approx$ 10-15% additional contribution to total time delay during the midday time period.

The only present method of making significant improvements over monthly average climatology in TEC predictions is through the use of an actual TEC measurement in the near time-space of where a prediction is required. The working group made several recommendations for further studies and for additional data sources to improve trans-ionospheric time delay predictions in the future.

G1-5
1600 The Application of Theoretical Modeling to Ionospheric Mapping and Predictions: David N. Anderson, NOAA/SEL, Department of Commerce, Boulder, CO 80303, and Charles M. Rush, NTIA/ITS, Department of Commerce, Boulder, CO 80303

Using the time-dependent continuity equation governing the distribution of ionization in the upper ionosphere, the diurnal variation of the maximum electron density, NmF2, at selected locations has been simulated. Observed values of NmF2 have been used to determine the parameters (particularly the neutral-air wind), necessary to reproduce the general features of the diurnal variation at a number of mid-latitude locations. These parameters were then used to determine NmF2 at other locations and the results compared to the actual observations in order to determine the accuracy afforded by use of theoretical considerations. The results were also compared with predictions of NmF2 obtained from various statistical and empirical models. The potential application of theoretical modeling as an aid in mapping the long-term and short-term variations of the F2 region in regions of the globe inaccessible to routine observations will be discussed in detail.

G1-6
1630 PREDICTION OF TRANSIONOSPHERIC SIGNAL TIME DELAYS USING CORRELATIVE TECHNIQUES:
H. SOICHER, COMMUNICATIONS SYSTEMS CENTER, US ARMY COMMUNICATIONS R&D COMMAND, FORT MONMOUTH, NJ 07703

ABSTRACT

Excess time delays of transionspheric radio signals introduce ranging errors in satellite-navigation and radar systems, which are directly proportional to the total electron content (TEC) along the propagation path. Correlations of TEC Values (based on linear regression analysis) at Fort Monmouth, N.J. (40.18°N, 74.06°W) and Richmond, FL (25.60°N, 80.40°W), as well as at Richmond, FL and Anchorage, AK (61.04°N, 149.75°W) were previously determined. The correlation analysis was performed at monthly and daily intervals for winter periods during the quiet phase of the solar cycle.

Average regression lines obtained by the analysis were then used to try to determine TEC at Richmond, assuming the availability of TEC in Fort Monmouth, and at Anchorage, assuming the availability of TEC at Richmond. In most cases, the "predicted" TEC was within one standard deviation of actual observed data for the former case, and within two standard deviations for the latter case.

LOW NOISE RECEIVERS - II
Monday Afternoon, 5 Nov., UMC 235
Chairman: A. R. Thompson, NRAO, Socorro, NM 87801

J2-1
1330 AN S-BAND NOISE ADDING RADIOMETER:

W.E. Blore and K.F. Tapping, Herzberg Institute of Astrophysics, National Research Council, Ottawa, Canada K1A OR6

A low-noise S-Band radiometer has been developed for radio astronomy. The low noise temperature of the receiver ($\sim$14° K) prohibited the use of Dicke switching techniques to minimise the effects of receiver gain-bandwidth fluctuations. A noise-adding radiometer system has been developed which uses high-power, solid state noise sources and integrated circuit analogue multipliers and dividers. The combination of these devices has made it possible to eliminate the sometimes troublesome gain control loop of the conventional noise adding radiometer technique while minimising the degradation of system noise temperature due to lossy front end components.

J2-2 1400 SIS QUASIPARTICLE TUNNEL JUNCTIONS AS LOW-NOISE MICROWAVE RECEIVERS:

T.M. Shen, P.L. Richards, R.Y. Chiao and M.J. Feldman, Department of Physics, University of California, Berkeley, California 94720 and R.E. Harris and F.L. Lloyd, National Bureau of Standards, Boulder, Colorado 80303.

The strong nonlinearity of the quasiparticle tunneling current in superconductor-insulator-superconductor (SIS) (Josephson) junctions near the full gap voltage $2\Delta/e$ can be used as an extremely sensitive microwave receiver in both the heterodyne mixing and the video detection modes of operation. Because of the absence of series (spreading) resistance, the junction capacitance can be resonated out by external microwave circuit elements. Consequently good performance is anticipated at short millimeter wavelengths.

The Pb(In, Au) alloy junctions used in our experiments were fabricated at NBS Boulder by two of the authors (R.E.H. and F.L.L.) using photoresist lift-off and RF sputter-oxidation techniques. The junction areas were about $2\mu m \times 2\mu m$ with normal impedances between 50 and 100Ω. Experiments to evaluate the use of these junctions as heterodyne mixers at 36 GHz yielded double-sideband conversion efficiencies of 0.36 and mixer noise temperatures as low as $T_M \lesssim 7K = 4\hbar\omega/k$. Photon-assisted tunneling effects were seen which indicate the approach to photon-noise limited operation. Measurements in the video mode at 36 GHz yielded a current responsivity of 3,500 A/W, which is within a factor of 2 of the quantum limited value $e/\hbar\omega$. The measured NEP of $2.6 \pm 0.8 \times 10^{-16} W/\sqrt{Hz}$ is the lowest value reported to date for a microwave video detector. The noise in the video device is limited by shot noise in the excess current near the full gap voltage. These experimental results will be compared with both standard classical analysis and with photon-assisted tunneling theory.

Higher conversion efficiencies in the heterodyne mode and lower noise in the video mode of operation can in principle be achieved by using other types of SIS tunnel junctions with lower leakage current and a sharper corner on the I-V curve. Linear arrays of Sn junctions have been fabricated by two of the authors (R.Y.C. and M.J.F.) using thermal oxidation techniques which have a very sharp corner on the I-V curve which closely approaches that of an ideal switch. Mixing experiments using series arrays of 50 Sn junctions with array impendances of 10 to 50Ω have shown strong quantum effects at 36 GHz. Theoretical analysis indicates that, in this strong quantum limit, the effects of a nonlinear "quantum" capacitence play an important role in the performance of the mixer. The performance of the SIS junction as a heterodyne mixer in the "ideal switch" limit will be discussed from both experimental and theoretical viewpoints.

J2-3
1430

PERFORMANCE OF A QUASI-PARTICLE PHOTON ASSISTED TUNNELING RECEIVER AT 115 GHz:

D.P. Woody*, T.G. Phillips† and G.J. Dolan, Bell Telephone Laboratory, Murray Hill, N.J. 07974.
*Permanent Address, Owens Valley Radio Observatory C.I.T., Pasadena, CA 91125, supported under NSF contract AST 76-13334. †Staff member of Owens Valley Radio Observatory.

A new type of cooled low noise receiver has been developed and tested on the OVRO 10m dish. The receiver utilized a small area ($\lesssim .5$ um^2) thin film superconductor-insulator-superconductor tunnel junction as a resistive mixer (G.J. Dolan, T.G. Phillips, and D.P. Woody, Appl. Phys. Lett., 34, 347-349, 1979; P.L. Richards et al., Appl. Phys. Lett., 34, 345-347, 1979). The I-V curve of the junction with and without LO power is shown below. The photon assisted tunneling steps induced in the quasi-particle current are apparent. The strong effect this quantum mechanical phenomenon had on the mixer performance is seen in the P_{IF} vs. V curve. The optimum performance was obtained when the Quasi-Particle Photon Assisted Tunneling (QPPAT) mixer was biased near the middle of the first step below the 2Δ energy gap. The total receiver noise temperature was 500K (SSB). The noise was dominated by the cooled 4 GHz GaAs FET IF amplifiers which had a noise temperature of $\simeq$ 60K. The mixer had a conversion efficiency of $\simeq$ -8 db and a noise temperature of $\approx$85K (SSB).

The QPPAT mixer proved to be a viable alternative to other cooled receivers. It didn't suffer the saturation and noise problems attendant with Josephson effect devices and required 50 db less LO power than Schottky diodes. The receiver has not yet been optimized, and significant improvements can be made. In particular, the use of cooled 1.4 GHz GaAs FET IF amplifiers will decrease the noise temperature by a factor of three, and improvements in the RF match will further improve the performance.

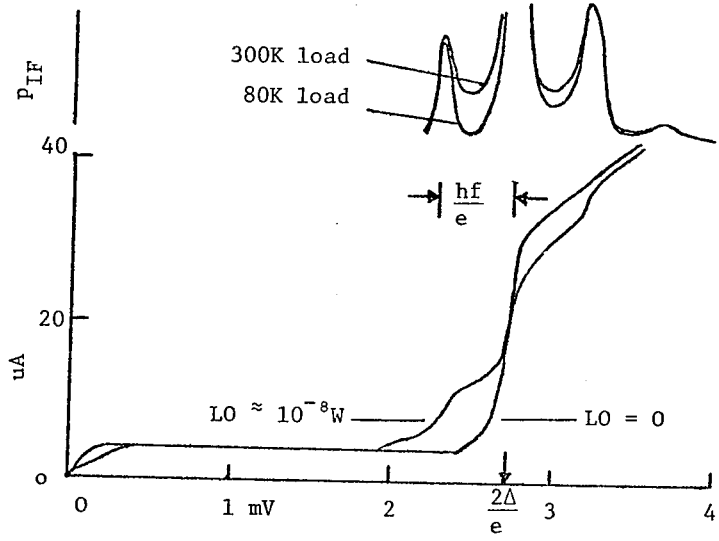

J2-4 VERY LOW NOISE 70-115 GHZ MOTT-DIODE COOLED MIXER

1520 S. Weinreb, Nat'l. Radio Astronomy Observatory, Charlottesville, Va. 22903 and R.J. Mattauch, E.E. Dept., U. of Va., Charlottesville, Va. 22903

Recent developments in semiconductor diode technology have resulted in a cryogenically-cooled (12°K) millimeter-wave mixer with T_{MXR} = 75°K and conversion loss, L = 4, at 91 Ghz. These values give a single-sideband receiver temperature, $T_{RCVR} = T_{MXR} + LT_{IF}$ of 155°K assuming a cooled-paramp IF amplifier with T_{IF} = 20°K. These figures neglect noise temperature contributions due to LO diplexing, polarization diplexing, feed loss, and atmosphere. However, with low-loss quasi-optical diplexers and a low water-vapor site, system temperatures of ∿ 250°K are expected.

Measured performance as a function of local oscillator power is shown in the figure below. Minimum T_{MXR} results at a surprisingly-low LO power of 18μW and high forward bias voltage of 950mV. The figure also shows T_{EQ} which is the temperature of an attenuator having identical noise temperature as the mixer. This quantity correlates well with the noise temperature of the DC biased (no LO) diode at the same DC current. The increase in T_{EQ} with DC current is believed due to hot-electron and intervalley scattering noise in gallium-arsenide. Measured values of T_{MXR} at 75 Ghz and 110.5 Ghz are 75°K and 180°K, respectively.

The diodes used in this mixer were fabricated at the semiconductor laborabory at U. of Virginia and had 2μ diameter anodes on 4 x $10^{16}/cm^3$ sulphur-doped epitaxial gallium-arsenide supplied by Plessey and anodically etched to an optimum thickness. Improved cooled-mixer performanced using thin, low-doped diodes has also been reported by Linke, Schneider, and Cho (IEEE Trans. MTT-26, #12, Dec. 1978, pp. 935-938) and by Keen, Haas, and Perchtold (Elect. Letters, 14, Dec. 7, 1978, pp. 825-826).

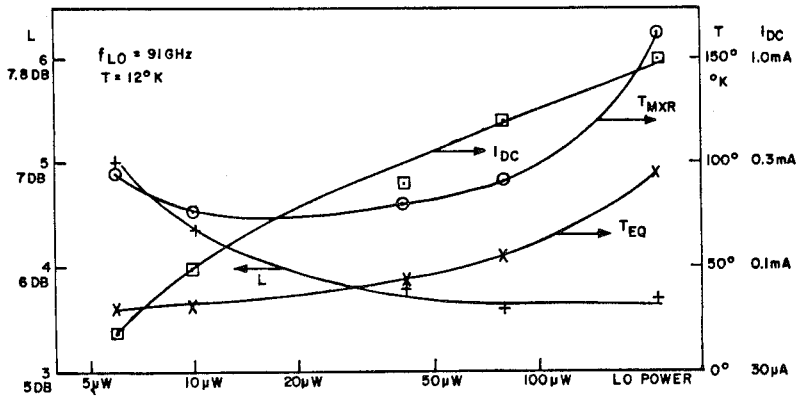

J2-5
1550

WIDEBAND - TUNABLE JOSEPHSON MIXER RECEIVER FOR SPECTRAL LINE OBSERVATIONS AROUND λ=1 MM

J.Edrich, University of Denver,Denver, CO 80208

Previous laboratory studies with a Josephson mixer receiver with batch cooling, adjustable point contacts and a narrow X-band if maser yielded a noise temperature of less than 1500 K with a tuning range of 100 GHz around 270 GHz (J.Edrich, D.B.Sullivan and D.G.McDonald, IEEE Trans.MTT, 25, 476-479,77). Further developments of this system have led to a permanent, temperature-cyclable Josephson junction followed by a more broadbanded C-band maser, and cooled by a closed-cycle refrigerator (J.Edrich, Dig. URSI Meet., 173, Jan. 1978).

Recently, this system has been improved by replacing the large and complex if maser by a more reliable and compact cooled GaAs FET if amplifier; it contains hybrids for better match, and is centered at the new if frequency of 1.3 GHz. As a result of these and other modifications the magnetic shielding problems associated with the large pump and dc magnetic fields of the maser have been eliminated. The closed-cycle refrigerator can now also be operated at higher temperatures ($4K < T < 9K$); this results in a more stable and reliable field operation. Details of this improved system including the tuning of the Josephson mixer, the cooled Schottky barrier multiplier, cooled FET and the LO injection are described.

Preliminary noise measurements indicate a DSB noise temperature of less than 800 K. The system is presently being integrated into a telescope receiver for wideband spectral line observations.

TUESDAY MORNING, 6 NOV., 0830-1200

COMBINED SESSION

UMC Center Ballroom
Chairman: W. E. Gordon, Rice University, Houston, TX

In Recognition of Henry G. Booker

CS-1
0845 *RADAR PROBING OF ELECTROJET PLASMA INSTABILITIES:*
D.T. Farley, School of Electrical Engineering, Cornell University, Ithaca, New York 14853

Scattering measurements using VHF radars provide a powerful tool for the remote probing of ionospheric plasma instabilities. A particular Fourier component of the spatial wave spectrum is selected by the scattering process, and the phase velocity distribution of these waves can be found from the Doppler shifts of the received scattered signals. A program of radar investigations of the instabilities in the equatorial E region electrojet has been carried out at the Jicamarca Radio Observatory in Peru since the early 1960's.

Two categories of irregularities have been identified and partially explained. Type 1 irregularities appear when the electrojet is strong, with an electron drift velocity exceeding the acoustic velocity, and their Doppler spectra are sharply peaked at a frequency corresponding to the acoustic velocity, a result which is not well explained by linear instability theory. Type 2 irregularities have a broad spectrum with a mean Doppler velocity proportional to the electron drift velocity, in agreement with linear theory, but are observed at shorter wavelengths than linear theory predicts. A nonlinear two-dimensional turbulent cascade of energy in k-space appears to be of vital importance in explaining the radar data. Both types of irregularities are strongly aligned with the magnetic field but differ in their distribution in the plane perpendicular to $\underline{B}$. Type 1 irregularities are strongest when traveling horizontally, while type 2 irregularities have an isotropic cross section distribution, a result of the turbulent cascade process. The cascade has some effect on type 1 also; without it vertically propagating type 1 waves could not be explained. Not only has this curbulence been directly observed with radar, it has also been successfully modeled in numerical simulations which have accurately reproduced some of the radar results.

Most recently we have used radar interferometry to study the electrojet instabilities. Signals are received separately on the east and west quarters of the large 50MHz Jicamarca array. By forming the complex cross spectrum of the two received signals, one can determine the size and angular position of individual localized scattering regions within the scattering volume. The temporal behavior of these indicate lifetimes and horizontal velocities as a function of altitude. Nighttime vertical observations show that type 1 echoes having

positive and negative Doppler shifts come from different portions of the scattering volume and are observed even when the apparent horizontal velocity of the scattering centers is substantially less than the acoustic velocity.

CS-2
0915 ACOUSTIC GRAVITY WAVES, TRAVELLING IONOSPHERIC DISTURBANCES, SPREAD F AND IONOSPHERIC SCINTILLATION: Henry G. Booker, University of California, San Diego, La Jolla, California 92093*

In the aggregate, acoustic gravity waves in the F region constitute a spectrum of geophysical noise extending from the frequencies involved in diurnal variations up to the Brunt-Väisälä buoyancy frequency. They drive a roughly uniform power spectrum of travelling ionospheric disturbances (TIDs) with vertical scales of the order of the atmospheric scale height H and with horizontal scales extending from the radius of the earth down to H. It has been known since the 1950's that this permits multiple normals onto the F region from an ionosonde, thereby creating the multiple-trace type of spread F on ionograms. At shorter scales the spectrum of TIDs decreases in strength and, below the mean free path of the neutral atmosphere, creates a spectrum of plasma turbulence aligned along the earth's magnetic field. Progressively shorter scales are responsible for phase scintillation, for amplitude scintillation and for blur-type spread F on ionograms. A weak extension of the spectrum to scales less than the ion gyroradius is responsible for spread F and transequatorial propagation in the VHF band. Under evening conditions in equatorial regions a band of TIDs with wavelengths of the order of 600 km can, at times, have a phase velocity that matches the drift velocity of the plasma (Röttger 1978). This band of TIDs is then amplified until it breaks (Klostermeyer 1978). The associated explosive increase in plasma turbulence creates the plume phenomenon discovered by Woodman and La Hoz (1976).

* Supported by NSF Grant ATM 78-02625

CS-3 0945 REVIEW OF SELECTED SCIENTIFIC ACHIEVEMENTS OF DR. HENRY BOOKER IN THE 1960's and 1970's:

C. M. Crain, The Rand Corporation, Santa Monica, California 90406

During the quarter century prior to 1960 Henry Booker had advanced radio science by forty or more major fundamental publications covering a variety of subjects including the general properties of the formulae of the magneto-ionic theory and their application to the ionosphere; mode theory of tropospheric, stratospheric, ionospheric and auroral scatter; radio star scintillation theory; application of impedance concepts to radiation and propagation problems; etc. This paper attempts to review more recent work and answer the question "What has Henry Booker done lately for radio science?" Although much of this work is in the literature many important contributions are not as widely known and appreciated. A brief review will be given of his pioneering work on advancing the understanding of certain man-made ionospheric effects including those due to missile transit and nuclear detonations; on ELF propagation under natural and disturbed conditions; on the role of ions in longwave propagation including easily applied means for determining reflection heights and transmission properties; on ionospheric transmission properties from 1 Hz to GHz; on HF antenna siting for obtaining very low angle radiation, etc. Also, the paper will outline the more significant national scientific committee work of Dr. Booker in recent years. Finally, his work dealing with the international organization of radio science will be reviewed.

CS-4 VIGNETTE OF GUIDED WAVES RESEARCH

1100 James R. Wait, ERL/NOAA
U.S. Department of Commerce,
Boulder, Colorado 80303

The guiding of electromagnetic waves in naturally occurring ducts in the earth's environment is exploited in telecommunications and remote sensing. In fact, this subject is one of the non-eroding cornerstones upon which URSI is based.

The primordial concept that the earth's surface and the lower edge of the ionosphere form a waveguide can be traced to Oliver Heaviside, G.N. Watson and others in the early part of the century. The role of tropospheric ducts in enhancing microwave transmission was actually suggested by Marconi in the 1930s, who is better known for his long wave trans-Atlantic experiment in 1901.

The subject of guided radio waves has matured since those early days. Probably the most notable achievement was made by Booker and Walkinshaw who developed the first recognizable normal mode theory of tropospheric radio propagation in the 1940s. The renaissance of long radio waves (i.e., VLF) in the 1950s led to various basic formulations of the earth-ionospheric waveguide that were relevant to global communication and navigation systems. Many parallel developments have been made by workers in underwater sound transmission that accompanied the technical development of SONAR and it's later refinements. In this same time period, the Soviets were not idle. Fock, Weinstein, Belkina and others made a number of important theoretical contributions, although these restricted attention to laterally uniform structures. Most recently the controlled guidance in optical fibers has been recognized as the basis of a whole new field of telecommunication science. This subject appears to have developed almost independently of closely related and much earlier work on radio propagation.

The theory of waveguiding in realistic models of both naturally occurring and artificial ducts is exceedingly difficult. Many of the groups working in parallel and related fields have been grappling with new analytical approaches that have not always been successful, e.g., the rigorous formulations lack physical insight and are not useful while the engineering approaches are usually empirical and lack credibility in a general sense. Actually, the bulk of the theoretical work has dealt with uniform structures in the sense that lateral variations of the cross sections have not been accounted for except in some *ad hoc* slowly varying sense; thus mode conversion is ignored or incompletely accounted for. Also the systematic interchangeability of ray representations and waveguide mode formulations has never been fully developed. A notable exception here is the fine theoretical achievements of L.B. Felsen and colleagues on hybrid ray/mode representations.

Here we will give a laconic review of recent analytical developments of guided wave theory and related studies in

surface waves. No claim for completeness is made, but an effort is put forth to show some of the links between current guided wave research in underwater sound, radio propagation, radio oceanography, tunnel transmission and optical fibers. It is intended this review will set the scene for one or more Commission B sessions on guided waves that are scheduled for Wednesday and Thursday morning . These will be concluded on Thursday afternoon by a workshop formed mainly by the special session speakers. Contributions from other interested persons are welcome, but they should contact the workshop co-chairmen (J.R. Wait and D.C. Chang) as soon as possible.

CS-5
1130 THE COSMIC MICROWAVE BACKGROUND RADIATION

R. W. Wilson, Bell Laboratories, Crawford Hill Laboratory, Box 400, Holmdel, N. J. 07733

The experiments and theory leading to the discovery of the CMBR will be described. Our present knowledge of its spectrum and isotropy will be summarized and the cosmological implications discussed.

TUESDAY AFTERNOON, 6 NOV., 1330-1700

EMI/EMC, MEASUREMENTS
AND TECHNIQUES
Commissions A and E, Session 1, UMC 158
Chairman and Organizer: John W. Adams, NBS, Boulder, CO 80303

A1/E1-1
1330

PERFORMING ELECTROMAGNETIC COMPATIBILITY MEASUREMENTS USING A TEM CELL:

M.L. Crawford, EM Fields Division,
Nat. Bureau of Stds., Boulder, CO 80302

Transverse electromagnetic (TEM) cells have shown great potential for performing electromagnetic interference/electromagnetic compatibility (EMI/EMC) measurements with substantially improved ease, versatility and accuracy (M.L. Crawford and J.L. Workman, "Using a TEM Cell for EMC Measurements of Electronic Equipment", NBS Technical Note 1013, April 1979).

The TEM cell consists of a section of rectangular, coaxial transmission line (figure 1) that serves as a broadband, linear phase and amplitude transducer (in the sense that it converts a TEM field to rf voltage or rf voltage to a TEM field) either to establish standard electromagnetic (EM) fields for susceptibility testing of electronic equipment or to detect radiated emanations from electronic equipment. The cell is also a shielded enclosure, thus providing electrical isolation for the tests being performed; and since it is a transducer, it eliminates the use of conventional antennas with their inherent measurement limitations.

This presentation will include a brief discussion of the TEM cell EMI/EMC measurement procedures and the factors which influnce the radiated measurement results. These include: defining the equipment under test (EUT), simulating EUT operation conditions, establishing the exposure field or detecting the radiated emanation from the EUT, evaluating EUT/test field/transducer/source interactions, accessing the EUT. and correlation of the measurement results with

open-field measurements or with operational conditions.

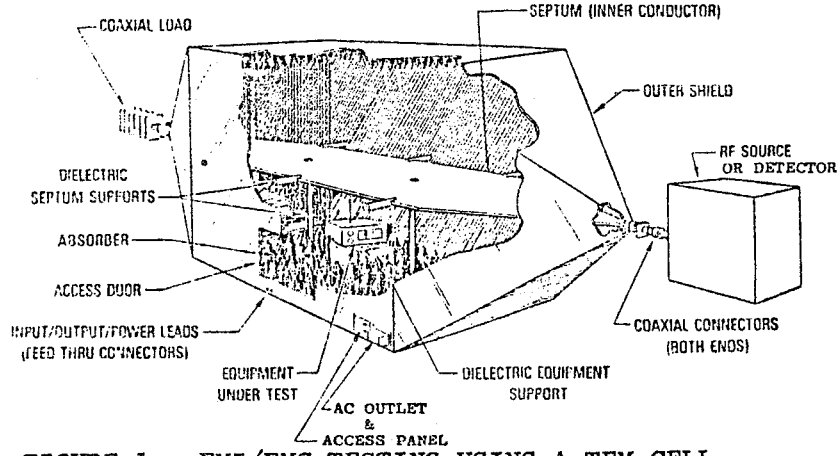

FIGURE 1. EMI/EMC TESTING USING A TEM CELL.

A1/E1-2
1400

A Whole Vehicle Electromagnetic Susceptibility Test Facility:

Don W. Briggs, Manager, EMC Test Facility,
General Motors Proving Ground,
Milford, Michigan 48042

This presentation will discuss the shielded, anechoic chambers at General Motors Proving Ground and the benefits and problems associated with the use of this type of test facility for conducting susceptibility tests. Discussion of the special problems associated with whole system testing of automobiles will be presented, such as the need for vehicle cooling, removal of exhaust fumes, and simulating accelerations and constant speed operations. Methods of obtaining knowledge about the field distributions around the vehicle inside the chamber and performance aspects of the vehicle and its on-board electronic systems will be discussed.

A1/E1-3 1430 ELECTROMAGNETIC INTERFERENCE (EMI) RADIATIVE MEASUREMENTS FOR AUTOMOTIVE APPLICATIONS: John W. Adams, National Bureau of Standards, Electromagnetic Fields Division, Boulder, CO 80303

This report describes the measured results of the electromagnetic (EM) environment encountered by three different-sized vehicles exposed to a selection of CB and mobile radio transmitters and broadcast stations. The vehicle in these situations is immersed in the near field of the radiating signals and the measured data is near-field data. This report gives measured data of electric and magnetic fields measured independently. The purpose of the report is to identify the EM environmental conditions under different circumstances in order to estimate EMC testing criteria for vehicles and their electronic systems.

A1/E1-4 1520 EMC OF PASSIVE RESTRAINT SYSTEMS (PRS): Harold E. Taggart, National Bureau of Standards, Electromagnetic Fields Division, Boulder, CO 80303

The use of electrical initiators for PRS (air bags), when the EM environment around vehicles cannot be controlled, poses severe EMC design requirements for the PRS systems. This in turn poses severe EMC measurment requirements.

This presentation will cover some EMC measurement techniques NBS is developing for the Department of Transportation, National Highway Traffic Safety Administration, and the automobile industry. It covers measurement of firing characteristics of initiators, such as current, thermal time constants, and frequency and wave shape dependence. It will also cover some EM environmental data around vehicles; more complete data will be available later.

A1/E1-5 LOW FREQUENCY MAGNETIC NOISE IN URBAN ENVIRONMENTS
1550

T. J. Beahn and P. A. McGrath
Laboratory for Physical Sciences, 4928 College Avenue, College Park, MD 20740

Measurements have been made of power spectra and statistics of low frequency (10 Hz to 1 kHz) magnetic noise observed in urban locations. Calibrated, portable instrumentation including 15 bit A/D, spectrum analyzer and tape recorder was transported to a number of urban locations, both inside and outside of buildings and near and remote from local power sources. Data was recorded for various conditions of bandwidth, polarization, etc.

The results to date show that the noise includes the expected strong CW components at power line harmonics as well as other line spectra from various sources, some of which could be identified. The spectrum of 60 Hz and its harmonics is typically 40 to 60 dB above a broadband noise floor, whose power spectral density decreases rapidly with increasing frequency. The broadband noise floor between line spectrum peaks was observed typically to be 20 dB or more above values at the same frequency measured in rural locations. Near 100 Hz the spectral density of H field noise was roughly 35 dB below $1\gamma/\sqrt{Hz}$, a value which did not change greatly, even for widely separated locations.

Sources of the noise and predicted maximum values to be expected in various environments will be discussed.

A1/E1-6 A NOVEL WINDOW FOR HARMONIC ANALYSIS
1620

F. I. Tseng, Electrical Engineering Department,
Rochester Institute of Technology
Rochester, New York 14623

This paper presents a new window design technique and discusses its effect on the detection of harmonic signals in the presence of nearby strong harmonic interference. The design yields a set of weightings whose frequency window has a near-in sidelobe level of any specified value and a sidelobe envelope of any asymptotic decay rate. Furthermore, it creates a wide deep dip at a given frequency, which is particularly useful in detecting and estimating the parameters of a weak tone in the presence of nearby strong tones.

Contrary to the conventional approach of initially specifying the continuous weighting, the new design technique starts with constructing the frequency window which meets the specifications and then employs the Fast Fourier Transform to compute the discrete weightings. No iterative sampling or perturbation procedure is required. A comparison of these with well-know windows in terms of beamwidth, near-in sidelobe, decay rate and processing gain is given. An example demonstrates the effectiveness of the new window in resolving closely spaced harmonic signals with large dynamic range.

Commissions B and J Session 3

LARGE ARRAYS AND RELATED TECHNIOUES
Tuesday Afternoon, 6 Nov., UMC 305
Chairman and Organizer: B. B. Steinberg, Moore School of Electrical Engineering, University of Pennsylvania, Philadelphia, PA 19104

B3/J3-1 1330 THE VLA: A. R. Thompson, National Radio Astronomy Observatory, Socorro, NM 87801

The Very Large Array is an instrument designed to produce maps of astronomical objects at centimeter and decimeter wavelengths, with angular resolution as fine as a few tenths of an arcsecond. Twenty-seven fully steerable antennas are arrayed in a three armed configuration, with the most distant ones 21 km from the center. Signals from the antennas are combined in pairs to form a complex visibility function from which the sky brightness distribution can be obtained by Fourier transformation.

The large size of the array results in numerous technical problems, some of which call for special solutions. To achieve the full sensitivity for objects with a large range of angular sizes, the antennas are movable to enable the resolution of the array to be varied. To bring the broadband IF signals to a common processing point low-loss, TE_{01}-mode waveguide is used. Calibration techniques are incorporated which continously monitor phase changes in the waveguide path length and the overall system gain. Variable time delays of up to 160 microseconds are used to compensate for the different transmission paths in space and in the waveguide. These are implemented digitally to avoid the bandpass variation encountered with analog delays. The reliability of the electronics is also a particularly important consideration in such a large system.

The high data collection rate imposes special requirements on both reduction and archiving facilities. Other data reduction considerations peculiar to the VLA include taking into account the deviation of the antenna baselines from a plane when large fields of view are synthesised. Also, the use of a phase-closure technique can reduce the effects of atmospheric phase instability over the array.

B3/J3-2
1400

HYBRID MAPPING OF RADIO SOURCES FROM VLBI DATA

A.C.S. Readhead, Owens Valley Radio Observatory
California Institute of Technology,
Pasadena, California 91125

Roughly half the extragalactic radio sources detected in high frequency radio surveys are very compact (<< 1 arc second). The structure of these objects can therefore only be studied by very long baseline interferometry.

Until fairly recently it was possible to make only crude models of these objects, because a small number (≤ 3) of telescopes was used, and only the visibility amplitude data were recovered. However observations are now made routinely with networks of four or more telescopes, and the visibility phase data are determined by use of the closure phase. Coupled with the convenience of operation of the new CIT/JPL processor, these advances have enabled us to make maps of radio sources with a resolution of milliarcsecond for the first time.

The sample of objects mapped so far is small, but a pattern is emerging which is of great importance to our understanding of these powerful sources: nearly all compact sources mapped thus far are found to consist of a bright flat spectrum core, and a one-sided steep spectrum jet.

B3/J3-3 LARGE SELF-COHERING ANTENNA ARRAYS
1430

C. Nelson Dorny, Valley Forge Research Center
The Moore School of Electrical Engineering
University of Pennsylvania
Philadelphia, Pennsylvania 19104

The staff of the Valley Forge Research Center is presently developing techniques suitable for cohering and using microwave arrays which are distributed thinly, randomly, and conformally over the surface of an aircraft, or which are distributed among several aircraft. The intent of the work is to provide very large apertures for the purpose of obtaining high resolution microwave images. Angular resolutions finer than 10^{-4} rad are anticipated. Such self-cohering systems must deal with uncertainty and motion in the relative positions of the array elements.

Techniques for self-cohering large poorly surveyed arrays have been proposed by Steinberg (e.g., Journal of the Franklin Institute, Vol. 296, 415-432, December 1973) and Dorny (e.g., IEEE Trans. A&P, November 1978). The techniques use signals from beacons or reflections from strong scatterers to assist in the formation of beams. The techniques differ in the requirements on the number of beacons, the accuracy of the beacon location information, the means of communication among the array elements, and in the field of view of the cohered system.

Present efforts are focused on loosening the requirements (geometrical restrictions, etc.) on both the beacons and the array elements, on the use of clutter returns as beacon signals, on extensions of the self-cohering techniques to synthetic aperture systems, and on exploration of properties of arrays large enough that the focal point is very near or within the array. Recent work will be summarized and related to previous self-cohering technology.

B3/J3-4 LARGE OPTICAL ARRAYS
1520

R.R. Shannon, Optical Sciences Center, University of Arizona, Tucson, Arizona 85721

Large diameter array telescopes for use in the optical wavelength region have always offered the possibility of improved light collection and resolution. Practical problems of atmospheric turbulence and environmental effects on large optical components and large structures have limited the application of the array concept. Present technology uses the approach of adaptive optics and speckle processing to minimize atmospheric effects. The mechanical problems are reduced by application of active structure control, and the production of large aspheric optical components has been aided by new methods of fabrication and test.

This paper will discuss the state-of-the-art of large telescope engineering, principally referring to the newly completed Multiple Mirror Telescope.

The tolerances required for a usable optical array will be presented and some methods for achieving these tolerances described. The tolerances are seen to depend on the aperture shape and dilution. An optical design configuration which can be used to provide phasing across a large field, and some separation of the tolerable errors will be presented. Some performance predictions based on present day technology will be made.

B3/J3-5 DYNAMIC BEAMFORMING OF A RANDOM ACOUSTIC
1550 ARRAY

W.S. Hodgkiss and V.C. Anderson, Marine Physical Laboratory, Scripps Institution of Oceanography, San Diego, CA 92152

Design trade-offs in a programmable time-delay-and-sum digital beamformer built by MPL will be discussed. This dynamic beamformer permits the incorporation of slow changes in element positions and/or beam steering direction while the beamformer carries out the real-time formation of 1300 beams from 32 input sensors. The sensors are distributed in a random but known manner over an aperture diameter of up to 800 λ (at 400 Hz).

Next, the implications of such a large output data rate on performing data analysis will be considered. Specifically, attention will be paid to computation, storage, and display of spectral information.

The paper concludes with a discussion on performance measures of random array beamforming. Here the focus will be on bearing response, array signal gain, and array gain.

ELECTROMAGNETIC THEORY
Tuesday Afternoon, Nov. 6, UMC West Ballroom
Chairman: R. Harrington, ECE, Syracuse University, Syracuse, NY 13210

B4-1 1330 AN APPLICATION OF ISOPERIMETRIC INEQUALITIES TO THE CALCULATION OF EQUIVALENT RADII:

D. L. Jaggard, Department of Electrical Engineering, University of Utah, Salt Lake City, Utah 84112

The concept of equivalent radii, which was apparently first introduced by Hallén [*Nova Acta Regiae Soc. Sci. Upsaliensis*, Ser. IV, II, 1-44 (1938)], has been useful in the solution of antenna and scattering problems which involve electrically thin wires of arbitrary cross section. Generally, the solution is first calculated for circular wires of an arbitrary radius and this radius is then replaced by the equivalent radius of a noncircular wire. In this way the original problem is reduced to that of finding the equivalent radius.

Here we bound and approximate the equivalent radius through the use of certain isoperimetric inequalities [see, e.g., Pólya and Szegö, *Isoperimetric Inequalities in Mathematical Physics*, Princeton University Press, Princeton (1951)]. From these considerations we are led to the following inequality for the equivalent radius r_{eq}:

$$\sqrt{A/\pi} \leq r_{eq} \leq P/2\pi$$

where A is the area of the wire cross section and P is the perimeter. Taking the arithmetic mean of the above bounds, we find an approximation to the equivalent radius. The bounds, approximation, and exact value for the equivalent radius of a rectangle are shown in the figure. It appears that in some cases the simple approximation found here is more accurate than the lengthy expression given by Uda and Mushiake [*Yagi-Uda Antenna*, Tohoku University, Sendai, Japan (1954)].

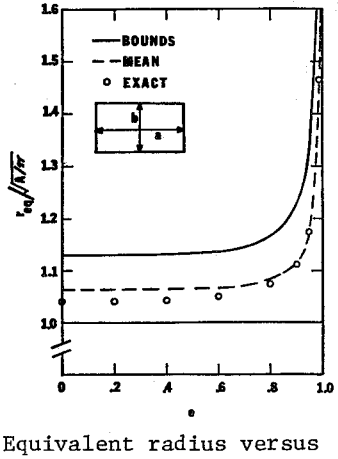

Equivalent radius versus eccentricity $e = \sqrt{1 - b^2/a^2}$ for a rectangle with sides a and b and area A = ab.

Applications of these concepts to scattering and shielding are given. In particular we note that for a given wire length and volume, the circular wire possesses the smallest equivalent radius of any wire with a given cross-sectional area.

B4-2
1350

A NEW LOOK AT THE EQUIVALENT ELECTROMAGNETIC PROPERTIES OF A THIN WIRE CIRCULAR CAGE BASED ON BOUNDARY CONNECTION SUPERMATRICES: Korada R. Umashankar and Carl E. Baum, Air Force Weapons Lab./ELT, Kirtland Air Force Base, Albuquerque, New Mexico 87117

The electromagnetic equivalence of an infinitely long loaded circular cylindrical wire cage scatterer with respect to a loaded hollow cylindrical scatterer is studied based on boundary connection supermatrices (BCS). The BCS representation of the transverse fields for the hollow cylindrical scatterer and for the wire cage scatterer points out a new and more proper interpretation of the electromagnetic scattering equivalence.

The question of electromagnetic equivalence of loaded circular cylindrical thin wire cages, used in hybrid and other electromagnetic pulse (EMP) simulators, as compared to a loaded hollow circular cylinder was investigated previously (K.R. Umashankar and C.E. Baum, Equivalent Electromagnetic Properties of a Concentric Wire Cage as Compared to a Circular Cylinder, Sensor and Simulation Note 252, March 1979) treating them as boundary value antenna problems. A detailed analysis was discussed for the infinitely long canonical wire antenna geometries with uniform impedance loading function. An electromagnetic equivalence criterion was also established by comparing the radiated far fields of the circular wire cage as against the radiated far fields of the hollow circular cylinder yielding equivalent wire cage parameters. It was shown that both the equivalent wire cage radius and the equivalent loading impedance function are in fact principally dependent on the geometrical parameters of the wire cage in the quasi-static limit, but in general are functions of the complex frequency and the far-field polar angular variation.

In this paper the canonical infinitely long wire geometries including the case of a circular hollow cylinder are analyzed, but as scatterers with an external incident plane wave excitation with specified polarization and incidence angles. Further a new approach to the study of equivalent electromagnetic properties of the loaded circular wire cage is given based on the BCS. The BCS form is obtained both for the hollow circular cylinder and the complex circular wire cage geometry. The elements of the BCS turn out to be independent of the incidence angles and mainly depend on the physical parameters of the boundary surface. This BCS representation yields a new interpretation of the equivalent electromagnetic properties of the wire cage structures.

B4-3
1410

A SURFACE WAVE INTERPRETATION FOR THE RESONANCES OF A DIELECTRIC SPHERE

J. D. Murphy, P. J. Moser, A. Nagl, and H. Überall
Department of Physics, Catholic University
Washington, DC 20064

The calculated radar and bistatic cross sections of dielectric spheres exhibit numerous resonances when plotted vs. frequency. These resonances may be related to the excitation of electromagnetic eigenvibrations of the sphere, with resonance frequencies calculable from a characteristic equation. We show that the resonance may be considered to originate from families of circumferential (surface) waves that are generated during the scattering process; at each eigenfrequency of the sphere, one of these surface waves matches phases after its repeated circumnavigations around the sphere, with the ensuing resonant reinforcement leading to the given scattering resonance. This mechanism explains the existence of electromagnetic eigenvibrations of a general smooth dielectric object; for the case of a sphere, it is shown that the surface waves suffer a phase jump of $\pi/2$ at each of their two convergence points. We calculate numerical values of the eigenvibrations of dielectric spheres, and obtain dispersion curves for the phase velocities of the surface waves.
(Supported by the Naval Air Systems Command, AIR 310-B).

B4-4
1430

COMPUTATION OF FRESNEL-ZONE FIELDS USING THE BESSEL-JACOBI SERIES IN THE WILCOX $1/R^n$ EXPANSION: V. Galindo-Israel and Rahmat-Samii, Jet Propulsion Laboratory, California Institute of Technology, Pasadena, CA 91103; and R. Mittra and A. Rushdi, University of Illinois, Urbana, IL 61801

The significance of Fresnel-zone computations has long been recognized in studies involving very large antennas and beam waveguide systems. A common problem is that antenna ranges are often too short for accurate far-field measurements, particularly for very low cross-polarization levels. The shorter ranges, however, are often sufficiently long for accurate Fresnel-zone measurements.

To overcome this and other problems, recent measurements have been made inside near-field ranges, with the data then being used to compute the far-zone fields. The Bessel-Jacobi series was recently applied to a computationally efficient plane-polar technique of near to far-field computations (1979 IEEE APS Seattle Symposium Record, p.569). The direct application of the Bessel-Jacobi method to the plane-polar near-field measurements yields only the far-zone fields and does not lend itself to computing the fields at intermediate ranges - e.g. The Fresnel-zone range. Since it is desirable to obtain the Fresnel as well as the far-zone field, several new techniques have been introduced to extend the applicability of the Bessel-Jacobi series (e.g. 1979 URSI Seattle Symposium Record, p.63).

An alternative technique discussed in this paper involves applying the Bessel-Jacobi series to the Wilcox vector $1/R^n$ expansion. First, it can be shown that the first two terms of the Wilcox expansion (the $1/R$ and the $1/R^2$ dependence terms) comprise the Fresnel-zone fields to the order $(1/R^3)$. Since all the higher order $(1/R^n, n>1)$ terms of this expansion are obtained from the leading far-field term, we then obtain the second, Fresnel-zone, term by differentiating the Bessel-Jacobi series under the summation signs. This differentiation is readily accomplished for the rectangular components of the plane-polar measurements. It is then possible to study the effects of measurements errors and compare the computed Fresnel fields with the true fields.

This technique is particularly useful for a near-zone measurement from which a computed Fresnel-zone field is used to compare it against the Fresnel-zone field that is measured directly on a short range. If these results compare well, then increased confidence is obtained in the accuracy of the far-zone fields computed directly from the near-zone measurements.

B4-5
1510

QUASI-STATIC ELECTROMAGNETIC PENETRATION OF A MESH-LOADED CIRCULAR APERTURE:

K.F. Casey, Dikewood Industries, Inc., Albuquerque, NM 87106

One method by means of which an aircraft window can be shielded against low-frequency electromagnetic penetration while preserving visibility is to embed a bonded-junction wire mesh of small optical coverage in the window. In this paper we consider the canonical problem of low-frequency electromagnetic penetration through a mesh-loaded circular aperture in a ground plane of infinite extent and determine the equivalent electric and magnetic polarizabilities of the loaded aperture via the solutions of two quasi-static boundary value problems. The boundary conditions to be applied at the mesh surface are developed in the quasi-static limit from the dyadic sheet-impedance operator which describes a bonded-junction square mesh. These boundary conditions are then used in the formulation of two mixed boundary-value problems, the solutions of which are expressed in terms of the solution of a single Fredholm integral equation of the second kind. Numerical results are presented to illustrate the behavior of the aperture polarizabilities as functions of the parameters descriptive of the loading, and simple equivalent-circuit representations for the loaded aperture are found.

B4-6
1530

INTEGRAL EQUATION SOLUTION FOR FIELD AND SUSCEPTANCE OF COAXIAL-TO-CIRCULAR WAVEGUIDE JUNCTION

Michael G. Harrison, Electromagnetics Division
Air Force Weapons Laboratory, Kirtland AFB, NM 87117
Chalmers M. Butler, Dept of Electrical Engineering
University of Mississippi, University, MS 38677

Accurate computation of the TEM susceptance introduced by truncating the inner conductor of a coaxial waveguide has been a problem of interest since the first treatment by Whinnery and Jamieson (Proc. IRE, vol 32, Feb 1944). Such a structure is effectively a junction of a coaxial and a circular waveguide, and the field in each region can be completely described by infinite sets of TEM (coaxial region only) and TM_{0n} modes if the excitation, assumed to be in the coaxial region, is ϕ symmetric. The expansion for the field components in each region can be used together with Fourier series techniques to obtain expressions for the unknown constants in the field expansions. These constants are expressed in terms of weighted integrals of the radial component of the electric field over the aperture formed at the discontinuity. An integral equation for the aperture electric field is obtained by constraining the transverse component of magnetic field to be continuous across the aperture. A numerical solution is obtained for the aperture electric field. The numerical technique includes a procedure to greatly enhance the convergence rate of the higher-order mode series rather than truncating the series after a certain number of terms. Most quantities of interest, including the field in either region and the TEM susceptance, can be calculated from the solution to the aperture electric field.

Aperture field distributions and TEM susceptance values are presented for several sizes of coaxial-to-circular waveguide junctions. It is demonstrated that the solution technique is not restricted to junctions where the outer radius of the coaxial waveguide is equal to the radius of the circular guide. It is also feasible to attach annular disks to either conductor at the junction. Results are also presented for the case where a shorting plate is introduced into the circular waveguide in order to create a one-port, cylindrical cavity.

The calculated susceptance values are compared to results presented in a paper by Razaz and Davies (Trans. MTT, vol 27, June 1979). In this paper, Razaz and Davies compare their results with the analytical and experimental work of earlier investigators and claim superior accuracy. The integral equation solutions compare extremely well with their calculations which are for capacitance only. The integral equation technique is equally applicable at higher frequencies where energy is converted into propogating modes in the circular waveguide.

B4-7
1550

ELECTROMAGNETIC TRANSMISSION THROUGH HOLES, SLOTS, AND CAVITIES IN THICK CONDUCTORS

Roger F. Harrington and David T. Auckland
Department of Electrical and Computer Engineering
Syracuse University, Syracuse, NY 13210

For electromagnetic transmission through small holes, most investigations to date use the concept of polarizability of apertures developed by Bethe for thin conductors. When the conductors have finite thickness, or are backed by conducting cavities, the polarizabilities alone are not sufficient to characterize the behavior of apertures. The admittance concept is required for this case. It can be shown that, for small holes, the polarizability is related to the susceptance of the hole. The real part of the admittance of the hole is a radiation conductance. When the hole is in a thick conductor, or when it is backed by a cavity, the susceptance of the hole can be resonated by the susceptance of the backing region, and exceptionally large transmission of energy may occur.

Perhaps the simplest problem of the type being considered is the two-dimensional one of a thin slot in a thick conducting plate. This general problem has been solved by the method of moments. When the slot is thin, an interesting simplification of the solution results. The distribution of the equivalent magnetic current (or tangential electric field) in the aperture becomes insensitive to aperture width and conductor thickness, and we can use a one-term moment solution. The equivalent circuit for the problem then reduces to a simple two-port parallel-plate waveguide circuit. To this approximation, the field in the parallel-plate waveguide region is the transmission-line mode. The lumped aperture admittances are the radiation admittances of a parallel-plate waveguide opening into half-space. The source is equal to the short-circuit current in the slot region when the aperture in the left-hand plane is short circuited.

A plot of the transmission width of a thin slot vs. the thickness of the conductor shows peaks occurring when the conductor thickness is a little less than an integral number of half wavelengths. In fact, as the slot width approaches zero, the transmission width approaches the value $1/\pi$ wavelengths. Hence, the peak transmission width for small slots is independent of the actual slot width. The sharpness of the peaks is determined by the slot susceptance, the bandwidth becoming narrower as the width approaches zero. This can be viewed as a resonance phenomena, the peaks occurring at frequencies for which the aperture susceptance is equal and opposite to the transmission line susceptance. Conductor losses will modify these results, the modification being greater as the slot width becomes smaller. The principal effects of losses will be to reduce the peaks and broaden the bandwidth of the resonances.

B4-8
1610

SINGULARITY IN GREEN'S FUNCTION AND ITS NUMERICAL EVALUATION: S. W. Lee, C. L. Law, and G. A. Deschamps, Department of Electrical Engineering, University of Illinois, Urbana, IL 61801

The free-space scalar Green's function g has an R^{-1} singularity, where R is the distance between the source and observation points. The second derivatives of g have R^{-3} -singularities, which are not generally integrable over a volume. This paper treats the derivatives of g as generalized functions in the manner described by Gel'fand and Shilov, and a new formula is derived that regularized a divergent convolution integral involving the second derivatives of g. When the formula is used in the dyadic Green's function formulation for calculating the E-field, we recover all previous results as special cases. Furthermore, it is demonstrated through numerical examples that our formula is particularly suitable for the numerical evaluation of the field at a source point, because it allows the exclusion of an arbitrary finite region around the singular point from the integration volume. This feature is not shared by any of the previous results on the dyadic Green's function.

---

*This work was supported by NSF under Grant ENG77-20820.

B4-9
1630

THE IMPORTANCE OF SOURCE MODELLING IN RADIATION PROBLEMS: Tapan K. Sarkar, Electrical Engineering Department, Rochester Institute of Technology, Rochester, NY 14623

Most radiation problems in electromagnetics can be formulated in terms of the operator equation.

$$Au = f \tag{1}$$

where A is a given integro-differential operator and f is the given source function. The objective is then to find the current distribution u on the body due to the forcing function f. In order to make this problem well-posed, it is necessary to ensure f is in the range of the operator A. This is expressed by the following theorem:

Theorem: If $f \notin R(A)$, there always exists a sequence $\{u_k\}$ such that

$$\lim_{k\to\infty} \left|\left| Au_k - f \right|\right| = 0 \tag{2}$$

and for any such sequence

$$\lim_{k\to\infty} \left|\left| u_k \right|\right| = \infty \tag{3}$$

Translated into physical concepts, this implies if the excitation f is such that f is not in the range of A and if one formally (blindly) applies the Method of Moments or Galerkins' method to this problem, one would find a solution u_k to this problem. But interestingly enough, as shown by the theorem, this sequence of solutions u_k diverges. And if the solution diverges it is meaningless to talk about the convergence of the current distribution on the structure.

These mathematical concepts will be illustrated by examples.

MULTIPLE-ACCESS COMMUNICATIONS
Tuesday Afternoon 6 Nov., UMC Forum Room
Chairman: M. Schwartz, Department of Electrical Engineering and Computer Science, Columbia University, New York, NY 10027

C3-1 1330 ON THE T-USER M-FREQUENCY MULTIPLE ACCESS CHANNEL WITH AND WITHOUT INTENSITY FORMATION: S. C. Chang and J. K. Wolf, Department of Electrical and Computer Engineering, University of Massachusetts, Amherst, MA 01003

C3-2 1415 THE BUFFERING DELAY PROBLEM IN RANDOM-ACCESS COMMUNICATIONS: A. Ephremides, Department of Electrical Engineering, University of Maryland, College Park, MD 20742

C3-3 1515 A STACK INTERPRETATION OF THE CAPETANAKIS RANDOM-ACCESS ALGORITHM: J. L. Massey, Department of System Science, University of California, Los Angeles, CA 90024

The basic serial "tree algorithm," devised by J. Capetanakis for random-accessing of a slotted channel with collision feedback information, guarantees finite average packet delay for an infinite population of identical transmitters generating packets at an average rate of λ packets per slot provided $\lambda < .375$.

It is shown that the above Capetanakis algorithm has a very natural interpretation as a "stack algorithm" in which transmitters involved in a collision are pushed down into the stack with probability 1/2 when collisions occur. The stack interpretation directly suggests Gallager's two-counters-per-transmitter implementation of the algorithm. It also suggests a "continuous-entry virtual-stack" modification that requires only one-counter-per-transmitter and yields finite average packet delay provided $\lambda < 1/e = .368$, the same maximum throughput as attained by the slotted-Aloha algorithm in its "equilibrium mode," although the latter algorithm actually gives an infinite average packet delay because of catastrophic failures.

C3-4 1545 INTRINSIC LIMITATIONS OF MULTIBEAM PACKET-SWITCHED PROCESSING SATELLITE SYSTEMS: I. Kadar, IBM Research Center, Yorktown Heights, NY 10598

C3-5 1615 Some Theoretical Observations on Spread-Spectrum Communications

J. E. Mazo, Bell Telephone Laboratories
Murray Hill, New Jersey 07974

We consider a simple direct-sequence model of spread-spectrum communication over a bandwidth W using signals of duration T. In addition to the dimension n=2WT of signal space, the other parameters of interest are the number (u+1) of simultaneous users of the system, the error rate Pe(u), and the number M of subscribers, or potential users. We investigate the relationships between these parameters, and, in particular, study the validity of the usual gaussian approximation often used to compute Pe(u). Basically we conclude that if M is larger than $n^2/2$ then the gaussian approximation is not a guaranteed error rate for (u+1) users, but rather an average over all possible (u+1) users. If M is somewhat less than this number (the exact value is not known) codes can be assigned so that a uniform performance at least as good as Pe(u) can be obtained, where, again Pe(u) is calculated from the gaussian approximation. Uniform performance guarantees are given for any value of M, but they (for M large) permit fewer simultaneous users that the gaussian approximation predicts. These bounds explicitly use the maximum cross-correlation between the signals of the different subscribers. This quantity played no role in the gaussian approximation.

SCATTERING FROM THE CLEAR ATMOSPHERE
Tuesday Afternoon, 6 Nov., UMC East Ballroom
Chairman: E Gossard, NOAA-ERL/WPL, Boulder CO 80303

F2-1
1330

DOPPLER RADAR MEASUREMENTS OF CLEAR AIR ATMOSPHERIC TURBULENCE STRUCTURE AT 1295 MHZ

Ben B. Balsley, Aeronomy Laboratory, National Oceanic and Atmospheric Administration, Boulder CO 80302, and Vern L. Peterson, Centennial Sciences, Inc., 3720 Sinton Road, Suite 205, Colorado Springs, CO 80907

We present Doppler radar observations of the refractivity turbulence structure constant, C_N^2, obtained with the Chatanika Radar Facility, near Fairbanks, Alaska, during a seven-day observing period in October, 1976. The radar is a steerable 26.8 m disk, operating at 1295 MHz (wavelength = 23.2 cm) and with a range resolution that is typically 1.5 km. By using a variety of scanning modes we can examine the variation of C_N^2 with time, height, azimuth and elevation. We find that: 1) At this operating frequency the turbulent irregularities do not scatter radio waves specularly, in contrast with observations at lower frequencies. 2) There is a weak aspect sensitivity of the strength of the radar echoes to the direction of the wind; this may be related to the geometry of the irregularities. 3) Turbulent irregularities occasionally occur in patches that remain identifiable from one scan to the next. None of the scanning modes employed during this series of observations was well suited for tracking the motion of those patches, and so a velocity vector of the patch can only be estimated. It appears that these patches of irregularities drift with the wind. 4) Vertical profiles of C_N^2 show peaks that can be correlated with maxima in wind shear, both in terms of wind speed shear and wind direction shear. However, the C_N^2 peaks normally do not coincide with peaks of wind shear; likewise, they do not normally occur at the tropopause. Caution needs to be exercised in "monitoring the height of the tropopause" with radar echoes alone. 5) A "typical" C_N^2 profile, defined by the median values of C_N^2 at each height from all the azimuth scan data, shows a decrease with altitude above 10 km of 1.3 dB/km; individual C_N^2 profiles show strong deviations from this value, however.

F2-2
1400

STUDIES OF ATMOSPHERIC STRUCTURE USING A FORWARD SCATTER RADAR SYSTEM

R.E. Post, J.P. Basart, and L.D. Bacon
Department of Electrical Engineering and the Engineering Research Institute, Iowa State University, Ames, IA 50011

The problem of characterizing the atmospheric structure responsible for the scattering of electromagnetic energy beyond the horizon has been the subject of study by engineers and scientists for many years. One system which has been found to be useful in such studies is the forward-scatter CW doppler radar incorporating a RAKE receiver. This system resolves the propagation path into a number of time delay shells which are concentric ellipsoids of revolution with the transmitter and receiver located at the foci. The signal resulting from the scattering processes in each shell can be isolated and studied on an individual basis. Thus, the propagation mechanisms present in each region of the common volume corresponding to a time delay shell can be inferred.

The objective of this study is to characterize the atmosperic structure responsible for the scattered signal in the individual time delay shells by interpreting the envelope statistics and the doppler spectrum of the scattered signal. The ability of the forward scatter radar-RAKE system to effectively divide the common volume into concentric shells combined with the sensitivity of the system in detecting the presence of partially reflecting layers makes it particularly well suited to studies of this nature.

The forward scatter CW radar system used in this research effort operates over a 406 km propagation path between Boone, IA and Arlington, WI at a frequency of 940 MHz. The carrier is bi-phase modulated at a 5 MHz rate with a pseudo-random code. This combination of path length and modulation frequency results in time delay shells separated by 0.2 μs, which corresponds to shell thicknesses ranging from 1.12 km at the lowest level to 0.4 km at tropopause heights. Coherent detection techniques, using a pseudo-random code identical to that impressed on the carrier but shifted in time, produce in-phase and quadrature components of the scattered signal. Received signal data blocks of one to two minutes in length are taken from the individual time-delay taps for subsequent processing and analysis. The envelope statistics are interpreted in terms of a Rayleigh distributed vector. This model is representative of a signal composed of an isotropically scattered field added to a partially-reflected field. The doppler spectrum of the received signal is also calculated and a comparison made between the statistical distribution and the doppler spectrum of signals from individual time-delay shells. Models of atmospheric structure which could be responsible for the characteristics of the received signals are proposed.

F2-3
1430

A NEW LIDAR/FLUORESCENT TRACER TECHNIQUE FOR ATMOSPHERIC RESEARCH:

T. G. Konrad and J. R. Rowland,
Applied Physics Laboratory, The Johns Hopkins University, Laurel, MD 20810

This paper describes a new remote sensing technique for the study of air motions and diffusion which uses microscopic fluorescent particles as tracers and lidar as the sensor. The technique has wide application in the study of atmospheric processes such as convection, sea and land breezes, shear layers, etc., and in pollution such as diffusion and fumigation of stack plumes.

The fluorescent particles are dispensed in the area of interest and excited by the laser. The backscattered signal is composed of (1) the elastic backscatter return at the laser frequency and (2) the return at the shifted fluorescent frequency. By filtering out the laser frequency and selectively detecting only the shifted, fluorescent frequency, the return from the background aerosols and other sources of clutter are eliminated. This results in increased detectability due to a large increase in signal-to-noise ratio. Thus, the fluorescent tracer provides a uniquely identifiable and easily detectable marker of atmospheric motions.

The technique was first tested in the fall of 1978 in a "proof of principle" experiment. Background data for optimizing the various elements of the system were collected. A series of laboratory measurements have been made to determine excitation and fluorescent spectra for a large number of pigments. Absolute cross section measurements have also been made. A second experiment was performed in the spring of 1979 at NASA/Wallops Island, VA, where a plume of tracer material was generated from a tower at the 150 foot level to simulate a stack plume. Vertical (RHI) and horizontal (PPI) sections through the plume were recorded on an intensity modulated scope. Details of the lidar system, the fluorescent tracer and the results of the laboratory and field tests will be presented.

F2-4
1520

CLEAR-ATMOSPHERE VARIATIONS OF CROSS-POLARIZATION DISCRIMINATION ON TERRESTRIAL MICROWAVE LINKS

R.S. Butler, Communications Research Centre
Department of Communications
Ottawa, Ontario K2H 8S2, Canada

The usefulness and reliability of dual polarization frequency reuse systems above 10 GHz is being investigated on two adjacent 16 km microwave paths. One path, which is entirely over land, uses a pair of closely spaced frequencies transmitted with orthogonal linear polarizations near 11 GHz and a second pair near 17 GHz. The other path, which crosses a 4 km wide river, has a single transmitted frequency near 11 GHz and another near 17 GHz. All twelve direct- and cross-polarized received signals are recorded.

In addition to clear air fades and enhancements which are attributable to multipath propagation and ducting, polarization-dependent variations of the received signals are observed during which the cross-polarization discrimination of the system is degraded significantly. The characteristics of the signal variations are quite different on the two paths, the over-water one being much more stable. This paper will deal with the phenomenology and statistics of these variations and discuss the possible mechanisms involved.

F2-5
1550 SIMULTANEOUS MULTIPATH MEASUREMENTS USING EIGHT AND FIFTEEN FOOT ANTENNAS: A. Fejfar and J. A. Wick, The Mitre Corporation, Tactical Communications Test Office, Drawer S, Ft. Huachuca, AZ 85613

In preparation for the test of a new digital troposcatter radio family, the AN/TRC-170, path loss and multipath spread were measured on four troposcatter links in Southern Arizona. This test was conducted by the USAF, Electronic Systems Division. Multipath measurements were made using pseudorandom probe (RAKE) equipment obtained from the Institute for Telecommunication Sciences.

On one of the troposcatter paths investigated, simultaneous RAKE observations were made using eight and fifteen foot antennas. The RAKE transmitter on this 143 mile path fed a 15 foot antenna. Under normal troposcatter conditions, it was found that the larger receive antennas showed no larger received signal level than the small antenna. During a brief interval of specular conditions, the RSL difference seen between the large and small antennas was nearly equal to the difference in their free space gains. During this interval, the multipath spread seen by each antenna was essentially the same.

Conclusions are drawn from the data concerning aperture-to-median coupling loss and the correlation between path loss and multipath spread variations.

F2-6
1620 MULTIPATH OBSERVATIONS ON A MIXED MODE TROPOSCATTER PATH: A. Fejfar and J. A. Wick, The Mitre Corporation, Tactical Communications Test Office, Drawer S, Ft. Huachuca, AZ 85613

Path loss and multipath spread were measured on four troposcatter links in Southern Arizona in preparation for the test and evaluation of a new troposcatter radio family, designated the AN/TRC-170. This test was conducted as a part of the development and test program of this new equipment by the Electronic Systems Division of the United States Air Force. Multipath measurements were made using pseudorandom probe (RAKE) equipment obtained from the US National Telecommunications and Information Administration.

Propagation on one of the links investigated was predominately by the diffraction mode with a weak troposcatter component evident. This is the first known RAKE observation of such a path. The magnitude of differential delays obtained on such a path have been posulated based upon geometric constructions and upon results inferred from adaptive digital modem performance observed on mixed mode paths. (Osterholz, J. et al, Ref 31, AGARD Conf. Proc. No 244, 3-7 Oct 77)

The observed impulse response of a mixed mode troposcatter path is shown and the effect of the relative magnitude of the troposcatter and diffraction components upon the apparent multipath spread is postulated. Fading characteristics of the mixed mode link investigated are discussed and the results are extrapolated to other links with varying mixtures of troposcatter and diffraction components.

RECENT RADIO BEACON RESULTS - I:
TOTAL ELECTRON CONTENTS
Tuesday Afternoon, 6 Nov., UMC 159
Chairman: K. Davies, SEL, NOAA, Boulder, CO 80303

G2-1
1330

TOTAL ELECTRON CONTENT OBSERVATIONS DURING THE FEBRUARY 26, 1979 TOTAL SOLAR ECLIPSE OVER NORTH AMERICA

E. A. Essex, J. A. Klobuchar, C. R. Philbrick, Air Force Geophysics Laboratory, Hanscom AFB, MA 01731
M. Mendillo, Astronomy Department, Boston University, Boston, MA 02215
R. E. Leo, Electrical Engineering Department, Montana State University, Bozeman, MT 59715

Ionospheric total electron content (TEC) observations were carried out from eight stations during the February 26, 1979 total solar eclipse over North America. The TEC's were determined from the Faraday rotation of the plane of polarization of the VHF signal from geostationary satellites. Local times of totality of the eclipse in the ionosphere observed from the various stations ranged from 0734 hours to 1400 hours. Depletion of the TEC from the non-eclipse average behavior varied up to a maximum of 40% for the ionosphere experiencing 100% eclipse. Maximum TEC depletion occurred at an average time of 33 minutes after maximum contact. Most of the results showed a rapid rate of depletion after about 30% obscuration, the rate of depletion reaching a minimum value at or before maximum obscuration. Before fourth contact was reached, the rate of increase of TEC generally had overshot the non-eclipse average, gradually returning to the non-eclipse average after fourth contact.

G2-2 1355 IONOSPHERIC TOTAL ELECTRON CONTENT AT OOTACAMUND, INDIA, DURING SOLAR MINIMUM: S. D. Bouwer and K. Davies, National Oceanic and Atmospheric Administration, Space Environment Laboratories, 825 Broadway, Boulder, CO 80302

Measurements of the total columnar electron content N_T of the ionosphere were made at a near equatorial station using the ATS6 Radio Beacon Experiment between October 1975 and July 1976. Seasonal variations of N_T can be accounted for by solar zenith angle and quiet magnetic variations. Sample diurnal variations show a deep predawn minimum and a variable early afternoon peak. The total content has a distinct dependence on the geomagnetic field.

G2-3 1420 ATS6-BOULDER PHASE III MEASUREMENTS OF TOTAL ELECTRON CONTENT: Kenneth Davies, NOAA/SEL, Boulder, CO 80303

Measurements of the total electron content of the ionosphere and plasmasphere have been made at Boulder using the ATS6 Radio Beacon. Preliminary analysis indicate that, during the winter of 1977-1978, the plasmasphere content has a peak near midday in contrast to the winter of 1974-1975 when the peak occurred at night. The total electron contents in 1977-1978 are considerably higher than those in 1974-1975 corresponding to increases in sunspot numbers.

G2-4
1515 Faraday, Protonospheric and total Electron Content Measurements at a Midlatitude Station during the third phase of ATS-6 Radio Beacon Experiment.

M. P. Paul, Department of Industrial Technology, Alcorn State University, Lorman, MS 39096

The launching of the radio beacon satellite ATS-6 (ATS-F prelaunch name) in May, 1974 heralded a new era for the exploration of the ionosphere and the overlying protonosphere from ground-based stations. This geostationary satellitecarries on board a radio transmitter which transmits signals at 40, 140 and 360 MHz. Both Faraday rotation of 40 and 140 MHz plane polarized signals and the group delay of the 1 MHz modulation phase of the 360 MHz signal measurements could be carried out yielding the ionospheric electron content and the total electron content from the ground-based receiving station to the point beneath the transmitting satellite. From a simultaneous measurement of both the quantities, the protonospheric contribution could be computed.

Under the sponsorship of the National Aeronautics and Space Administration a field station was set up on the Alcorn State University campus having the geographical coordinates 31.5° N latitude and 91.06° W longitude and the above mentioned observation at 140 and 360 MHz began during the third phase of ATS-6 radio beacon experiment around Decemebr, 1976 when the satellite was positioned at the present longitude 140° W. Our Faraday and group delay measurements cover the period from December, 1976 to June, 1977. In the report we will discuss the temporal behavior and other salient features of the Faraday, total and protonospheric electron contents during this period of our observation.

G2-5 1540 PRELIMINARY RESULTS FROM THE COLLEGE, ALASKA ATS-6 RBE FARADAY ROTATION AND MODULATION PHASE MEASUREMENTS: Robert D. Hunsucker, Geophysical Institute, University of Alaska, Fairbanks, Alaska 99701

Faraday rotation and modulation phase measurements of the 140 and 360 MHz ATS-6 geostationary satellite Radio Beacon Experiment (RBE) transmissions have been recorded almost continually since October, 1978, at College, Alaska. The ray path from ATS-6 to the College earth station is unique because of its geometry. The path is tangential to the lower protonosphere near L = 2.0 and intersects the ionosphere near F-layer maximum (h ≈ 300 km) at L = 4.0.

Data from a very extensive array of geophysical instrumentation including ionosondes, riometers, magnetometers, telluric current recorders and the Chatanika incoherent scatter radar are available and aid in the interpretation of the ATS-6 RBE data.

This preliminary report concerns three general areas: 1. "Scintillation onset in relation to auroral substorms" - which outlines the general relation of the latitudinal variation of a substorm (measured by Alaska IMS instrumentation chain data) with occurrence of F-region scintillation at 140 and 360 MHz near L = 4.0; 2. "Power spectral analysis of scintillation", relating the spectral signatures of scintillation to various geophysical parameters; and, 3. "Total electron content (TEC) variations" - mainly large-scale variations in TEC diurnal behavior related to storm behavior.

G2-6
1605

SOLAR CYCLE AND SEASONAL VARIATIONS OF THE SOLAR AND LUNAR DAILY VARIATIONS OF TOTAL ELECTRON CONTENT AT LUNPING

Yinn-Nien Huang, Telecommunication Laboratories, M. O. C., Chung-Li P. O. Box 71, Taiwan, R. O. C.

The solar and lunar daily variations of the ionospheric total electron content observed at Lunping (25.00°N; 121.17°E geographic) were analyzed by Chapman-Miller method. The total electron content data observed from March 4, 1977 to January 31, 1979 by measuring Faraday rotation angle of the 136.1124 MHz beacon signal transmitted from Japanese ETS-II geostationary satellite were used for analysis. The subionospheric point of ETS-II observed at Lunping is located at 23.0°N; 121.9°E geographic coordinate which is near to the crest zone of the so called equatorial anomaly.

The luni-solar diurnal variation, L_1, and lunar semi-diurnal variation, L_2, were found to have significant seasonal variations with amplitude increasing steadily from summer to winter. The hours for L_1 and L_2 variations to attain their respective maximum values also increase steadily from summer to winter. The seasonal variation of the semi-diurnal variation, L_2, was found to be explainable by the additional fountain effect caused by the similar seasonal variation of the lunar semi-diurnal electric field induced at the equatorial region. However, the seasonal variation of the luni-solar variation, L_1, was found not to be explainable by the additional fountain effect. Seasonal variations for the harmonic components of the solar daily variation were found to be different from those of lunar daily variation. Solar cycle variations of the harmonic components of the solar and lunar daily variations were found and described.

G2-7
1630

INTERPRETATION OF TROPOSPHERIC EFFECTS OBSERVED WITH RADIO BEACONS

C. Fengler, Department of Electrical Engineering, McGill University, Montreal, Que., H3A 2A7

Tropospheric effects have been reported from radio beacon observations at various frequencies. On the base of meteorological data and terrestrial propagation measurements the possible causes of these disturbances are considered. The feasibility of predicting their occurence is discussed.

ACTIVE EXPERIMENTS FROM THE SPACE SHUTTLE
Tuesday Afternoon, 6 Nov., UMC 157
Chairman: R. W. Fredricks, TRW Defense and Space Systems Group, Redondo Beach, CA

H1-1
1330

A VLF TRANSMITTER ON THE SPACE SHUTTLE

U. S. Inan, T. F. Bell and R. A. Helliwell,
Radioscience Laboratory, Stanford University
Stanford, Ca. 94305.

The use of a VLF transmitter on the space shuttle has been suggested as a means of studying VLF cyclotron resonance wave-particle interactions in the magnetosphere. In these interactions the waves are observed to be amplified by up to 30 dB and the particles are scattered in pitch angle and energy, resulting in the precipitation of some of the particles into the atmosphere.

In the present paper we discuss the power budget of the particle scattering experiment and relate the shuttle transmitter power (into the dipole antenna) to the wave power in the magnetosphere necessary to perform the experiment. Two key features of the analysis, namely (i) the antenna characteristics and (ii) the distribution of the ray paths in the ionosphere are discussed. The antenna impedance and radiation resistance are computed as a function of the local plasma parameters and antenna length and orientation. The propagation of the excited waves in the inhomogeneous magnetoplasma is studied using a raytracing analysis. A unique feature of a space-borne transmitter is the capability to excite waves over a wide range of wave normals. It is shown that injected waves can be focused by the plasmapause or other large scale density structures, making those regions very likely places for strong wave-particle interactions.

H1-2
1400

OSS-1 AND SPACELAB 2 PLASMA DIAGNOSTICS PACKAGE

Stanley D. Shawhan
Department of Physics and Astronomy, University of Iowa, Iowa City, IA 52242

A Plasma Diagnostics Package (PDP) which houses instruments for the measurement of plasma fields, waves, composition and suprathermal particles is to be flown on the Office of Space Science OSS-1 "Pathfinder" and on the Spacelab 2 Missions. Instrumentation includes a triaxial fluxgate magnetometer (12 mγ - 1.5 gauss), a dc electric field meter (2 - 2000 mVm^{-1}), a plasma wave analyzer with magnetic search-coil and electric dipole sensors to measure the peak and average wave spectrum (5 Hz - 800 MHz), an ion mass spectrometer for 1 to 64 AMU (20 to 2 $\times$ 10^6 cm^{-3}), an ion retarding potential analyzer and differential ion flux probe to determine the energy distribution and streaming velocity direction (< 16 eV, < 15 km sec^{-1}), a Langmuir Probe for assessment of electron density irregularities (< 20% up to 1 kHz), and a quadrispherical low energy proton and electron differential energy analyzer to determine the suprathermal particle distribution functions (2 eV - 50 keV).

On OSS-1 the PDP is manipulated by the Remote Manipulator System (RMS) to diagnose the beam from the VCAP Fast Pulse Electron Gun (1 keV, 100 ma, 600 nsec--continuous beam) and to assess the resulting Orbiter charging effects and plasma wave emissions. On Spacelab 2 the PDP is released to become an Orbiter subsatellite. As the PDP separates from the Orbiter, the wave propagation and mode coupling characteristics of the Shuttle EMI noise spectrum can be evaluated. During the plasma depletion experiments the PDP is to make in situ measurements of the changes in ionospheric composition and density and in associate fields and wave phenomena. On both missions, the PDP is to determine the characteristics of the plasma wake created by the Orbiter's motion through the ionosphere. The PDP measurements on the early Shuttle flights provide essential background information for the extensive follow-on wave injection (WISP) and particle beam (SEPAC) experiments.

H1-3
1430 ELECTROMAGNETIC WAVE GENERATION AND INJECTION IN THE IONOSPHERE BY A LONG ORBITING WIRE

D.A.Arnold, M.Dobrowolny, M.D.Grossi
Radio and Geoastronomy Division,
Harvard-Smithsonian Center for Astrophysics,
Cambridge, MA 02138

The National Aeronautics and Space Administration is currently developing a facility to use long Shuttle-borne tethers, with lenghts up to 100 Km, to perform unprecedented scientific experiments. In particular, if the tether is constructed of metal, either uncoated or coated with a dielectric, its electrodynamic interactions with the ionosphere can give rise to a number of unusual phenomena. The basic concept behind these electrodynamic uses is the polarizing electric field $\overline{E} = -\overline{V}_o \times \overline{B}$ that is established along the tether owing to its motion, with velocity $\overline{V}_o$ across the lines of force of the earth's magnetic field $\overline{B}$. For a tether length L= 100 Km and a Shuttle velocity V_o= 7.8 Km/sec, a voltage as high as 23 KV can develop between the two ends of the tether, thus causing the system to act as a kind of self-powered generator (unipolar inductor) capable of exciting a variety of wave and particle phenomena in the ionosphere. These include the generation of waves in various frequency bands, such as ULF, VLF ,etc., and the possible acceleration of electrons to high energies toward the earth's atmosphere.

There is a close analogy between the electrodynamic tether and the Jovian moon Io, which moves in the Jupiter's magnetosphere. In developing this analogy, the authors review the interactuons Io/Jupiter's magnetosphere and point out similarities and differences with the electrodynamic phenomena associated with the orbiting tether.

The authors discuss in detail the mechanisms that produce electron acceleration through the charged-sheath region that surrounds the conducting balloon at the free end of the tether, and the consequent generation of accelerated electron beams, of HF electromagnetic waves and of artificial auroral lines in the optical band. It is shown that these emissions can be detected and measured with stae-of-the-art instrumentation, at ground level and in orbit.

H1-4
1530

SHUTTLE-TO-SUBSATELLITE DIFFERENTIAL DOPPLER PROBING OF TRAVELLING IONOSPHERIC DISTURBANCES BY VHF BISTATIC SOUNDER :

M.D.Grossi, Radio and Geoastronomy Division,
Harvard-Smithsonian Center for Astrophysics,
Cambridge, MA 02138

Forthcoming Shuttle missions are expected to perform experiments on wave injection in space plasma, inclusive of the differential doppler probing of Travelling Ionospheric Disturbances (T.I.D.s). This observational technique consists in using a VHF bistatic sounder, with the transmitting terminal on board the Shuttle and the receiving terminal on a subsatellite. The latter will be able to acquire a variety of relative positions with respect to the former, at a relative distance that will span from a few hundred meters up to several hundred kilometers.

The instrumentation required to perform these measurements has been already developed and built for space use and is ready for adaptation to the Shuttle and its subsatellite. The bistatic sounder operates at 162 and 324 MHz (phase-coherent pair of frequencies). The observed differential doppler is a measure of the component along the doppler baseline Shuttle-to-Subsatellite of the ionospheric electron density gradients. Measurement accuracy in differential doppler frequency is better than 1 millihertz for a 10 second integration time. This corresponds to a minimum detectable electron density gradient of the order of 10^3 el/m^4.

This bistatic sounding technique is expected to provide valuable information on the T.I.D. phenomenology, such as spatial extent of the wave train, envelope shape, number of cycles in the train, spatial wavenumber, group velocity and phase velocity .

H1-5
1600 Large Scale Waves in the Ionosphere Observed by the AE Satellites

S. H. Gross, Polytechnic Institute of New York,
C. A. Reber and F. Huang, Goddard Space Flight Center, NASA

The AE series of satellites have made insitu measurements of the density and temperature of plasma and neutral species in circular orbits at altitudes of about 250km. The fluctuations of these measurements are spectrally analyzed for large scale, long period waves, such as gravity waves. The spectra are found to exhibit considerable coherence between the different species indicating their likely origin from a common source. Data are presented for many orbits exhibiting some of the characteristics of these waves for low and high inclination satellite orbits. The possible association of these waves to other finer scale phenomena will be indicated.

H1-6
1630 PLASMA EFFECTS ON THE IMPEDANCE OF THE ISIS SOUNDER DIPOLE ANTENNA DURING TRANSMISSION: H. G. James, Communications Research Centre, Department of Communications, Ottawa, Ontario K2H 8S2, Canada

It is planned to investigate antenna impedance and the interaction of an antenna with a plasma using powerful radio transmitters in wave injection experiments on Shuttle/Spacelab. Data from the ISIS topside sounder spacecraft have been studied in order to anticipate some of the expected phenomena.

The voltage at the output of the power amplifier in the ISIS sounder transmitter is routinely recorded over the entire frequency range of 0.1 MHz to 20 MHz. A large quantity of data from the ISIS I and ISIS II spacecraft has been processed and the dependence of the output voltage on frequency has been investigated under a variety of plasma conditions. In cases where the plasma frequency is low, around 0.1 MHz, the voltage response is essentially what would be expected in free space. At higher plasma frequencies, there is a significant departure from the free-space case at frequencies close to the plasma and gyro frequencies. For a given working frequency and given plasma parameters, the voltage exhibits a slight dependence on antenna orientation. The ISIS I sounder has both a 100-watt and a 400-watt mode of operation; there are no important differences between the voltage responses obtained in the two modes. It will be possible to study responses through a much wider range of transmitter power using the wave injection equipment planned for Shuttle/Spacelab.

The theoretical curve of voltage versus frequency for ISIS I and ISIS II has been computed using an equivalent circuit representation of the amplifier, the antenna matching network and the long and short sounder dipoles. Various theories have been applied to calculate the impedances of the dipoles, with qualified success. Good agreement with the observed free-space curve is obtained by using standard textbook equations for the vacuum cylindrical dipole, but only by including stray capacitance at the antennas. Plasma theory accounts roughly for the changes observed in the curve near the characteristic frequencies. However, there are important differences between the observed and calculated curves. The failure of the linear theory is just one kind of evidence that the sounder pulse profoundly changes the nature of the plasma near the dipole.

GUIDED WAVES: OPTICAL AND MILLIMETER
Commission B, Session 5, UMC West Ballroom
Chairman: D. C. Chang, Electromagnetics Laboratory, Department of Electrical Engineering, University of Colorado, Boulder, CO 80309

B5-1
0830 NUMERICAL SOLUTION OF INTEGRAL-OPERATOR EQUATION FOR NATURAL MODES ALONG HETEROGENEOUS OPTICAL WAVEGUIDES:
D.R. Johnson and D.P. Nyquist, Department of Electrical Engineering and Systems Science; B. Drachman, Department of Mathematics, Michigan State University, East Lansing, MI 48824

An integral-operator formulation for the EM field excited in cladded, heterogeneous, dielectric optical waveguides was previously developed by the authors. The validity of that formulation was confirmed by analytical solutions for the homogeneous-core configuration. In this investigation numerical solutions for heterogeneous-core, graded-index waveguides are obtained by the method of moments (MoM).

A 2-d electric-field integral equation (EFIE) for the source-free, natural-mode electric field $\vec{E}(\vec{r})=\vec{e}(\vec{\rho})\exp(\pm j\beta z)$ along a graded-index (described by refractive index $n(\vec{\rho})$) optical waveguide is

$$\vec{e}(\vec{\rho})-\frac{1}{2\pi n_c^2}\nabla\sum_{i=1}^{N}\oint_{\Gamma_i}\{[n^2(\vec{\rho}_+')-n_c^2]\hat{n}'\cdot\vec{e}(\vec{\rho}_+')-[n^2(\vec{\rho}_-')-n_c^2]\hat{n}'\cdot\vec{e}(\vec{\rho}_-')\}$$

$$K_0(\gamma|\vec{\rho}-\vec{\rho}'|)d\ell'-\frac{1}{2\pi}\nabla\sum_{i=1}^{N}\int_{(\Delta S)_i}\frac{\vec{e}(\vec{\rho}')\cdot\nabla' n^2(\vec{\rho}')}{n^2(\vec{\rho}')}K_0(\gamma|\vec{\rho}-\vec{\rho}'|)dS'$$

$$-\frac{k_o^2}{2\pi}\int_{c.s.}[n^2(\vec{\rho}')-n_c^2]\vec{e}(\vec{\rho}')K_0(\gamma|\vec{\rho}-\vec{\rho}'|)dS'=0\quad\ldots\text{ for }\vec{\rho}\in c.s.$$

where $\vec{e}$ is the unknown natural-mode field over cross section c.s.; γ is a parameter depending upon β; and N is the number of cross-section subregions $(\Delta S)_i$ with continuous index variations bounded by contours of index discontinuity Γ_i. Numerical solutions to the source-free EFIE for natural modes along graded-index optical waveguides are obtained by application of the MoM. Eigenmodes are identified by numerically locating roots to the singular system matrix equation, providing the desired eigenvalues and corresponding natural-eigenmode fields.

Solutions were obtained by this method for several waveguide systems. TE and TM natural modes are computed along slab waveguides for various index profile variations. The effects of various profiles on waveguide dispersion are studied. Natural modes are also computed along homogeneous rectangular waveguides for various height/width ratios.

B5-2
0850

INTEGRAL EQUATION FORMULATION FOR SCATTERING FROM OBSTACLES IN DIELECTRIC OPTICAL WAVEGUIDES

S. V. Hsu, E-Systems Inc., Garland Division, P.O. Box 226118, Dallas, Texas 75266, U.S.A., Dennis P. Nyquist, Department of Electrical Engineering and System Sciences, Michigan State University, East Lansing, Michigan 48824, U.S.A.

An Integral equation formulation is described as an alternative to the conventional boundary-value analysis for waves scattered from the obstacles in a cladded dielectric waveguide.

The heterogeneous core and the region of discontinuity in the dielectric waveguide are replaced by equivalent current distributions which maintain a scattered field in the otherwise uniform, infinite cladding. The total electric field in the waveguide consists of the superposition of an impressed excitatory field and the scattered field. Expansion of the scattered field in terms of the normal modes of the system results in the following 3-D electric field integral equation (EFIE) for the unknown electric field in the device region:

$$\vec{E}(\vec{r}) + j\omega\epsilon_o \int_V (n^2(\vec{r}') - n_b^2(\vec{r}'))\, \vec{E}(\vec{r}') \cdot \overleftrightarrow{G}(\vec{r},\vec{r}')\, dV' = \vec{E}^{inc}(\vec{r})$$

where n and n_b are reflective indices of the device and the unperturbed waveguide region, and $\overleftrightarrow{G} = \overleftrightarrow{G}_D + \overleftrightarrow{G}_R$ is a tensor green's dyadic with

$$\overleftrightarrow{G}_D(\vec{r},\vec{r}') = \sum_n \vec{e}_n(\vec{\rho})\vec{e}_n(\vec{\rho}')\, \exp(-j\beta_n|z-z'|)$$

and $\overleftrightarrow{G}_R(\vec{r},\vec{r}')$ is contributed by the continuous radiation mode spectrum.

Application of the above EFIE to a dielectric slab waveguide with a slice gap discontinuity is studied and numerical results are obtained by the Method of Moments to determine the modal amplitudes for the scattered fields. This subsequently yields the transmission and reflection coefficients. Other potential applications of this technique include integrated dielectric lens, dielectric step discontinuities etc..

B5-3
0910

APPROXIMATED BOUNDARY VALUE PROBLEM IN A RIB WAVEGUIDE:

Hiroshi Shigesawa, Mikio Tsuji, Shigefumi Suhara, and Kei Takiyama, Department of Electronics, Doshisha University, Karasuma-Imadegawa, Kamikyo-ku, Kyoto, 602 Japan

This paper deals with the transmission properties of a dielectric rib waveguide by means of the approximated mode-matching method. It is anticipated that dielectric waveguides will be used as the fundamental transmission line for integrated optical, submillimeter and millimeter wave circuits. A rib waveguide will become one of the most important waveguides because of its simplicity, single-mode operation, mechanical stability and precision of construction.

However, there are many difficulties in analyzing its mode properties rigorously because of the geometrical structure of the boundary. The propagation characteristics of such a waveguide have been estimated by several approximate treatments which use the effective refractive index method, the numerical method and the variational method. On the other hand, a more accurate method based on the Rayleigh expansion theorem has been also developed.

Our analytical considerations in this paper are based on the last method, named as the mode-matching method. In our analysis for both the eigen value and the eigen function, the cross section of a rib waveguide is subdivided into several sub-sections having a simple geometry of the boundary, i.e., that of a slab waveguide. After approximating the field in each sub-section only by the guided propagation modes trapped by the slab waveguide, the boundary value problem is treated so as to minimize the mean-squares deviation in the approximated fields on the boundary under consideration. This minimization is, of course, done for both the unknown field amplitudes and propagation constant.

To prove the accuracy of our analytical results, a number of experiments have been performed in the 50 GHz region. In our experiments, a newly proposed technique using the "movable metal grating coupler" has been applied to obtain the precise eigen values, and reasonable agreements between experimental and theoretical values have been found.

Finally, the relative merits of the present analysis and the others are discussed, and our analysis will be improved by considering the non-trapped radiation modes in a slab waveguide.

B5-4
0920 EXPERIMENTAL INVESTIGATION OF SURFACE WAVE RADIATION FROM A TAPERED DIELECTRIC SLAB: Robert German, Edward F. Kuester and David C. Chang, Electromagnetics Laboratory, Department of Electrical Engineering, University of Colorado, Boulder, CO 80309

Radiation of surface wave from a tapered dielectric waveguide is often associated with the problem of prism couplers in an integrated optics environment, as well as the problem of splicing in fibers. In order to understand the physical phenomena involved, we have devised an experimental study consisting of a foam slab sandwiched in between two large, closely spaced parallel metal plates for modelling a two dimensional dielectric slab structure. Operating at X-band, one end of the slab is extended into a multimode waveguide horn and a single surface-wave mode of the TE-type is launched. At the other end, one side of the foam slab is cut into a wedge shape and the radiation pattern is detected by an electric probe inserted into holes drilled on the upper conducting plate. Radiation coupling between two tapered slabs is also investigated by placing a second slab with identical wedge angle at several different locations, as well as orientation near the first slab. Some results unique to the problem of a weakly-guided structure (i.e. the case where the refractive index contrast between the slab and surrounding material is very small), are observed. Among them is the observation that coupling between two tapered guides is sensitive to the alignment and the tip-to-tip spacing of the two slabs, but relatively insensitive to the way the face of the wedge is slanted.

B5-5
1000

AN APPROXIMATE DYNAMIC GREEN'S FUNCTION IN THREE DIMENSIONS FOR FINITE LENGTH MICROSTRIPLINES

Y.L. Chow, Department of Electrical Engineering, University of Waterloo, Waterloo, Ontario, Canada N2L 3G1

A spatial Green's function in 2-D for straight and infinite microstriplines has been shown to be accurate [1] at frequencies that the dynamic effects cannot be neglected. It is reasonable, therefore, to expect that a similarly accurate spatial Green's function in 3-D can be constructed for finite and curved microstriplines.

Based on the same image model of charges and currents as in 2-D, this paper constructs the 3-D Green's function. The Green's function is then applied, through Harrington's moment method, to calculate the input impedance of a few microstriplines, viz: a matched microstripline, straight and hairpin open ended stubs.

As an example of the above calculations, the table of the input impedance of the open circuited straight stub is presented below. The stub has a length ℓ=70.5 mm, width w=2.54 mm, substrate thickness b=1.27 mm, and dielectric constant ε_r=3.

Frequency	20MHz $\ell\sim\lambda/38$	346.6 MHz $\ell\sim\lambda/8$	693.1 MHz $\ell\sim\lambda/4$
Z_{in} from this paper	2.43×10^{-5} $-j1.26\times10^{3}\Omega$	8.75×10^{-3} $-j57.9\Omega$	4.55×10^{-2} $-j8.48\times10^{-1}\Omega$
R_{in} from Lewin[2]	$2.65\times10^{-5}\Omega$	$7.96\times10^{-3}\Omega$	$3.18\times10^{-2}\Omega$
X_{in} from TEM solution[3]	$-1.24\times10^{3}\Omega$	-55.7Ω	1.67Ω

The table shows that at frequencies at or below 346.6MHz, the agreements of Z_{in} in this paper with the available low frequency data are excellent.

References:

1. Y.L. Chow and I.N. El-Behery, IEEE Trans. on Microwave Theory and Techniques, 26, 978-983, 1978.
2. L. Lewin, Proc. IEE, 107, Part C, 163-170, 1960.
3. P. Silvester, Proc. IEE, vol. III, 43-48, 1968.

B5-6
1020

ANALYSIS OF BROADSIDE-COUPLED MICROSTRIP LINES

I.J. Bahl, Department of Electrical Engineering,
University of Ottawa, Ottawa, Canada K1N 6N5
P. Bhartia, Defence Electronics Division,
Defence Research Establishment, Ottawa, Canada

Broadside-coupled striplines have been used extensively in the design of many passive and active components, such as directional couplers, filters, baluns and digital phase shifter networks. This configuration has been used widely for realizing tight couplers. In order to ease the mounting of solid state devices and simplify the fabrication process, the best choice for circuit design is broadside-coupled microstrip lines. This configuration consists of two parallel strip conductors etched on two sides of a dielectric substrate and placed in the middle of two ground planes.

In this paper, the variational method is described to evaluate the capacitance between the strip conductor and the ground plane. The geometry can support two orthogonal TEM modes called even and odd modes. For calculating the capacitances for these modes, the symmetry of the structure is used. For the even modes (both the strip conductors are at equal positive potential), a magnetic wall is considered in the plane of the conductors at the plane of symmetry, whereas in the case of odd modes (both the strip conductors are at equal potential but of opposite sign), an electric wall is considered at the plane of symmetry. After applying boundary and the continuity conditions to the potential distribution (in the Fourier transform domain) on the strip in terms of the Fourier transform for the charge distribution, the variational expressions for the line capacitance are obtained. The line capacitances for the even and odd modes are calculated, and the characteristic impedances are then obtained from these capacitances. The theoretical results for $\varepsilon_r = 1.0$ are in good agreement with the available data for broadside-coupled striplines demonstrating the validity of the method. The coupling coefficients for 50 ohm as the input and output impedance are calculated and it is noted that coupling increases when the spacings between the strip conductors, and the widths of the strips decrease.

B5-7
1040

COMPLETE AND PARTIAL REFLECTION OF A TEM WAVE OBLIQUELY INCIDENT ONTO A GROUNDED DIELECTRIC SLAB:

David C. Chang, Edward F. Kuester and Robert Johnk, Electromagnetics Laboratory, Department of Electrical Engineering, University of Colorado, Boulder, CO 80309

Excitation of a grounded dielectric slab by a TEM wave incident normally from a parallel-plate horn has long been investiaged in conjunction with the launching of surface waves. Little attention however, was given to the case of an oblique incidence until more recently, when it was realized that such a structure represents the canonical problem essential to the understanding of a wide microstrip structure. Physically, the problem is more complicated because of the possible excitation of both the LSE- and LSM-type of waves on the slab. In addition, since the field variation along the edge of the upper plate is governed by the incident TEM-wave, surface-wave as well as the sky-wave can be either propagating or decaying away from the parallel plate horn, depending upon the angle of incidence. Complete reflection of the TEM-wave is therefore possible for an incident angle beyond a certain critical angle and this phenomenon essentially forms the basis for the wave-guiding of a wide microstrip when the TEM wave under the conducting strip is allowed to bounce back and forth between the two ends, without being attenuated.

In this work, the problem is analyzed by using the well known Wiener-Hopf technique. Using the conventional Jones's formulation, spectrum representation of the charge distribution (which corresponds to $\nabla \cdot \bar{J}$ where $\bar{J}$ is the induced current on the upper plate) and the normal component of $\nabla \times \bar{J}$ are derived separately up to two undermined constants. These constants are determined by requiring both the longitudinal and the transverse currents to vanish outside the conducting plate. Analytical expression for the reflection coefficient as well as the end admittance are then derived, with numerical results obtained for both the case of complete and partial reflections of the TEM wave.

B5-8
1100 MICROSTRIP LINE ON FERRITE SUBSTRATE IN THE CASE OF TRANSVERSAL MAGNETIZATION IN THE APPROXIMATION OF HARMONIC FUNCTIONS: Yu. Lauchius and V. Shugurov, Vilnius V. Kapsukas University, Vilnius, U.S.S.R.

In the case of the microstrip line on ferrite substrate with transversal magnetization H_0 it is a necessity to take into account the longitudinal components of the electric and magnetic fields. The last satisfy the system of two coupled second order differential equations. Qualitative consideration of the equations shows that harmonic functions might be taken as approximate solutions with accuracy obtainable in the TEM-approximation.

The idea of approach to the problem follows. The longitudinal components are represented as analytic functions in the form of contour integrals satisfying Laplace equations and having two unknown distribution functions. The transversal components of the fields can be then obtained by differentiating. The boundary conditions lead to the singular integral equations for the distribution functions. The zero of the system determinant gives the propagation constant which depends on geometry of the line, magnetic field H_0 and frequency (fig.I). The method enables computation of the field configuration, the density of longitudinal or transversal currents on metal surfaces. The algorithm does not depend on the number of strips and the shape of the line cross-section. We've gotten good agreement with experiments.

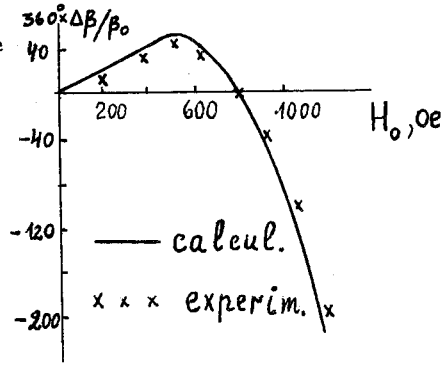

Fig.I

B5-9
1120

CHARACTERISTICS OF MICROSTRIP SLOT LINES

T. Itoh and D. Zimmerman, The University of Texas at Auston, The Department of Electrical Engineering, Austin, TX 78712

Characteristics of a new printed transmission line, the coupled microstrip-slot line, are studied. This transmission line is believed to have a number of advantages over other printed lines, such as microstrip lines, at millimeter-wave frequencies. For instance, the new transmission line has an additional degree of freedom in design process which may be used advantageously to realize low attenuation constants. Also, tightly coupled line structures may be realized with relatively large separation between lines.

In this paper, this transmission line is analyzed by using the spectral domain technique. For the formulation, we used a recently developed spectral domain impedance method which reduces analytical labor considerably, and the formulation is done almost by inspection. In addition, this formulation method tells us clearly when the surface wave poles or radiation type singularities are encountered.

NON-GAUSSIAN NOISE THEORY AND MEASUREMENT
Wednesday Morning, 7 Nov., UMC 158
Chairman and Organizer: A. A. Giodano, GTE Sylvania, 77 "A" St., Needham Heights, MA 02194

E2-1 0830 CPFSK AS A MODULATION ON THE ATMOSPHERIC IMPULSIVE NOISE CHANNEL: Thomas A. Schonhoff, The MITRE Corporation, Bedford MA 01730

Continuous phase frequency-shift keying (CPFSK) is investigated as a potential modulation on Atmospheric Impulsive Noise Channels. Theoretical estimation and Monte-Carlo simulation are used to evaluate the error rate performance in terms of E_B/σ^2 where E_B is the energy per bit and σ^2 is the received atmospheric noise variance. Two analytically tractable noise models are used in the analysis.

The error rate performance is determined for linear receivers as well as nonlinear receivers consisting of linear receivers preceded by a zero-memory nonlinearity, such as a clipper or a hole puncher. It is found that the use of CPFSK as a modulation on channels with additive atmospheric noise requires less E_B/σ^2 to achieve a given error rate than is necessary using more conventional modulations such as PSK or MSK.

E2-2 0900 MODELING AND DETERMINATION OF NON-LINEAR RECEIVER PERFORMANCE IN IMPULSE NOISE: J. W. Modesto, Rensselaer Polytechnic Institute, Troy, NY 12181

E2-3 0930 EFFECT OF THE PROPAGATION PATH ON LIGHTNING INDUCED TRANSIENT FIELDS: Robert L. Gardner, Cooperative Institute for Research in Environmental Sciences, University of Colorado, Boulder, CO 80309

A lightning flash is initiated when a stepped leader forms a conducting charged path from cloud to ground. The charged column then discharges, emitting electromagnetic energy at radio frequencies. This discharge is called the first return stroke. Learning about the discharge current pulse from observed transient waveforms is difficult because lightning flashes do not occur consistently at a given distance from the observer. Comparing measurements from lightning strokes at different distances from an observer is complex because the earth-ionospheric waveguide does not attenuate all frequencies uniformly nor does it preserve wave polarization. Colinear multi-station measurements would therefore be desirable but are not always available.

In this paper we examine the effect on a known transmitted waveform of a uniform conducting ground and ionosphere. Propagation of VLF and ELF signals in the earth-ionospheric waveguide is well studied and the propagation model we use is a combination of several well known theoretical techniques. Below 1000 Hz the earth and ionosphere are approximated by almost perfect isotropic conductors so a modal analysis technique like that of Wait (Electromagnetic Waves in Stratified Media, 2nd ed., Pergamon, 1970) is used. Above 1000 Hz asymptotic expansions near the source axis and near the interface are used for the Sommerfeld integrals in the ground wave, as in Banõs (Dipole Radiation in the Presence of a Conducting Half-Space, Pergamon, 1966). The sky wave is treated as a perturbation of the total field using anisotropic reflection coefficients in a ray-optic approximation as in Wait (Proc. IRE, 50, 1624-1647, 1962). Propagation out to distances from the flash of 200 km are covered in this way. The earth is assumed flat throughout.

The return stroke is modeled as a series of straight line segments, modeling the three dimensional tortuosity of the lightning channel. The discharge current pulse is a triple exponential waveform propagating along the tortuous channel at a constant velocity somewhat less than the speed of light. The model is fully three dimensional in that all three source current orientations are used in the model and all field components are calculated.

The model predicts that the leading edge (high frequency component) of the transient waveform is preferentially attenuated. The preferential attenuation result agrees with the measured waveforms of Uman, et al. (Radio Science, 11, 985-990, 1976).

E2-4 1020 MINIMUM SHIFT KEYING (MSK) MODEL PERFORMANCE IN VLF ATMOSPHERIC NOISE: Roger K. Cernius, Naval Ocean Systems Center, San Diego, CA 92152

Performance of multichannel MSK using combinations of linear and nonlinear receivers, channel bit rates, and post detection error detection and correction (6,5 Wagner) schemes has been empirically measured in a wide range of VLF impulsive noise.

Results are compared to analysis of linear and nonlinear coherent detection in atmospheric noise simulator. VLF statistical noise parameters such as amplitude probability distribution, crossing rates, pulse width and pulse space statistics are also given.

E2-5 1050 ATMOSPHERIC STATISTICAL NOISE ANALYZER AND RELATED INSTRUMENTATION:

Lawrence E. Christensen, Maureen E. O'Brien, and Donald J. Adrian, MEGATEK Corporation, 1055 Shafter Street, San Diego, California 92106

The MEGATEK atmospheric noise analyzer provides signal environment information required to advance the design of modems used in VLF and LF communication systems. Radio atmospheric noise impulse signals are characterized in terms of amplitude probability distributions, pulse width and space distributions and statistical moments of these distributions.

An advanced design VLF/LF radio receiver is coupled into a minicomputer which processes the data in real-time and controls the output of both raw and reduced data to a magnetic tape record/playback unit, a teletype and a graphical plotter. Both on-line and off-line plotting of statistical data in four different colors is provided. The system has 120 dB dynamic range, selectable figure eight or omnidirectional receiving patterns, and 4 selectable bandwidths. Operating frequency and monitoring cycles are under computer control.

The noise analyzer is supplemented by a portable atmospheric noise recording system which employs amplitude compression prior to tape recording followed by amplitude expansion on playback. The system provides 80 dB dynamic range in the VLF band and can play directly into the statistical noise analyzer.

E2-6
1120

WIDEBAND ATMOSPHERIC NOISE MEASUREMENTS:

A. Giordano, X. DeAngelis, H. Sunkenberg, K. Marzotto, R. Freudberg, Sylvania Systems Group, GTE Sylvania, 189 "B" Street, Needham Heights, MA 02194

This paper describes a wideband digital recording system used to record atmospheric noise at medium frequency (MF). The system consists of an RF receiving system employing quadrature demodulation to baseband, a portable digital recording system, a digital transcription system used to transfer data from high density field tape recordings onto magnetic tape, and a digital/analog real time playback system. Atmospheric noise data is recorded in 5-minute intervals at MF in Nevada using bandwidths up to 100 KHz. The recorded data is statistically analyzed to estimate noise moments, the amplitude probability distribution, power spectrum, autocorrelation function, and pulse spacing and pulse duration distributions. The results should prove useful in yielding better noise models and better estimates of communication performance for receivers operating in atmospheric noise.

SEASAT I - ATLANTIC COAST EXPERIMENT
Wednesday Morning, 7 Nov., UMC East Ballroom
Chairman and Organizer: R. C. Beal, Applied Physics Laboratory, The Johns Hopkins University, Laurel, MD 20810

F3-1
0830 A SUMMARY OF WIND AND WAVE CONDITIONS FOR 28 SEPTEMBER EXTRACTED FROM "CONVENTIONAL" DATA SOURCES: P. DeLeonibus and J. Ernst, NOAA/NESS, Washington, DC 20233

Waves of about .5 meter height from both northeast and southeast propagated through the Cape Hatteras area during SEASAT overpass number 1339 which occurred on 1500 GMT, September 28, 1978. Waves from the northeast were associated with a fetch near a high pressure ridge oriented roughly parallel to the east coast on September 27th. The high pressure ridge moved slowly to the northeast as a cold front approached. The cold front was located several hundred miles northwest of Cape Hatteras during overpass. Longer period waves from the southeast were associated with a low pressure trough several hundred miles southeast of Cape Hatteras.

F3-4 0920 A COMPARISON OF AIRCRAFT MEASUREMENTS OF SURFACE ENVIRONMENTAL CONDITIONS TO OBSERVATIONS BY SEASAT-A

Duncan Ross, Peter Black, Linwood Jones, and Robert Beal

A P3C aircraft belonging to the National Oceanographic and Atmospheric Administration's Research Flight Facility has been used to obtain surface measurements of windspeed, wave height and direction, sea temperatures, and rain distribution concurrent to the overpass by Seasat-A during Rev 1339 on 28 September 1978. The satellite pass observed an ocean area which included a developing low pressure system and an extensive range of surface wind and wave conditions. Available data from the Seasat environmental sensors will be compared to aircraft measurements. Of particular emphasis will be the snapshot of the weather system which emerges using the combined data sets as compared to conventional analysis.

F3-5
1000

MICROSCALE STRUCTURE OF OCEAN WIND FIELD AS MEASURED BY THE SEASAT-A SAR

W. Linwood Jones
E. M. Bracalente
W. L. Grantham
NASA Langley Research Center
Hampton, VA 23665

Images of the ocean surface produced at L-band by the Seasat Synthetic Aperture Radar have shown roughness patterns of order kilometer length that are postulated to be caused by changes in the wind stress at the ocean's surface. These patterns have been analyzed for revolution 1339 in the Atlantic Ocean near the Outer Banks of North Carolina as a part of the "DUCKEX" (Duck N.C. Experiment). SAR data were used to infer ocean surface friction velocity from a model of the form:

$$\sigma^\circ \propto U_*^x \cos 2\Psi$$

where σ° is the normalized radar cross section
U_* is the magnitude of wind friction velocity
x is the wind friction velocity exponent
Ψ is angle between radar azimuth and wind direction

Correlations are presented between changes in the SAR image intensity (converted to relative σ°) and ocean surface wind friction velocity inferred from the Seasat-A Satellite Scatterometer and low flying aircraft.

F3-6
1020

LOW ENERGY OCEAN WAVE DETECTION WITH THE SEASAT SAR:
R. C. Beal, Applied Physics Laboratory, The Johns Hopkins University, Laurel, MD 20810, and D. Ross, AOML/NOAA, 15 Rickenbacker Causeway, Miami, FL 33149

One of the primary purposes of the Seasat synthetic aperture radar (SAR) was to explore the possibility for synoptic monitoring of ocean wavelength and direction from space. A number of aircraft studies in the past few years have indicated that ocean swell can be imaged with SAR reliably at least for some values of wind velocity when there is a substantial component of the swell traveling along the line-of-sight of the radar. The bounds of wind, wave and geometric conditions over which reliable ocean wave detection occurs, however, remain elusive for want of an extensive experimental data base. Seasat provided a unique, although limited, opportunity to re-examine the wave detection problem without some of the artificial constraints of aircraft measurements. "Duck-X" (an acronym for the Duck, North Carolina Experiment) was one of three major Seasat SAR wave detection experiments conducted with extensive coincident surface truth during the limited lifetime of the SAR.

On the 28th of September, a well organized low energy (H_s < 1 m) 11 second swell system was detected with the Seasat SAR and successfully tracked from deep water, across the continental shelf, and into shallow water. In addition, a less organized 7 second system has been tentatively identified in the imagery. Both systems were independently confirmed with simultaneous wave spectral measurements from the Duck pier, aircraft laser profilometer data, and Fleet Numerical Spectral Wave Forecasts.

Finally, an intercomparison of the SAR radar backscatter power versus the SASS-inferred wind speed indicates a power law dependence of σ_o(L-band) ~ $U^{0.65}$ over a surface wind speed range of 2-14 m/s.

F3-7
1040

AN INTERCOMPARISON OF THE WIND MEASURING INSTRUMENTS ON SEASAT:

L.S. Fedor, NOAA/ERL/Wave Propagation Laboratory, Boulder, CO 80303
C.T. Swift, NASA/Langley Research Center Hampton, VA
E.M. Bracalente, NASA/LaRC
W. Grantham, NASA/LaRC
G.S. Brown, Applied Science Associates, Apex, NC
F. Gonzales, NOAA/ERL/Pacific Marine Environmental Laboratory
R.C. Beal, Johns Hopkins Univ./Applied Physics Laboratory

Of the five microwave instruments on board the SEASAT satellite, four are capable of measuring surface wind speeds. The SEASAT Scatterometer System (SASS) was designed to provide measurements of the ocean surface wind vector based on Bragg-scattering from centimeter-length capillary waves. The altimeter is a sub-satellite pointing microwave radar where scatter is produced by specular points distributed in height. The scanning multi-channel microwave radiometer (SMMR) measures emmissivity variations caused by surface wind stresses. And optical film density measurements of the synthetic aperature radar (SAR) imagery are used to infer surface winds.

A total of eight orbital segments were selected to intercompare windspeeds as derived from the altimeter, SASS, and SMMR. For one of these orbits (1339) the SAR had been turned on. Orbit 1339 windspeeds derived from the four instruments are studies in detail. Background information about the comparison surface data base, instrument calibration, spatial and temporal sampling, and algorithms used are presented. Intercomparison statistics are given to complete the discussion.

F3-8
1100 AN INTERCOMPARISON OF SIGNIFICANT WAVE HEIGHT (SWH) AS MEASURED BY THE SEASAT-1 RADAR ALTIMETER WITH THAT ESTIMATED BY THE FNWC SPECTRAL OCEAN WAVE MODEL (SOWM) DURING DUCK-X: W. F. Townsend, E. J. Walsh, and D. W. Hancock III, NASA Wallops Flight Center, Wallops Island, VA 23337

SEASAT-1 was a proof-of-concept mission dedicated to establishing the use of microwave sensors for remote sensing of the Earth's oceans. In this regard, a radar altimeter system was on-board and represented the first attempt to achieve 10 cm altitude resolution from orbit. Additionally, this system provided a real-time measurement of Significant Wave Height (SWH) along the sub-satellite ground track to an accuracy of ± 0.5 m or 10%, whichever is greater, over a range of SWH of 1 to 20 m, as well as providing the information required to compute the ocean backscatter coefficient (σ_o) from which wind speed along the sub-satellite ground track can be inferred. Although the SEASAT-1 spacecraft ceased operating after 99 days of on-orbit sensor operations, a high quality global data set covering that period was obtained from which a great deal can be learned.

On September 28, 1978, during revolution #1339, the SEASAT-1 ground track passed south of Duck, NC where an extensive data taking exercise involving pier mounted measurement systems and instrumented aircraft, as well as other remote sensing satellite systems, was on-going. During this pass a full complement of data was collected by the SEASAT-1 Radar Altimeter. In particular, real time measurements of SWH and return pulse shape were acquired. The return pulse shape data can be used to derive a more accurate, independent estimate of SWH as well as an estimate of the skewness of the observed surface height distribution. This independent estimate of SWH along with the real time SWH measurement will be compared against each other and against the SWH estimated by the FNWC Spectral Ocean Wave Model (SOWM). Additionally, it has recently been shown (Huang and Long, submitted to Journal of Fluid Mechanics, 1979) that the estimate of skewness can be related to the dominant ocean wavelength. Results of this analysis will also be presented and compared with that derived from the FNWC SOWM.

RECENT RADIO BEACON RESULTS - II: SCINTILLATIONS
Wednesday Morning, 7 Nov., UMC 159
Chairman: G. H. Millman, General Electric, Syracuse, NY

G3-1
0830 THE STRUCTURE OF ISOLATED SCINTILLATION ENHANCEMENTS AT THE EQUATORWARD BOUNDARY OF THE DIFFUSE AURORA

C. L. Rino and J. Owen, Radio Physics Laboratory, SRI International, Menlo Park, CA 94025

A prominent feature in nighttime auroral-zone scintillation data as measured by low-altitude ($\sim$ 1000 km) polar orbiting satellites is a pronounced localized scintillation enhancement at the point where the propagation vector intercepts the local L-shell. The phenomenon is described in Fremouw et al. (Geophys. Res. Letts., 4, 539-542, 1977), and it has been attributed to a geometrical enhancement caused by sheet-like irregularities (Rino et al., Geophys. Res. Letts., 5, 1039-1043, 1978). These structures evidently persist throughout the major nighttime precipitation regions that encompass the diffuse and the discrete aurora. During November 1977, Wideband satellite data were simultaneously recorded at Poker Flat and Fort Yukon, Alaska. The two stations are separated by $\sim$ 200 km along the geomagnetic meridian.

The data show that, although on a statistical basis there is the expected shift in the location of the geometrical enhancement, the individual patterns of the scintillation observed at the two stations are very different. The most pronounced enhancements occur when the edge of the diffuse aurora, as indicated by total electron content (TEC) data, is at or very near the point of L-shell alignment.

We have attributed this feature to a narrow columnar ionization enhancement that extends well into the F-region. By using incoherent scatter radar data from the nearby Chatanika radar, we have developed a latitudinal ionization model that accurately reproduced the TEC variations at the edge of the diffuse aurora. We believe that the structured, columnar F-region electron density enhancement is a semipermanent feature of the plasma-trough diffuse auroral boundary under nonsubstorm conditions.

G3-2
0900

PHASE AND AMPLITUDE SCINTILLATIONS OVER DISCRETE AURORA

Jules Aarons, Air Force Geophysics Laboratory, Hanscom AFB, MA 01731
John P. Mullen, Air Force Geophysics Laboratory, Hanscom AFB, MA 01731
Herbert E. Whitney, Air Force Geophysics Laboratory, Hanscom AFB, MA 01731
Michael Cousins, SRI International, Menlo Park, CA 94025
Robert C. Livingston, SRI International, Menlo Park, CA 94025

Observations have been made at Goose Bay, Labrador of phase and amplitude scintillations of the WIDEBAND satellite and of other satellites. The observational position of the site (65°C.G.L.) allows for noting the equatorward irregularity boundary during the day of the noon pass of WIDEBAND and of the poleward boundary of the irregularity region in the midnight time period. North of the poleward boundary of irregularities activity is lower in general although variations of the polar cap irregularities are not as yet available.

Levels of phase fluctuations at 137 MHz of several radians are seen polewards of the scintillation boundary during the day; at night levels of 5-10 radians at 137 MHz have been noted over discrete aurora in this initial analysis of winter data.

G3-3 0930 RADAR MEASUREMENTS OF THE ELECTRICAL PROPERTIES OF THE AURORAL-ZONE IONOSPHERE

James F. Vickrey, Richard R. Vondrak, and Stephen J. Matthews, Radio Physics Laboratory, SRI International, Menlo Park, CA 94025

Much interest has developed recently in the electrodynamic coupling between the high and low latitude ionosphere. Improvements in the model calculations of the coupling processes are limited by an inadequate description of the highly variable auroral-zone phenomena. The Chatanika radar can survey these phenomena over the latitude range 62° to 69° with a time resolution of approximately 10 minutes. Three days of observations have been analyzed to examine the diurnal variations of the auroral-zone electric field, E, conductivity, Σ, and current, J, during both quiet and active magnetic conditions. The time-varying relationships between E, Σ, and J are examined in an attempt to relate their behavior empirically to magnetic activity.

G3-4 1030 HIGH-LATITUDE IONOSPHERIC ELECTRON AND ION TEMPERATURE VARIATIONS

J. D. Kelly, Radio Physics Laboratory
SRI International, 333 Ravenswood Avenue,
Menlo Park, California 94025

This paper presents ground-based measurements of ion and electron temperatures in the high-latitude thermosphere. The structure of the thermosphere at high latitudes is strongly influenced by the highly variable auroral energy inputs. The measurements were made with the incoherent-scatter radar located at Chatanika, Alaska (L = 5.6).

The data were selected so that conditions during summer, winter, and near the autumnal equinox were sampled. In addition, the data were chosen so that both active and quiet geomagnetic conditions existed. Consequently, the variations in electron and ion temperatures and ion composition due to diurnal, seasonal, and auroral effects have been examined.

During the quiet periods, the F-region electron temperatures varied as much as 1000 K over the day/night cycle. The ion temperatures varied only 100 K over the same period. These quiet time results are similar to measurements made at midlatitudes.

The temperature variations during particle precipitation and joule heating events are quite dramatic. During precipitation, the electron temperature increased as much as 1000 K above the neutral gas temperature. The ion temperature also increased by a similar amount during a large joule heating event (30 ergs/cm^2-s).

G3-5 1100 SIMULTANEOUS INCOHERENT SCATTER AND SCINTILLATION/TOTAL ELECTRON CONTENT OBSERVATIONS IN THE MID-LATITUDE IONOSPHERE :

Sunanda Basu, Santimay Basu, Emmanuel College, Boston, MA 02115, S. Ganguly, Department of Space Physics and Astronomy, Rice University, Houston, TX 77005, and J. A. Klobuchar, Air Force Geophysics Laboratory, Bedford, MA 01731

Small scale electron density irregularities ($\sim$ 1 km) causing scintillations on VHF transionospheric communication links observed near Arecibo (dip 50°N) are associated with long period ($\sim$ 30 mins to one hour) total electron content (TEC) fluctuations. From simultaneous high resolution (height resolution 600 m; time resolution 85 secs) electron density profiles obtained by the incoherent scatter technique at Arecibo, it is found that the temporal variation of electron density at discrete heights in the bottomside F-region shows fluctuations of the same period. This indicates that the major contributions to TEC fluctuations are obtained from the region below the F-layer peak. Spectral analysis of these large scale perturbations in electron density are consistent with the ionospheric response to the passage of internal gravity waves. Measurements of ion transport made at Arecibo during such scintillation/TEC fluctuation events indicate large fluctuations of ion velocity perpendicular to the magnetic field in the meridional plane (i.e., E-W electric field) with similar periods. Possible plasma instability mechanisms responsible for the generation of small scale irregularities which may be associated with such electric field fluctuations are discussed.

G3-6 1130 FREQUENCY COHERENCE FOR TRANSIONOSPHERIC RADIOWAVES

C. L. Rino and V. H. Gonzalez, Radio Physics Laboratory, SRI International, Menlo Park, CA 94025

The Wideband satellite transmits seven phase-coherent equispaced UHF signals covering an $\sim$ 70-MHz bandwidth. These data are ideally suited for measuring the single point, two-frequency coherence function that characterizes the random frequency dispersive effects of the disturbed ionosphere. In this paper we report the results of a series of measurements made using disturbed equatorial passes.

To interpret the data, we used the phase-screen model that fully accommodates strong scattering and anisotropy. There is good overall agreement between the data and theory. In particular, the model is sensitive to the irregularity anisotropy and power-law spectral index. The data fit the theory best when highly elongated irregularities are assumed and the slope of the integrated phase spectral density function is somewhat less than 3.

The complex signal is dominated by large dispersive phase variations. The frequency coherence function is sensitive to this "quasi-deterministic" component; thus, as with the dispersive phase itself, the frequency coherence function contains a component that is measurement-interval dependent. The theory accommodates this component. Under strong-scatter conditions, the diffractive term always dominates.

ACTIVE EXPERIMENTS FROM THE SPACE SHUTTLE - II AND WAVES IN PLASMA

Wednesday Morning, 7 Nov., UMC 157

Chairman: S. H. Gross, Polytechnic Institute of New York, Farmingdale, Long Island, NY

H2-1
0830 ACTIVE IONOSPHERIC EXPERIMENTS INVOLVING STIMULATED NONLINEAR PHENOMENA: Robert F. Benson, Laboratory for Planetary Atmospheres, NASA/Goddard Space Flight Center, Greenbelt, MD 20771

Most of the plasma resonances stimulated by ionospheric topside sounders can be interpreted strictly in terms of linear plasma wave theory. Examples are the nf_H resonances where f_H is the electron cyclotron frequency and n=2,3,4... . A few resonances, however, require nonlinear mechanisms. Examples are the sequence of diffuse resonances designed by f_{Dn} where f_{D1} lies between f_H and $2f_H$, f_{D2} lies between $2f_H$ and $3f_H$, etc. (see, e.g., the review by Benson, Radio Sci., 12, 861, 1977). The $3f_H$ resonance, which is normally observed with a long time duration on topside ionograms, becomes so weak during the formation of the f_{D2} resonance that it cannot be detected. The mechanism by which the linear $3f_H$ resonance is so strongly affected by the nonlinear f_{D2} resonance is not clear. In the case of the f_{D1} resonance, two nonlinear mechanisms have been proposed which each require the linear $2f_H$ resonance (Oya, Phys. of Fluids, 14, 2487, 1971; Kiwamoto and Benson, J. Geophys. Res., in press, 1979). The $2f_H$ resonance, however, is observed with a long time duration during all of the development phases of the f_{D1} resonance.

This is one of several outstanding problems in the interpretation of the sequence of diffuse resonances. Others include the following: to determine (1) the extent of the hot plasma region, initiated by the high power sounder pulse, which drives the instability that gives rise to the non-resonant f_{Dn} waves, (2) the mechanism by which this hot region is initiated, and (3) the dependance of the proposed nonlinear mechanisms on the intensities of the various waves involved. Experiments performed from the space shuttle, using a highly flexible wave injection facility, could provide the necessary data to solve these problems.

H2-2
0900 SOUNDER OBSERVATIONS OF EQUATORIAL BUBBLES:

Robert F. Benson, Laboratory for Planetary Atmospheres, NASA/Goddard Space Flight Center, Greenbelt, MD 20771 and Wynne Calvert, Institute for Physical Science and Technology, University of Maryland, College Park, MD 20742 (permanent address: Lockheed Palo Alto Research Laboratory, 3251 Hanover Street, Palo Alto, CA 94304)

The HF sounder aboard Space Shuttle will permit extending the studies of equatorial bubbles already begun with Alouette and ISIS. Thus far it is clear that bubbles involve substantial depletions of the electron density and that they are aligned along the magnetic field [Dyson and Benson, Geophys. Res. Lett., 5, 795, 1978]. Thin, field-aligned irregularities frequently occur within a bubble. They support ducted propagation and give rise to the principal echoes observed by a sounder inside. Although weak O-mode echoes are sometimes seen, the strongest signals are X-mode. Echoes are observed from both ends of the irregularities where they intercept the equatorial anomaly, north and south of the magnetic equator. Multiple near-end echoes indicate that the irregularities are tubular in shape and probably less than one kilometer across. Z-mode echoes are also observed, but only near the magnetic equator. The Z echo has a distinctive high frequency termination which corresponds to the plasma frequency at the apex of the field line. The occasional appearance of ground echoes and terrestrial interference at low frequencies indicate that the bubble depletion may sometimes extend to the bottom of the ionosphere.

H2-3
0930 TOPSIDE Z-O COUPLING: Wynne Calvert, Institute for Physical Science and Technology, University of Maryland, College Park, MD 20742 (permanent address: Lockheed Palo Alto Research Laboratory, 3251 Hanover Street, Palo Alto, CA 94304)

The coupling of wave energy between the Z-mode and the O-mode has been used to explain the cusp triple-splitting sometimes observed with ground ionosoundes. Since topside ionograms do not exhibit triple-splitting, it has been concluded that Z-O coupling does not occur above the F-layer peak. However, Z-O coupling could be detected differently, as follows: When the peak electron density is sufficiently low, Z-mode waves with frequencies between f_ZF2 and f_HF2 can penetrate the ionosphere directly. These waves are normally absorbed in the topside near $f=f_H$. However, if the F-layer is thin and $f-f_N$ is encountered first, they could couple to the O-mode and reach a satellite at higher altitudes. ISIS-1 observes bands of man-made noise with a sharp height-frequency cutoff near f_HF2 which fit this model and could be evidence for topside Z-O coupling. Shuttle wave experiments, using a subsatellite, would permit a direct study of the Z-O coupling mechanism.

H2-4
1030

A DUCT MODEL FOR THE HALF-GYROFREQUENCY GAP IN MAGNETOSPHERIC WHISTLER-MODE SIGNALS: Wynne Calvert, Institute for Physical Science and Technology, University of Maryland, College Park, MD 20742 (Permanent address: Lockheed Palo Alto Research Laboratory, 3251 Hanover Street, Palo Alto, CA 94304); and Kaichi Maeda, Laboratory for Planetary Atmosphere, NASA/Goddard Space Flight Center, Greenbelt, MD 20771

The whistler-mode signals received by satellites in the equatorial plane outside the plasmapause exhibit a missing band at half the electron gyrofrequency. A new explanation of this frequency gap is proposed, involving ducted propagation along magnetic-field-aligned electron-density irregularities. The signals below $f_H/2$ are attributed to ducting in enhancement irregularities (crests) comparable to those which guide lightening whistlers. The signals above $f_H/2$ are attributed to ducting in similar depletion irregularities (troughs). Crest ducting occurs only below $f_H/2$. For weak irregularities and small wave angles, trough ducting occurs at frequencies near and above $f_H/2$. Where the magnetic field strength varies between the source location and the observing location, crest ducting will be limited by the smallest $f_H/2$, and trough ducting by the largest. Thus the two components will separate in frequency and produce a gap. This explanation suggests that trough irregularities also exist, along with crest irregularities, and that they affect the observations of whistler-mode signals outside the plasmapause.

H2-5 THE FOCUSING EFFECT OF RADIO WAVES IN MAGNETOPLASMA:
1100 M. C. Lee, Megatek Corp., San Diego, CA 92106

Focusing instability of the heater waves in ionospheric modification experiments seems to be responsible for the temporal variation of f.a.s.(Fialer, 1974). This instability is also needed to explain the discrepancy between the theoretical prediction and the experimental observation of f.a.s.(Lee and Fejer, 1979). We investigate the spatial growth of the focusing instability of e.m. waves in magnetoplasma, so that we can assess the power flux enhancement of o-mode heater waves.

The threshold power flux to produce this instability is less than 1 $\mu w/m^2$ in ionospheric F region. An o-mode radio wave of 6 MHz is estimated to increase its power flux by this instability from an initial value of 50 $\mu w/m^2$ to a final value of about 200 $\mu w/m^2$, before it trasfers its energy to a spectrum of plasma waves via parametric instabilities near its reflection point.

H2-6
1130

NONLINEAR PLASMA RESONANCE CONE SURFACES:

H.H. Kuehl, Electrical Engineering Department, University of Southern California, Los Angeles, CA 90007.

When a magnetized plasma is excited by a spatially-localized radio-frequency source with a frequency that is either below the smaller of the plasma and cyclotron frequencies (lower branch) or between the larger of the plasma and cyclotron frequencies and the upper hybrid resonance frequancy (upper branch), the electric field is enhanced on a surface called the resonance cone. Because the field is relatively large on the resonance cone, it is expected that nonlinear effects may be significant. In a two-dimensional geometry, the nonlinear distortion of the resonance cones is governed by the complex modified Korteweg-de Vries equation. However, in many cases of practical interest in which the resonance cones are excited by a small localized source, such as an antenna immersed in a plasma, the geometry is three-dimensional. Therefore, we consider the nonlinear modification of the equation describing the resonance cone surface in a three-dimensional geometry when the exciter is a spatially-localized radio-frequency source in a magnetized plasma. The nonlinearity is assumed to be due to the ponderomotive force. The nonlinear modification of the slope of the resonance cone is most pronounced near the plasma and upper hybrid frequencies, and is inversely proportional to the distance from the exciter. For frequencies of the lower branch the slope is decreased, whereas for the upper branch frequencies the slope is increased.

GENERAL SESSION
Wednesday Morning, 7 Nov., UMC 235
Chairman; M. H. Cohen, Caltech, Pasadena, CA 91125

J4-1 0830 QUASAR PROPER MOTION STUDY: VLBI OBSERVATIONS OF 1038+528:

M. J. Reid, F. N. Owen, and D. B. Shaffer, NRAO, Charlottesville, VA 22901; K. I. Kellermann and A. Witzel, MPIR, Bonn, W. Germany

The radio source at 1038+528 consists of two radio quasars separated in angle by only 33 arcseconds. These quasars possess substantially different redshifts (0.7 and 2.3), and thus their extremely close proximity in the plane of the sky is almost certainly a chance projection effect. These sources offer an opportunity to determine the relative proper motion of two independent objects with relative positional accuracies at the micro-arcsecond level. If over a period of years a relative proper motion is discovered, it would have profund implications regarding standard interpretations of the Hubble expansion. On the other hand, the absence of a detectable proper motion would strongly suggest that these objects are very distant--independently of their redshift distance.

We report on an experiment using the MPI 100-m and the NRAO 43-m telescopes in which we observed 1038+528 at a frequency of 5 GHz. Both quasars were detected with this interferometer. The northern quasar appears unresolved, while the southern one possesses structure on a milli-arcsecond scale. Given a model for the southern source, the relative position of the two sources is determined to an accuracy of about 50 micro-arcseconds. A second experiment to investigate potential time variations of the source structure, to considerably improve the relative positional accuracy, and to examine other source pairs will be attempted. In concluding we discuss the practical limitations of QSO proper motion studies, and comment upon the possibilities of future improvements using the enhanced capabilities of the Mk III VLBI system.

J4-2 0855 TESTS FOR COHERENCE IN RADIO PULSES FROM M87:

I.R. Linscott, Dudley Observatory, Schenectady, NY 12308

Radio pulses were detected during observations of M87 at Arecibo in May 1979, using the 430 MHz, 606 MHz, and 1420 MHz feeds. The pulses appear as narrow enhancements in Fourier spectra which drift slowly down in frequency with time. The full Fourier amplitude and phase of contiguous spectra were recorded in real-time during the observations. Consequently, predetection dispersion removal and coherence measurement have been performed on these pulses. The degree of coherence after dispersion has been removed is presented as a function of observing frequency.

J4-3 0920 MULTI-FREQUENCY OBSERVATIONS OF PULSE STRUCTURE:

B.J. Rickett, Department of Electrical Engineering and Computer Sciences, University of California, San Diego 92093 and J.M. Cordes, Department of Astronomy, Cornell University, Ithaca, New York 14853

Pulsar observations were made at Arecibo using the log periodic dual polarization feed and frequency-agile receiver over the range 70 to 450 MHz. The receiver can be set to a new frequency in less than 10 milliseconds by on-line control of the local oscillator. By exploiting the dispersion delay, we sampled the same pulse at several frequencies (from three for short period pulsars to twelve for long period pulsars). In each case total intensities were recorded from two bandwidths, chosen to give a time resolution of one millisecond. Polarization studies must await calibration of the feed polarization.

The large volume of data recorded from several pulsars is being analyzed to yield subpulse structure versus frequency. The effects of interstellar scintillation will be identified and corrected for by studying total pulse energy versus frequency and time, or by comparing leading with trailing components in double pulsars. The motivation for the observations is to look for evidence on the intrinsic bandwidth of the emission process. By studying subpulse widths, delays and detailed shape versus frequency and longitude, we hope to distinguish between narrow band emission from a range of heights and broad band emission from a single height. System performance and preliminary results will be presented.

J4-4 0945 VERY LARGE ARRAY OBSERVATIONS OF SOLAR ACTIVE REGIONS, Kenneth R. Lang and Robert F. Willson, Department of Physics, Tufts University, Medford, MA 02155

Very Large Array (V.L.A.) synthesis maps of the total intensity and the circular polarization of three active regions at 6 cm wavelength are presented. The radiation from each active region is dominated by a few intense cores with angular sizes of $\sim 0.5'$, brightness temperatures of $\sim 10^6$ K, and degrees of circular polarization of 30 to 90%. Some of the core sources within a given active region exhibit opposite senses of circular polarization, suggesting the feet of magnetic dipoles, and the high brightness temperatures suggest that these magnetic structures belong to the low solar corona. We also present comparisons between our V.L.A. maps of circular polarization and Zeeman effect magnetograms of the lower lying photosphere. There is an excellent correlation between the magnetic structures inferred by the two methods, indicating that synthesis maps of circular polarization at 6 cm can be used to delineate magnetic structures in the low solar corona.

GUIDED WAVES I: RANGE DEPENDENT
MODES AND HYBRID REPRESENTATIONS
Commission B, Session 6, Commissions F and G, Session 4
UMC Forum Room
Chairman: J. R. Wait, ERL/NOAA, Boulder, CO 80303

B6/F4
G4-1
1355

WAVE DUCTING IN LATERALLY NON-UNIFORM MEDIA

F. S. Chwieroth, R. D. Graves, A. J. Haug, A. Nagl, H. Überall, and G. L. Zarur
Department of Physics, Catholic University
Washington, DC 20064

Studies on the propagation of scalar fields in laterally non-uniform ducts have been performed, with application to acoustic propagation in under-ocean sound channels. The method of calculation used was the adiabatic mode theory of A. D. Pierce (J. Acoust. Soc. A. 37, 19 (1965))and D. M. Milder (J. Acoust. Soc. Am. 46, 1259 (1969)). This theory, however, in addition furnishes mode coupling terms which have also been considered by us for some cases.

The following examples have been treated by us: (a) adiabatically: a homogeneous wedge-shaped duct; a parabolic wave number profile which opens up with range; a numerically given general profile with general range dependence; (b) including mode coupling: the parabolic profile opening up with range. A program for the generally z- and r-dependent case has also been written, with results now being obtained.

The same approach has also been used for the problem of coupled mode propagation in the ionospheric day-night transition region. A computer program has been written and will be discussed.

(Supported by the Office of Naval Research, Code 486, and by the Naval Research Laboratory, Washington, DC, Code 8120).

B6/F4/G4-2 1330

Range - Dependent Modes: A Survey of Asymptotic Techniques

L. B. Felsen, Department of Electrical Engineering, Polytechnic Institute of New York, Farmingdale, N. Y. 11735

When the medium properties of a guiding channel vary along the direction of propagation, the modes defined with respect to the longitudinally invariant structure become coupled. If the longitudinal variations, which may include curvature of the axis, are small over an interval corresponding to the local wavelength, one may employ asymptotic methods to allow local adaptation of a mode field to the changed conditions, thereby eliminating the weak coupling between forward propagating unperturbed modes. Various approaches have been employed to deal with this problem, depending on whether guiding occurs due to the presence of reflecting boundaries, due to refraction in a transversely inhomogeneous medium, or due to a combination of these. They involve local treatment of standing wave fields, modal ray congruences and their associated caustics, and evanescent fields. These methods are reviewed, with emphasis on their physical implications.

B6/F4/
G4-3
1420

TRANSMISSION AND REFLECTION SCATTERING COEFFICIENTS IN AN IRREGULAR SPHEROIDAL MODEL OF THE EARTH-IONOSPHERE WAVEGUIDE

E. Bahar, Electrical Engineering Department,
University of Nebraska, Lincoln NE 68588

Using a full-wave approach (E. Bahar, Radio Science, 11, 137-147, 1976), propagation of low frequency radio waves in an irregular spheroidal model of the earth-ionosphere waveguide, is investigated. The perturbation considered here results in the variation of the effective height of the ionosphere along the propagation path. For simplicity the waveguide parameters and the fields are assumed to be independent of the azimuth angle ϕ. Using a complete expansion of the fields and imposing the boundary conditions at an irregular surface, Maxwell's equations are converted into sets of coupled ordinary differential equations for the wave amplitudes. The wave amplitudes which are subject to mixed boundary conditions, are expressed in terms of auxiliary functions with unmixed boundary conditions to obtain rigorous numerical solutions to the differential equations.

The analysis can be used to compute the perturbed fields inside and outside the irregular regions of the earth ionosphere waveguides. Since low frequency radio waves are used for navigation, special attention is given to the phase anomaly and the advantages of exciting the earth detached mode are considered in detail.

An illustrative example is presented and the transmission and reflection scattering coefficients that characterize wave scattering by a perturbed ionosphere excited in both directions, are given. The results are in agreement with reciprocity relationships in electromagnetic theory. Since an irregular spheroidal model is analyzed, rather than an approximate cylindrical model, this work can be used to investigate antipodal effects.

B6/F4/G4-4 1505 NUMERICAL TECHNIQUE TO SOLVE THE COMPLEX ROOTS OF MODAL EQUATIONS APPLIED TO VLF RADIO PROPAGATION IN SPHEROIDAL WAVEGUIDES: E. Bahar and M. Fitzwater, Electrical Engineering Department, University of Nebraska, Lincoln, NE 68588

While various efficient techniques have been developed to solve modal equations with real roots, more versatile numerical techniques need to be developed to compute the complex roots of modal equations for dissipative layered structures, characterized by complex electromagnetic parameters, such as the earth-ionosphere waveguide. Some of the numerical methods currently employed are based on use of the two-dimensional Newton-Raphson technique together with good initial estimates of the complex values of the roots. Other numerical techniques are based on the phase integral properties of analytic functions of complex variables with isolated poles.

In general the attenuation coefficients do not progressively increase as the corresponding phase velocities increase. For example, in the earth-ionosphere waveguide, the attenuation coefficients for some of the lower order earth-detached modes may be larger than the attenuation coefficients for the regular earth-ionosphere waveguide modes. Thus a rectangular region in the complex plane, where all the significant modes lie, cannot in general be identified with certainty. Furthermore, for modes of grazing incidence at the earth's surface, the amplitude and phase of the reflection coefficient for vertically polarized waves fluctuate very rapidly. In these regions it is difficult to evaluate phase integrals.

Using the numerical technique developed in this work, a common locus on which all the complex roots lie is determined. As the phase velocity is increased along this locus the roots of the modal equation are determined. It is not necessary to obtain good initial estimates of the complex roots, nor is it necessary to extract the poles of the modal equation and to perform phase integrals in rectangular regions of the complex plane, in order to determine the roots. Furthermore, only one analytic form of the modal equation (involving spherical Bessel functions) is used for all the computed modes. Since the dimensions or the electromagnetic parameters of the waveguides vary along the propagation path, the locus of each root of the modal equation is determined for the given propagation path.

B6/F4/
G4-5
1530

Hybrid Ray-Mode Representation of Parallel Plane Waveguide Green's Functions

A. Kamel and L. B. Felsen, Electrical Engineering Department, Polytechnic Institute of New York, Farmingdale, N. Y. 11735

Source-excited propagation in a multimode parallel plane waveguide can be analyzed exactly in terms of a guided mode expansion and approximately in terms of a ray-optical expansion involving direct and multiply reflected rays. If the waveguide is strongly overmoded, either summation scheme is inconvenient. It is then desirable to employ an alternative representation comprising an appropriately chosen mixture of rays and modes, which is numerically much more efficient than either the ray series or the mode series. The hybrid formulation is derived from the rigorous Green's function for waveguides with perfectly conducting and impedance boundaries, and also from partial Poisson summation of the ray or mode series. It is found that a few rays can account for a cluster of far-from-cutoff modes whose characteristic plane wave propagation directions are nearly axial, whereas a few near-cutoff modes can account for the cumulative effect of rays undergoing many reflections. The accuracy of the hybrid representation is illustrated by numerical results computed for various ray-mode combinations and physical parameters.

B6/F4/G4-6
1555

A HYBRID REPRESENTATION FOR OPTICAL WAVE PROPAGATION IN AN OVER-MODED SLAB DIELECTRIC WAVEGUIDE:

David C. Chang, Edward F. Kuester and Setsuo Nakayama,
Electromagnetics Laboratory, Department of Electrical Engineering, University of Colorado, Boulder, 80309

The problem of optical wave propagation in a single-mode step-index fiber, as well as in a parabolic graded-index fiber guide has been investigated extensively in the literature. Although these waveguides are inherently broad band, and hence, more suitable for long-range trunk communication, many of the current applications of fiber optics are limited to large fibers and fiber bundles excited by incoherent light sources (i.e. LED) primarily because of the low cost and long life time. These fibers are typically so large that virtually hundreds of surface wave modes can exist. Since each of these modes propagate at a different phase velocity, interference among the modes in a fiber become an important consideration. Perhaps also because of this reason, very little has been done in the literature in trying to understand the propagation of optical waves in this type of waveguide system.

Based upon an assumption that the bulk of optical power is carried by low-order modes where the corresponding "rays" are paraxial, a simple theory concerning the propagation of an optical wave in an over-moded slab waveguide can be constructed without resorting to a detail modal analysis. The theory is devised from an earlier observation of the so-called Fresnel images which stated that an optical beam propagating in an over-moded guide can be split into a different number of individual beams at discrete distances along the guide. For distances in between those where the multiple beams are formed, a representation analogue to the Gaussian beam propagation in free-space can be used, provided of course, secondary sources due to the reflective boundaries are taken into account. We shall discuss in this paper, the physical implication of the new hybrid representation in analyzing fiber-to-fiber coupling problems.

B6/F4/G4-7
1620

High Frequency Fields Inside Regions with Concave Boundaries

E. Topuz, S. H. Cho, E. Niver and L. B. Felsen,
Electrical Engineering Department, Polytechnic Institute of New York, Farmingdale, N. Y. 11735

This investigation deals with the determination of high frequency fields due to an axial line source located arbitrarily in a region bounded by a perfectly conducting concave cylindrical surface. It has previously been shown that if the source and observation points are placed on the boundary, a purely ray-optical treatment will fail because ray optics cannot account for ray fields undergoing many reflections. Therefore, alternative field representations, such as hybrid ray-mode formulations, must be introduced to overcome this inadequacy. As the source and(or) observation points move sufficiently far off the boundary, high order reflected ray fields do not contribute, and one may show that ray optics is satisfactory, except in the vicinity of ray caustics that arise due to focusing effects of the concave boundary. To deal with the caustic transition regions, uniform asymptotic methods can be utilized. However, this approach becomes complicated when the caustics form cusps and when several caustics or caustics and cusps become contiguous. The transition problem can be avoided by resorting to alternative field representations. One of these involves a hybrid ray-mode mixture wherein a properly chosen number of whispering gallery (W.G.) modes and a number of rays less than the maximum, is utilized. Another, which applies especially near the boundary, involves the maximum number of admissible rays plus a canonical integral to account for the high order reflected fields.

The validity of these various representations is examined by comparing numerical results derived from them for a broad range of source and observation point locations with those of a rigorous reference solution comprised of the complete W.G. mode series plus a continuous spectrum integral, with emphasis also on the physical interpretation of the various forms of the solution. Also discussed is the corresponding problem for surface-guided waves in a plane duct with transversely inhomogeneous refractive index.

ANTENNAS
Wednesday Afternoon, 7 Nov., UMC West Ballroom
Chairman: J. Mink, U.S. Army Research Office, Research Triangle Park, NC 27709

B7-1
1330 INVESTIGATION OF AN ARBITRARILY ORIENTED THIN-WIRE ANTENNA NEAR A BODY OF REVOLUTION:
Allen W. Glisson and Chalmers M. Butler, Department of Electrical Engineering, University of Mississippi, University, MS 38677

The problem of an arbitrarily oriented thin-wire antenna located near a body of revolution is analyzed. The usual integro-differential equation for a thin wire in unbounded space is generalized to account for scattering from the nearby body. The presence of the body is accounted for by a numerical, dyadic Green's function. The modified wire equation is solved by standard numerical techniques to obtain the current distribution on the wire.

Numerical and measured input admittance data have been obtained for several cases of interest. Effects of various bodies on input admittance are compared with results for an isolated antenna. Measurements were performed to determine the input admittance for a monopole above a ground plane located near several different bodies of revolution resting on the ground plane including a hemisphere, several closed- and open-ended cylinders, and a truncated cone. Experimental and theoretical results are found to be in good agreement. For the case of a wire near a sphere, measured results are compared with numerical results obtained both by the numerical Green's function approach and an analytical Green's function approach.

B7-2
1350

DESIGN OF A SQUARE WAVEGUIDE FEED:

C.Q. Lee, Sharad R. Laxpati, Wilson Ishu+, and Frank Hamma+, Department of Information Engineering, University of Illinois at Chicago Circle, Box 4348, Chicago, IL 60680

A feed element for a large reflector antenna is usually characterized by pattern symmetry, low sidelobes and backlobes. Naturally, pyramidal and sectoral horns with and without corrugations are the frequent choices. Recently, Donn, et al. (1979 AP-S Symposium Digest, pp. 282-5) discussed a square corrugated horn feed.

This paper presents experimental design study of a coaxial, square waveguide antenna that would be suitable as a reflector antenna feed. The structure investigated is a square waveguide with coaxial circular conductor and is operating in x-band. The waveguide element is designed to support TE_1 mode only (Lee and Christian, Proc. IEEE, 61, pp. 1754-5, 1973). The geometrical and mode pattern symmetry should result in an equal E- and H-plane radiation patterns.

The laboratory measurements show that the antenna has almost symmetric pattern with a half power beamwidth of about 45 degrees over a reasonable frequency band. The paper will discuss the design considerations and the measured data. It will also discuss a technique for varying the beamwidth.

+Northrop Defense Systems Division, Rolling Meadows, IL.

B7-3 1410 OFFSET BIFOCAL DUAL REFLECTOR ANTENNAS WITH PROFILE OPTIMIZATION: V. Galindo-Israel and R. Mittra, Jet Propulsion Laboratory, California Institute of Technology, Pasadena, CA 91103; and M. Sheshadri and A. Cha, University of Illinois, Urbana, IL 61801

A bifocal dual reflector antenna has two perfect geometrical optics focii in a given profile. Hence each feed, placed at a focal point, will produce a perfect plane phase front, each in a distinct direction. The bifocal reflector antenna thus provides the possibility of improved wide angle scanning or multi-beam operation of a reflector antenna. Considerable work has already been done in the synthesis, analysis, and construction and testing of the bifocal reflector antenna in the U.S.S.R., Britain, Japan, and the U.S.

The synthesis procedure published to date has generally been for a cylindrical geometry with symmetry about a given axis. Extension to three dimensions has been accomplished by rotation of the cylindrical profile about the axis of symmetry - thus generating a surface of revolution (for the main and sub-reflectors) with an approximate focal 'ring'.

Since many spacecraft antennas which require multiple beams are often unable to tolerate substantial aperture blockage, we have extended the synthesis procedure so as to generate an offset (clear aperture) bifocal dual reflector antenna profile (cylindrical design). The generation of a three dimensional offset geometry can then be accomplished by one of several means - depending upon the design objectives. That is, either a perfect two focal point design can be sought or an approximate but wider focussed region can be designed.

The synthesis procedure for either the symmetric or offset profiles generates a series of points (and slopes) dividing segments of the main and subreflector profiles. The reflector profiles are constrained to pass through these points with the correct slope in order to satisfy the bifocal requirement. In one case, these 'constraining points' become lines when the offset cylindrical profile is used to generate a three dimensional offset bifocal antenna. It does not appear to be well understood that only one segment between the constraining points of the profile can be specified independently. The remaining segments on both reflectors are then determined uniquely by the same iterative bifocal procedure by which the constraining points (and slopes) were first determined. However, the degree of freedom afforded by the arbitrariness of any one profile segment can be used to enhance the focal properties of the reflector pair at a third point between the two perfect focii. Optimization of the feed off-focus position (B. Claydon, Electronics Letters, 1973) gives further improvement.

B7-4
1430 ILLUMINATION SYNTHESIS FOR WIDEBAND NULLS IN LOW SIDE-LOBES RADIATION PATTERNS: Giorgio V. Borgiotti and Timothy Carey, Raytheon Co., Bedford, MA

A technique has been established for the synthesis of antenna illuminations generating radiation patterns having nulls in arbitrarily specified directions that are preserved on a wide band. The synthesis method is direct, in the sense of not being based on iterative optimization techniques, and is computationally straightforward. Also, it is very general being applicable to linear and planar arrays or continuous apertures, with unperturbed illuminations - prior to the nulls placements - that are not restricted to special classes and can be arbitrarily chosen. The method has the desirable feature of producing only local modifications in the neighborhoods of the null directions of the antenna pattern that remains elsewhere virtually identical to the desired unperturbed pattern. The idea at the basis of the method consists in determining an illumination that has a minimum quadratic deviation from the unperturbed illumination under the constraint of having its radiation on pattern and a chosen number of its derivatives equal to zero at the direction of the null. It is shown that the problem consists mathematically of finding, in an appropriately defined Hilbert space, a vector (representing the illumination sought) having the minimum distance from an assigned vector (the unperturbed illumination) and constrained to be orthogonal to a certain subspace whose dimensionality is equal to the number of pattern nulls multiplied by the number of constraints per null. As numerical examples the pattern of an array of 73 elements with an unperturbed sampled Taylor illumination with 25 dB nominal sidelobe level, has been calculated, with nulls having a number of constraint ranging from one to five. Three constraints are sufficient, to guarantee a null depth greater than -70 dB below the peak of the beam on a 10 % bandwidth.

B7-5
1510

ANALYSIS OF AN ANNULAR SLOT IN A PARALLEL-PLATE WAVEGUIDE EXCITED BY A RADIALLY-TRAVELING TEM WAVE

Chalmers M. Butler and Talya L. Keshavamurthy,
Department of Electrical Engineering, University of Mississippi, University, MS 38677

A parallel-plate waveguide with an annular slot of uniform width in its upper plate is considered in this paper. The guide is excited by a known, radially-traveling TEM wave which is incident upon the slot. An integral equation is formulated for the unknown electric field in the slot and it is solved numerically for several combinations of plate separation, slot width, and contrast between interior and exterior dielectric constants. From the solutions for the slot electric field, one determines the scattering parameters for the discontinuity due to the presence of the slot as well as the pattern of the fields radiated by the slot. Data are presented for several cases of interest.

B7-6
1530

MICROSTRIP OPEN-CIRCUIT NEAR-FIELD ANALYSIS

T.M. Ruehle and L. Lewin, Electromagnetics Laboratory, Department of Electrical Engineering, University of Colorado, Boulder, Co. 80309.

Using the near-field Poynting vector method (L. Lewin, **Proc. IEE, 125**, 633-642, 1978) the radiated power and the end-effect reactance of a microstrip open-circuit resonator have been solved for. It is desirable to try to obtain a relatively simple correction to the quasi-static method of obtaining the reactance correction of a microstrip resonator because the quasi-static solution breaks down at higher frequencies while other methods (T. Itoh, **IEEE Trans., MTT-22**, 946-952, 1974) tend to require large amounts of computer resources and the results, because they are not analytic, are difficult to generalize. The radiated power obtained using the near-field Poynting vector method agrees identically with results using the far-field method. The reactance obtained gives some improvement on the quasi-static results in a comparison with the more complex numerical methods of Itoh.

The radiated power results contain terms that are length-independent and are identical to the semi-infinite results obtained by Lewin, and terms that are due to the mutual influences between the ends, and which decrease as the length of the resonator gets large. These results are also identical with those obtained by Watkins (J. Watkins, **IEEE Trans., MTT-21**, 636-639, 1973) and Danielson and Jorgensen (M. Danielson and R. Jorgensen, **IEEE Trans., AP-27**, 146-150, 1979).

The reactive results can be separated into two groups; the first one represents a quasi-static reactance per unit length, and the second contains a term which refers basically to a high frequency phonomenon. The reactance per unit length can be interpeted as a line fringe capacitance, but this feature was not an intended goal of the analysis and represents an additional 'spin-off' of the method. Combining the quasi-static end capacitance result (A. Gopinath **Calculation of Microstrip Discontinuity Circuit Parameters**, Annual Report, RU 24-13, School of Electronic Engineering Science, Univ. college of North Wales, Bangor) and the high frequency term, the final result compares more favorably with the results obtained by Itoh.

B7-6
1530

MICROSTRIP ANTENNA WITH POLARIZATION DIVERSITY:

Daniel H. Schaubert and Frederick G. Farrar, US Army ERADCOM, Harry Diamond Laboratories, 2800 Powder Mill Rd., Adelphi, MD 20783

A microstrip antenna has been developed with the unique property that its polarization can be altered by changing the position of shorting posts in the antenna. Four types of polarization (horizontal linear, vertical linear, right-hand circular, and left-hand circular) may be obtained from a single microstrip radiator without changing its dimensions or feed location. Circular and square patch radiators have both given excellent results.

Linear polarization diversity is achieved with the square patch by feeding it along a diagonal and placing shorting posts midway along opposing sides of the patch. Vertical polarization is achieved when the posts are at the left and right sides, and horizontal polarization is achieved when the posts are at the top and bottom. Cross polarization levels 25 dB below the desired polarization are typical. Replacing the shorting posts with rf switching diodes permits electronic selection of the polarization.

Circular polarization is obtained from the same basic antenna by moving the shorting posts near the center of the patch. The axial ratio is controlled by the spacing between the shorting posts and the sense of polarization is controlled by the orientation of the posts relative to the feed. The antenna is well-matched for both polarizations, and axial ratios of less than 2 dB are achieved over a large portion of the beam.

B7-8 1610 ANALYTICAL/NUMERICAL METHOD FOR THE EVALUATION OF THE RADIATION PATTERN OF AN APERTURE ON A CONDUCTING CYLINDER COVERED BY A RADIALLY INHOMOGENEOUS LOSSY DIELECTRIC:

Giorgio V. Borgiotti, Raytheon Co., Bedford, MA

The electromagnetic field of an aperture radiating through a lossy radially inhomogeneous dielectric is obtained by numerically solving the system of ordinary differential equations, with variable coefficients, representing a propagation in the radial direction of the coefficients of the longitudinal and azimuthal Fourier expansion of the field. The enforcement of the appropriate boundary conditions on the conducting cylinder and on the outer surface of the dielectric layer uniquely specifies the solution. Once the tangential electric field on the dielectric outer surface is obtained, the radiation pattern is evaluated through a straightforward well known procedure. This analytical/numerical approach has been found more desirable than the alternative method of modeling the dielectric layer in a stepwise fashion as a multilayered system. Comparison of the two methods shows that the direct numerical integration of the field equations has the primary computational advantage of not requiring the evaluation of Hankel functions of complex argument, a most difficult task. Other secondary advantages are reduced computer storage and simpler Fortran coding. As numerical examples the radiation patterns of a circular aperture having a transverse electric field distribution equal to that of the dominant mode of a circular waveguide have been calculated for different radial profiles of the complex constant within the dielectric layer.

B7-9 1630 AN APPROACH FOR DETERMINING INTERBEAM ISOLATION IN MULTIPLE BEAM APPLICATIONS: Y. Rahmat-Samii and C. Coyle, California Institute of Technology, Pasadena, CA 91103

The use of multiple beam antennas in satellite communications has created a need to obtain detailed knowledge of the interaction of individual beams in the far field. Accurate data on isolation is vital to any study which attempts to optimize beam shape and separation to obtain desired coverage, frequency reuse, etc. Reasonable results to this end have been achieved using an upper envelope approximation to the sidelobes of interfering beams providing a kind of upper-bound analysis (IEEE Communications Society Magazine, Mar. 1977, pgs. 9-15). This method, especially in cases with many simultaneous beams, would likely provide an overly pessimistic conclusion as to the quality of separation.

Accurate calculation of the isolation can become rather tedious if one uses the standard way of evaluating the radiation integral as it involves computing numerous antenna patterns for various azimuth angles, both principal and cross-polarized, and evaluating these for multiple positions within each beam coverage area. This presentation deals with a novel method of accurately determining isolation among beams using a very efficient method of determining the far field [IEEE Antenna and Propagat. May 1979, pgs. 294-304]. Associated with each beam is a set of coefficients which are independent of observation points allowing one to obtain the far field at any point. Vector far fields for all beams are then computed at a point on the footprint of the desired beam using the coefficients in a Jacobi-Bessel series expansion of the field. The isolation factor is obtained as the incoherent sum of the copolarized components of the power densities of all the interfering beams normalized to the power density of the desired beam for a particular polarization. Studies have been conducted for both linear and circular polarizations for a multiple feed system illuminating an offset parabolic reflector. In the linear case, the direction of polarization along which isolation is measured is taken as the major axis of the E-field ellipse of the desired beam. This assumes that the receiver will be polarized for maximum signal strength. Extensive numerical results will be presented for patterns as well as contour plots of the isolation among various beams for various practical configurations.

NOISE AND INTERFERENCE, MODELS AND SYSTEM DESIGN
Wednesday Afternoon, 7 Nov., UMC 157
Chairman: M. Nessenbergs, NTIA/ITS, Boulder, CO 80302

E3-1
1330

ON WORST-CASE ADDITIVE INTERFERENCE FOR M-ARY SIGNALING AND CORRELATION RECEIVERS:

J. M. Morris, Naval Research Laboratory,
Communications Sciences Division,
Washington, DC 20375

Specification of the worst-case additive interference for M-ary signaling and recievers using pre-decision correlation is obtained. The interference is constrained by average power and peak amplitude upperbounds on its Fourier transform. In addition, no statistical description is assumed. The performance measure is a weighted (± 1) sum of the correlations between the received corrupted-signal Fourier transform $R_m(f)$ and each member of the signal set Fourier transforms $\{S_m(f)\}$. This measure also depends on the signal-present probability p. Functional analysis concepts are utilized to state and solve the resulting generalized-Lagrange-multiplier problem in L_2.

The worst-case interference function $W^o(f)$ is shown to have an average power equal to the average power upperbound and is independent of p. A key parameter may need numerical techniques for evaluation. This power level is achieved with W^o as a clipped multiple of $|\Sigma S_m|$ that follows the phase of $\Sigma S_m(f)$. The clipping level is the peak amplitude upperbound.

The worst-case performance is explicitly expressed in terms of W^o. Upper and lower bounds are also derived with respect to arbitrary signal sets. Additional bounds are obtained for interference functions independent of the signal set magnitudes and/or phases. As a recommendation to minimize the worst-case performance, the communicator should transmit with a high average probability per signal pM^{-1} for a given fixed sum $\Sigma S_m(f)$ and $\tilde{S}_m(f)S_n(f) = 0$, $m \neq n$, $\forall m, n$. However, to weaken the effectiveness of some sub-worst-case interference, compared with the worst-case, the communicator should transmit with low average probability for signal pM^{-1} and a phase of $\Sigma S_m(f)$ close to π. Further investigation of good signal sets is warranted.

E3-2
1400

NEW CANONICAL NON-GAUSSIAN EM NOISE AND INTERFERENCE MODELS AND RECEIVER PERFORMANCE THEREIN [Ref. A]

David Middleton, Contractor, National Telecommunications and Information Administration, Institute for Telecommunication Sciences, Boulder, CO 80303

The aim of this paper is to provide a concise technical summary of the principle noise/interference model results ([1]-[11], cf. Ref. A. below), developed by the author to date, and to consider their implications for: (1) measurement; (2) performance prediction and evaluation. [A. "Canonical Non-Gaussian Noise Models: Their Implications for Measurement and for Prediction of Receiver Performance", Proc. 3rd Int'l. Symp. on Electromagnetic Compatibility, Rotterdam (The Netherlands), May 1-3, 1979; also, IEEE Trans. EMC, Vol. EMC-21, No. 3, August, 1979.] The discussion is illustrated by a short review of model statistics and methods of estimating model parameters. A selection of typical signal detection problems are similarly employed to illustrate the very large potential improvement possible when optimum processing algorithms are employed, vis-a-vis currently used systems, which are conventionally (nearly) optimized for gaussian noise/interference. These new noise models make possible, for the first time, a systematic treatment of real world EMI environments, both for measurement, assessment, and receiver performance therein.

E3-3
1430

THE ROBUSTNESS OF THE LOCALLY OPTIMUM DETECTORS FOR NON-GAUSSIAN NOISE:

A.D. Spaulding, National Telecommunications and Information Administration
Institute for Telecommunication Sciences
Boulder, CO 80303

In this paper the performance of various nonlinear detection schemes are compared with the performance of the locally optimum threshold (small signal) detector. It is shown that, for a wide range of non-Gaussian impulsive noise conditions, performance is degraded only slightly by using appropriate suboptimum nonlinearities (e.g., hard limiter and adaptive clipper) in place of the optimum nonlinearity. In addition, this paper also investigates the robustness of the various nonlinearities (optimum and suboptimum) as the interfering noise changes. It is shown that the optimum nonlinearity (for a given impulsive noise situation) maintains good performance (i.e., is robust) over a wider range of different noise conditions than do the suboptimum nonlinearities.

E3-4
1520

MEASUREMENTS OF IGNITION-NOISE INTERFERENCE TO TELEVISION RECEPTION:

Y-H. Lin, R.K. Moore and S. Sucharitpanich
Department of Electrical Engineering, University of Kansas, Lawrence, KS 66045

The fact that "noisy" automobile ignition systems cause interference to television reception is well-known, but heretofore no quantitative data were available on the magnitude of the effect. Measurements reported here show that the interfering signal must be quite large to cause serious degradation of the TV picture.

A TV receiver was modified to serve as both receiver and impulse peak-amplitude detector. Thus, the amplitude of the peak noise within the band of interest could be determined and compared with the peak TV signal. A 60-volt 30 ns pulse generator was constructed and used to create simulated ignition interference at different pulse-repetition rates corresponding to autos with different characteristics and different speeds. Signals with the differing interference levels and pulse rates were recorded, using the same TV picture for each to avoid effects of varying picture content. The tape was played before a moderate-sized audience, and members of the audience rated their perception of the picture degradation under different signal-to-noise and PRF conditions. The experiment was repeated with a tape produced using actual ignition pulses. Results are reported here.

E3-5
1550 ON EFFICIENT SPECTRUM UTILIZATION FROM THE STANDPOINT OF COMMUNICATION THEORY:

C.P. Tou and D.A. Roy, Department of Electrical Engineering, Nova Scotia Technical College, Halifax, Nova Scotia, Canada, B3J 2X4

The radio spectrum is an invaluable resource. Proper management is essential for efficient spectrum utilization as ever-increasing demands for frequency spectrum are made. One of the most important measures which has been adopted is radio frequency allocation. Radio frequency allocation in spectrum management is based on the propagation characteristics of the radio wave, the electromagnetic environment, the type of signal and service, technological advances, and social and economic considerations. The efficiency of spectrum utilization may be evaluated in terms of several parameters such as frequency bandwidth, radiated power, service area, transmission path, antenna pattern, polarization, signal waveform, immunity to interference and noise, quality of performance, and cost of the system used. Traditional techniques of spectrum management constrained signal and equipment parameters and geographical locations in the different radio services involved to permit frequency sharing within and between services.

In order to increase the efficiency of spectrum utilization, it is necessary to continue exploring new modulation techniques. Various modulation techniques, such as amplitude-, frequency-, and phase-modulation and frequency- and time-multiplexing techniques have been applied for effective spectrum use. Recently, the idea of using combined modulation has been considered to be very promising for the possibility of making rational use of the spectrum. Combined modulation is a multi-parameter modulation, such as amplitude phase-shift-keying (APSK), which means two or more parameters are varied instead of only one carrier parameter and the carrier wave becomes a carrier of multi-channel information. As a result, the combined modulation process may offer various possibilities of improving the characteristics of communication systems by increasing the channel efficiency and providing a more efficient use of the radio spectrum and the transmitter power.

This paper discusses the rational of possible bandwidth reduction by combined modulation techniques. The present state-of-the-art will be reviewed and the future prospect of using combined modulation techniques to improve the efficiency of spectrum utilization will be discussed with reference to bandwidth reduction, transmitter power, interference and noise immunity, and degree of reliability.

RADIO OCEANOGRAPHY
Wednesday Afternoon, 7 Nov., UMC East Ballroom
Chairman: D. Barrick, Wave Propagation Laboratory, NOAA, Boulder, CO 80302

F5-1
1330 THE IMPACT OF SURFACE CONTOUR RADAR SYSTEM CHANGES ON ITS RADIO OCEANOGRAPHIC CAPABILITIES: E. J. Walsh, NASA Wallops Flight Center, Wallops Island, VA 23337 and J. E. Kenney, Naval Research Laboratory, Washington, DC 20375

The Surface Contour Radar (SCR) scans a pencil beam (0.85° X 1.2°) laterally within ± 15° of the perpendicular to the aircraft wings to produce a real-time topographic map of the surface below the aircraft. During each sweep of the antenna beam the range interrogated by the radar is scanned about mean sea level (MSL) in a saw-tooth pattern which has 51 legs. In its original configuration the mean power and the centroid of the return power were determined for each leg and the centroid was used to determine the elevation of that point with respect to MSL. This presented problems when the SNR was low since noise could contaminate the magnitude of the mean signal power and shift the position of the centroid. Since the centroid of the noise would generally be near the center of the scan leg (near MSL) it would lower the apparent returned power centroid position for a crest and raise it for a trough. The result would appear to be the same as a spatial filtering effect of a large illuminated spot.

The system has been modified to determine the peak power and the position of the peak power on each range scan leg. The result is that the correct values of those quantities will be determined as long as the peak instantaneous signal power is even slightly above the peak instantaneous noise on a particular leg. SCR data using the new configuration will be shown and the effect of using the peak power instead of the mean power to determine such quantities as the electromagnetic bias which radar altimeters are subject to will be discussed.

F5-2
1400 COMPARISON OF REMOTELY-SENSED SURFACE WINDS FROM SATELLITE AND AIRCRAFT SCATTEROMETERS WITH IN-SITU WINDS FROM A LOW-FLYING AIRCRAFT:

V. E. Delnor, Kentron International, Inc., Hampton Technical Center, Hampton, VA 23665; W. L. Jones, NASA Langley Research Center, Hampton, VA 23665; D. Ross, NOAA, Atlantic Oceanographic and Meteorological Laboratories, Sea-Air Interaction Laboratory, Miami, FL; and P. Black, NOAA National Hurricane and Experimental Meteorology Laboratory, Miami, FL

Surface winds over a 187 n.m. long strip of ocean southeast of Cape Hatteras were measured simultaneously by a NOAA aircraft at 500 ft altitude and a NASA aircraft at 22,000 ft altitude. The flights were timed to coincide with the passage of the SEASAT oceanographic satellite over the same area. Wind-sensing instruments aboard the NOAA aircraft included a gust probe and the inertial navigation system (INS).

Those aboard the NASA aircraft included a microwave scatterometer which measured sea surface roughness from which winds speed and direction is inferred, and the INS. The satellite carried a scatterometer similar in function to that on the NASA aircraft.

During the experiments, the low altitude aircraft passed through several wind speed and stability regimes. We present here comparisons of the remotely-sensed winds from the two aircraft and the satellite.

F5-3
1450 FINE TIME SCALE SERIES OF SEA SURFACE SPECTRA AT SELECTED WAVELENGTHS TAKEN FROM JONSWAP SEA PHOTOGRAPHS:

T. G. Konrad and F. M. Monaldo,
Applied Physics Laboratory, The Johns Hopkins University, Laurel, MD 20810

The fine time scale variation in the spectral energy at selected wavelengths in the 3 to 30 centimeter range has been extracted from two dimensional sea surface spectra obtained from sea photographs. The photographs of the sea surface were taken at a rate of four per second from the PISA tower during the Joint North Sea Wave Project (JONSWAP). Two dimensional wave slope spectra were produced using the optical Fourier analysis technique. Spectral energy in the depression plane or "look direction" was measured using a traveling diode and mask in the Fourier plane. Cross correlation of the time series for the centimeter sized waves provides information concerning the hydrodynamic interaction between the short waves while a comparison with that for the "DC spot" indicates the correlation of the short with the very long waves under certain circumstances.

Bulk processing of large numbers of sea photographs has been made possible with the development of automatic, computer controlled data reduction and recording equipment.

F5-4 1520

FORWARD SCATTERING FROM WATER WAVES - PART II

C. I. Beard, Naval Research Laboratory, Washington, DC 20375

In Part I (June 1979 URSI Meeting in Seattle), an assumption in the spherical-wave method for finding the surface correlation length (L_x) along the ocean wave propagation direction was that wave heights had previously been found. A remote sensing method for finding significant wave height emerges from recasting Ament's [1953] theoretical expression for the coherent reflected field into a series of curves vs grazing angle (ψ), with wave height (σ_w) as a parameter. With the limitation that $(\sigma_w \sin\psi)/\lambda \leq 0.1$, plotting the measured reflection coefficients on this graph then yields significant wave height ($4\,\sigma_w$) directly. Examples will be given with 23-cm wavelength data.

In contrast to Beckmann's [1967] spherical wave theory of the coherent reflected field for Gaussian surfaces closely following over-ocean data [Beard, 1961], plane wave theories for non-Gaussian surfaces also follow the over-ocean data. Probability density functions for these surfaces, and the p.d.f. for Wagner's [1967] non-shadowed surface, will be discussed in this context. As Wagner's shadowing function is a function of the ratio of the slope of the incident ray to the rms slope of the surface, shadowing at low grazing angles may offer another method for finding L_x by forward scattering.

IONOSPHERIC IRREGULARITIES
Wednesday Afternoon, 7 Nov., UMC 159
Chairman: K. C. Yeh, University of Illinois, Urbana, IL 61801

G5-1
1330

NIGHTTIME EQUATORIAL UHF RADIO SCINTILLATION AND E AND F REGION IRREGULARITIES

R. G. Rastogi, Air Force Geophysics Laboratory, Hanscom AFB, MA 01731

A detailed comparison of the amplitude scintillations of 137/140 and 360 MHz radio beacons from satellite ATS-6 received at Huancayo and the corresponding vertical incidence ionospheric sounding records at Huancayo for the nighttime hours for the period October 1974 - May 1975 is being made. Besides the broad category of F region irregularities into range and frequency spread, more detailed study has been made between the type of irregularities and the scintillations. During a strong blanketing type of irregularity in the E region (Es-b) not preceded or followed by spread F, the scintillations were found to be slow and weak (of the order of 1-3 dB). The uniformly distributed irregularities in the F region producing diffused ionogram with clear minimum height with group retardation again was ineffective in producing scintillations. An ionogram indicating P'-f trace at a height constant with frequency was associated with strong scintillations. The scintillations were strongest when the ionogram indicated a number of scattering levels in the F region. Thus the equatorial scintillation is shown to be strong in the presence of sharp plasma gradient regions at a number of heights rather than due to a very thick uniformly populated irregularity region. Evidence of the spread F and the scintillations well after sunrise suggest the persistence of the irregularities when these rise sufficiently above the F layer peak.

G5-2
1400

EQUATORIAL BUBBLES, PLUMES AND SCINTILLATION PATCHES:

Santimay Basu and Sunanda Basu, Emmanuel College, Boston, MA 02115, J. Aarons, Air Force Geophysics Laboratory, Hanscom AFB, MA 01731, J. P. McClure and W. B. Hanson, University of Texas at Dallas, Richardson, TX 75080

Coordinated VHF radar backscatter, multifrequency (VHF-GHz) scintillation and in-situ measurements of total ion-concentration and their spatial fluctuations by Atmospheric Explorer-E (AE-E) satellite are studied to explore the relationship between the plumes (extended 3 m irregularity structures) the bubbles (plasma density depletions) and scintillation patches in the nighttime equatorial ionosphere during the various phases of irregularity development and decay. It is shown that in the developed phase of equatorial irregularities, the plasma bubbles detected by the AE-E satellite exhibit highly structured density fluctuations containing considerable spectral power at irregularity wavelengths in the range of 1 km to 100 m and are associated with extended 3 m plume structures and scintillations over the entire VHF-GHz band. Later, the spatial structures of the plasma bubbles become less steep. At this time only weak and fragmentary VHF backscatter and weak GHz (but strong VHF) scintillations are observed. In the post-midnight period, the bubbles persist but exhibit more gradual spatial fluctuations with consequent reduction of spectral power at small irregularity wavelengths. Such bubbles are conspicuous by the absence of any VHF radar backscatter and scintillations in the VHF-GHz band although VHF scintillations are observed with moderate intensity. A striking case of an early morning bubble in association with weak and thin VHF backscatter return from the topside ionosphere and very weak ($\sim$ 2 dB) VHF scintillation is also discussed.

G5-3
1430

MODEL COMPUTATIONS OF RADIO WAVE SCINTILLATION CAUSED BY EQUATORIAL IONOSPHERIC BUBBLES

A. W. Wernik*, C. H. Liu and K. C. Yeh,
Department of Electrical Engineering, University of Illinois, Urbana, IL. 61801

Based on the available in situ data of the electron density measurements and theoretical considerations, a two-dimensional model of the irregularities associated with the equatorial ionospheric bubble is developed. The parabolic equation for a wave traversing such a bubble is solved numerically. The computed wave amplitude pattern suggests that wave diffraction on structures formed by sharp horizontal electron density gradients may be a possible cause of scintillation at gigahertz frequencies. Comparison with the results obtained for a model of random irregularities with the same power spectrum shows that the medium characterized by sharp electron density gradients leads to stronger scintillation in a wide range of wave frequencies.

The amplitude pattern, scintillation index frequency dependence and scatter plots computed for the model are compared with radio beacon observations.

*On leave from Space Research Centre, Polish Academy of Sciences, Warsaw, Poland.

G5-4 DEEPLY MODULATED PHASE SCREENS WITH POWER LAW SPECTRA:
1530 Barry J. Uscinski, Department of Applied Mathematics and Theoretical Physics, Cambridge, England CB39EW*

Deeply modulated phase screens ($\phi_o^2 >> 1$) with a power law spectrum of phase irregularities of the form k^{-n}, i.e. where there is no scale size, are widely used to describe diffraction phenomena. This paper studies a phase spectrum of the form $(1+L^2k^2)^{-n/2}$, $2 \leq n \leq 4$, which allows us to show how a finite scale L affects the intensity fluctuations produced by such a screen, and also to determine the conditions under which the k^{-n} spectrum can be used.

The case $(1+L^2k^2)^{-1}$ corresponds to a phase autocorrelation function $\exp(-|\mathbf{x}|/L)$ and analytic expressions are obtained in this case for S(q), the spectrum of intensity fluctuations produced by the screen. It is shown that only when $z << kL^2/z\phi_o^2$ (z = distance from screen, $k = 2\pi/\lambda$) can the scale size L be treated as infinite and the k^{-2} spectrum used validly. Physically this condidion means that the observer must be so close to the screen that intensity fluctuations produced by irregularities of size L and larger, and of phase depth ϕ_o^2, are negligible. When this condition is violated the effect of the scale L must be included, and the form of S(q) becomes more complicated.

The spectrum $(1+L^2k^2)^{-2}$ corresponds to a phase autocorrelation function $(1 + |x|/L)\exp(-|x|/L)$ which behaves like $(1-|x|^2/L^2+\ldots)$ for small x, and therefore closely resembles certain physical spectra. The form of S(q) in this case has a more complex dependence on L. It behaves like $\exp(-q^2)$ at high frequencies but exhibits dependences like $\exp(-q)$ and q^{-2} in other ranges. The effect of letting $L \to \infty$ is also studied in this case.

---

*Visiting scientist at University of California, San Diego.
Supported by NSF Grant ATM-02625.

G5-5
1600 EFFECT OF THE REFRACTIVE INDEX OUTER SCALE ON THE INTENSITY SCINTILLATION SPECTRUM: W.A. Coles and V.H. Rumsey, Department of Electrical Engineering and Computer Sciences, University of California, San Diego, La Jolla, CA 92093

Records of the spectrum of intensity fluctuations due to propagation of an electromagnetic wave through a random medium contain much useful information about the medium. The theory that connects the medium with the intensity spectrum usually requires extensive machine computation, which necessarily introduces effective inner and outer scales. The effect of this computational artifact on the interpretation of computed spectra is subject to some doubt. For this reason, and others, there is a need for exact solutions that are free of this artifact. Such a solution has been worked out for one dimensional scintillations such as are typical of propagation through the ionosphere. Simple expressions for the phase spectrum and correlation, the angular spectrum and mutual coherence, and the intensity spectrum are used to examine such questions as the effect of an outer scale, and the validity of weak and strong scattering approximations.

G5-6
1630

The Effect of Sporadic E on Television Reception

Ernest K. Smith, California Institute of Technology, Jet Propulsion Laboratory, Pasadena, CA 91103, and Edwin W. Davis, CBS, Inc., 51 West 52nd St., New York City 10019

Long distance propagation by sporadic E is an important source of interference at VHF, particularly to low-band television reception. This much has been known for 40 years but accepted methods for determining sporadic-E interference have been slow in coming. We are presently at the predicted maximum of solar cycle 21 and concern with long-distance F2 propagated interference is understandably high. However the next seven years will see a steady decrease in the F2 problem but not in the sporadic-E one, inasmuch as intense temperate latitude sporadic E shows no significant correlation with the solar cycle. As crowding of the VHF spectrum builds up and needs for higher reliability grow, concern with sporadic-E interference and how to combat it is bound to increase.

Progress has been made towards quantifying our estimates of long-term sporadic-E interference. We first offer a brief historical review of the events and developments in sporadic-E field strength prediction at VHF. We then compare the approaches of the principal published methods (all Japanese) and illustrate the differences with sample calculations. We next consider the justification for the CCIR choice of the Miya method (K. Miya, K. Shimizu and T. Kojima, Radio Science 13, 559-570, May-June, 1978), and use this method to illustrate the interference problem vis-a-vis television reception in the U.S., in Japan, and in Europe. Japan is seen to have by far the worst sporadic-E problem and has made a drastic adjustment. The U.S. has also made adjustments. Finally we offer some guidelines for determining unacceptable interference in the VHF band in terms of allowable outage times for the different services, and acceptable signal-to-interference ratios for the various types of modulation employed.

RADIO TELESCOPES
Wednesday Afternoon, 7 Nov., UMC 235
Chairman: S. Gulkis, Jet Propulsion Laboratory, Pasadena, CA 91103

J5-1
1330

THE U.S. NAVAL OBSERVATORY RADIO ASTROMETRY PROJECT

G. Westerhout and W.J. Klepczynski
U.S. Naval Observatory
Washington, DC 20390

Since October 1978 the NRAO interferometer in Green Bank, WV, has been operated exclusively for the use of the U.S. Naval Observatory in an astrometric program. The 35-km baseline is used for the daily determination of Earth Rotation parameters. Because it is a single baseline, only UTO and one component of Polar Motion can be determined at this time. Construction of a second remote station and a new microwave link is planned for 1980, which will result in the ability to determine both UTO and Polar Motion without any input from other sources. Astronomers from NRL are collaborating in this joint program.

The standard observing program consists of observations of approximately 20 radio sources, each observation of about ten minutes duration, 24 hours per day. The data are reduced using the Naval Observatory computer in Washington. Because no instrumental parameters are changed in this continuing program, and the same sources are observed over and over, it is possible to detect ever more subtle atmospheric and instrumental effects, study their origin and take steps to correct them or apply corrections to the data. This process is presently going on. It was found that after improving some hardware subsystems, data reduction software and source positions, it is now possible to determine two-day averages of the 35 km baseline length to a precision of 2-8 mm. This indicates that it will be possible to achieve our goal of determining UTO to a daily precision of 1 millisecond and to provide absolute source positions to an accuracy of 0.01 arc seconds. The main sources of error, which need to be monitored and modeled in order to remove most or all of their effect, are the differential delays caused by the ionosphere (which is rather active at present) and by the troposphere (mainly water vapor). It is expected that over the next few years sources will be added to build up an accurate catalog containing around 50 sources.

Data will be presented describing the first year of operations. In particular, a comparison will be made of the interferometer values of UTO-UTC with those derived from the BIH data. In addition, a comparison of UT1-UTC derived from the simultaneous use of the interferometer and Doppler satellite data with the BIH values for UT1-UTC will be presented.

J5-2
1350

THE CULGOORA RADIOHELIOGRAPH AND CORRELATOR RECEIVER

D. J. McLean, Division of Radiophysics, CSIRO, Sydney, Australia and G. A. Dulk, Department of Astro-Geophysics, University of Colorado, Boulder, CO 80309

The Culgoora radioheliograph is a circular array of 96 dishes, each of 15m diameter, forming a 3 km aperture. At present the instrument works at 3 frequencies, 43, 80 and 160 MHz; a fourth frequency, 327 MHz, will be available within a year. The east-west resolution at the four frequencies is 7!6, 3!8, 1!9 and 0!9 respectively; the north-south resolution is degraded by $\sec(\delta + 30°)$. The receiver system is presently analog with 48 beams formed simultaneously.

A new correlator receiver consisting of nearly 10,000 correlators has been designed and is being design-tested. When installed, the receiver and processing system will dramatically improve the sensitivity of the heliograph for most applications. For the sun it will allow images to be formed in real time at a rate of 10 per second, while for cosmic observations it will allow a large field to be synthesized with a sensitivity of a few mjy. By making use of the redundancy in the array and the oversampling at small (u,v), phasing errors due to the equipment and the ionosphere are expected to be corrected immediately, giving a greatly reduced sidelobe level and improved dynamic range. These improved characteristics will make the radioheliograph an exceptionally powerful instrument for a variety of solar and cosmic studies.

J5-3 1410 RECENT IMPROVEMENTS IN POINTING AND APERTURE EFFICIENCY AT ARECIBO OBSERVATORY:

Michael M. Davis
Arecibo Observatory, P. O. Box 995
Arecibo, Puerto Rico 00612

Arecibo Observatory is the world's largest radio-radar telescope. Recently, Observatory personnel have readjusted the 1000-foot diameter reflector to provide a smoother surface. Two thousand precision targets spaced uniformly on the surface were measured with T3 theodolites and adjusted, with a final random error (including reobservation) of less than 1mm rms. The remaining 36,000 adjustment screws were set by interpolation within this "hard-point" grid, using a taut-wire fairing tool. All measurement and adjustment work was carried out at night, to reduce thermal effects. The final rms deviation of the surface from the best-fit sphere is now measured as less than 3 mm.

Improvements have also been made to the pointing system to remove the effects of backlash in the azimuth drive. With the new hydraulic drive and servo system, pointing is now accurate to better tahn 10 arcseconds rms, and shows promise of still further improvement. A new computer control package provides safe, convenient and flexible interaction between pointing and data-taking.

The improved reflector efficiency and pointing accuracy significantly enhance the performance of the Arecibo S-band radar system, at 2380 MHz, and permit 6 cm wavlength operation for the first time. A cooled receiver and 450-foot aperture feed are now available for 4.5 to 5 GHz observations.

Arecibo Observatory is part of the National Astronomy and Ionospheric Center, operated by Cornell University for the National Science Foundation.

J5-4
1450 THE COCOA-CROSS ARRAY: W. M. Cronyn and J. J. Rickard, Clark Lake Radio Observatory, Department of Physics and Astronomy, University of Iowa, Borrego Springs, CA 92004

The University of Iowa COCOA-CROSS is a phased array radio telescope with a total collecting area of 7.2×10^4 m^2 and an observing bandwidth of 0.6 MHz centered at 34.3 MHz, designed specifically for IPS (interplanetary scintillation) observations at large elongation angles ($\gtrsim 40^o$). Observations already reported (Erskine, et. al., J.G.R. 83, 4153-4164, 1978) have demonstrated the utility of the IPS technique using the COCOA-CROSS. Early observational programs were hampered by four major problems: 1) excessive down time due to vulnerability to heavy flooding (a recent and recurrent Clark Lake phenomenon); 2) poor signal/noise ratio due to high line attenuation preceding the first amplifier stage; 3) tedious hand scaling of low dynamic range analog chart records; and 4) cumbersome and unreliable telescope pointing with a card reader based control system. Each of these problems has now been successfully alleviated by 1) elevating all signal and control lines; 2) installing bipolar/VMOS FET amplifiers in the telescope; 3) and 4) using a Poly 88 microcomputer system for both telescope control and acquisition of digital data which is processed and plotted using a NOVA microcomputer system.

Recent observations demonstrate the improvement in telescope performance.

J5-5
1510

ACCURACY OF RADIATION PATTERNS DETERMINED FROM SPATIALLY LIMITED NEAR-FIELD MEASUREMENTS:

T.S. Craven and E.B. Joy, School of Electrical Engineering, Georgia Institute of Technology, Atlanta, GA 30332

The problem of determining the sampling window truncation error in calculating the far field radiation pattern of an antenna from near-field measurements made over a finite portion of a planar surface located near the antenna is discussed. The method of determining the error is not restricted to a specific type of antenna, but applies to a broad, general class of antennas.

Three things are known about the planar near field of an antenna which help in determining this error. First, the total power on the infinite near-field plane is finite. Secondly, the near-field plane is located a finite distance from the antenna so that the higher order evanescent modes have attenuated and the near field is approximately bandlimited in the Transform domain. Third, the field attentuates as 1/r as r approaches infinity. It is known that such a bandlimited finite power function can be reconstructed outside a finite window by expressing the function as a summation of prolate spheroidal wave functions fitted to the function within the window and that such a summation approaches 1/r as r approaches infinity. By expressing the measured near field as such a summation, an expression is obtained for the error. An upper bound on this error is obtained as a function of the ratio of power measured to the total power by using the method of Lagrangian Multipliers. The total power passing through the infinite measurement plane is bounded by measuring the input power to the test antenna.

The method has been tested by measuring the near-field of an S-band antenna over a large near-field sampling window. The far-field was then calculated using the standard procedure. The near-field data was then truncated to two smaller window sizes and the far field calculated from the truncated data. The error bound was then calculated using the method described above. The actual error was determined by comparing the far field calculated from the truncated sampling windows with the far field calculated from the full size sampling window data. The far field of the antenna was also measured on a conventional far-field range and the calculated far field was compared to the measured far field. The results of these tests will be presented.

This material is based on work supported by the National Science Foundation under Grant No. ENG78-01587

GUIDED WAVES - II: ENVIRONMENTAL INFLUENCES
Commission B, Session 8, Commissions F and G, Session 6
UMC Forum Room
Chairman: E. F. Kuester, Electromagnetics Laboratory, Department of Electrical Engineering, University of Colorado, Boulder, CO 80309

B8/F6/G6-1 0830 EFFECTS OF A LARGE PATCH OF SPORADIC-E ON NIGHTTIME PROPAGATION AT LOWER ELF:
R.A. Pappert, Electromagnetic Propagation Division, Naval Ocean Systems Center, San Diego, CA 92152

A simple surface propagation model coupled with a moments method has been used to estimate the effect of a patch of sporadic-E on propagation in the lower ELF band. The results indicate that a sporadic-E patch of 1 Mm by 1 Mm which causes phase rate shifts and attenuation rate enhancements consistent with full wave modal evaluations can account for 6-8 dB fades observed in connection with 1.6 Mm Wisconsin Test Facility (WTF) transmissions. Patches 1 Mm by 0.5 Mm can account for more commonly observed fades in the 3 to 4 dB range. Deepest fades require the center of the disturbance to be well within the first Fresnel zone. The 1 Mm by 1 Mm patch can produce 2 to 4 dB fades out to ranges of 10 Mm and more even with the disturbance considerably removed from the terminals of the path.

B8/F6/G6-2 0850 SUBSURFACE ELECTROMAGNETIC FIELD PENETRATION FROM A LOW-FREQUENCY DIPOLE SOURCE IN THE IONOSPHERE: Edward F. Kuester, Electromagnetics Laboratory, Department of Electrical Engineering, University of Colorado, Boulder, CO 80309 (summer faculty fellow at JPL); and Y. Rahmat-Samii and Ernest K. Smith, Jet Propulsion Laboratory, California Institute of Technology, Pasadena, CA 91103

The use of transmissions from orbiting satellites for low frequency (ELF-VLF) communication with receivers located below the surface of the Earth has been considered from time-to-time for two decades. Antenna efficiency is potentially higher for the satellite case as compared to a ground-based antenna but is still poor, as is the power transfer efficiency between the satellite antenna and the Earth-ionosphere waveguide. However, propagation can be quite good in the Earth-ionosphere waveguide and considerable subsurface penetration can be achieved. In this paper, the authors investigate the fields produced below the plane surface of the Earth (e.g., in the sea) by a horizontal electric dipole source located in the ionosphere. In this simple model, the ionosphere is taken to be homogeneous and isotropic, and to extend to infinity in the vertical direction. With an atmospheric layer of finite height, this forms a three-layer Sommerfeld problem which is formulated in the usual way. At ELF, the height of the atmospheric layer will be electrically small, but the complex refractive indices of the ionosphere and of sea water will be quite large, impairing field penetration between regions, and making most conventional quasi-static approximations inapplicable. The subsurface fields are examined and found to consist of contributions from Earth-ionosphere waveguide modes, as well as a saddle-point contribution corresponding to a ray-like field. A numerical examination of these terms will be made, and conclusions drawn about the dipole moment needed to produce a reasonable field strength at the receiver. The applicability of this model to situations such as submarine and mine-disaster communications will be discussed.

B8/F6/G6-3 0910

ELECTROMAGNETIC PROPAGATION ALONG A MULTICONDUCTOR TRANSMISSION LINE IN A TUNNEL - APPROXIMATE ANALYSIS:

Ronald J. Pogorzelski, TRW Defense and Space Systems Group, One Space Park, Redondo Beach, CA 90278

The propagation of electromagnetic waves along a complex of thin wires parallel to the axis of an underground tunnel of circular cross section is a theoretically complicated phenomenon. Although the problem can be formulated exactly, the resulting mode equation can only be solved by searching for its roots in the complex plane numerically. This is often a complicated and time consuming process which provides little physical insight regarding the fundamental phenomena contributing to the behavior of the system. On the other hand, an approach based on perturbation theory, while providing certain physical insights, leaves one with a disturbing concern about its accuracy. Wait has shown that, for the case of a single thin wire in a tunnel, the exact mode equation can be solved approximately yielding a rather simple result for the propagation constant. (J.R. Wait, IEEE Trans. AP-25, 441-443, May 1977.) The relationship between Wait's approach and the usual perturbation theory has been elucidated by Pogorzelski who has pointed out that an important part of Wait's work is the appearance of a modified tunnel wall admittance which "bridges the gap" between the high and low frequency extremes of the quasistatic regime. (R.J. Pogorzelski, 1979 URSI/AP-S Symposium, Seattle, Washington.)

In the present work, the approximate analysis is generalized to a case involving an arbitrary number of thin wires parallel to the axis of a circular tunnel. That is, Λ, Ω, and Z_s in Wait's single wire formula for the propagation constant are replaced with corresponding quadratic forms in the eigenmodal wire currents to generalize the formula to an arbitrary number of wires. The foundations of this approximate approach in standard perturbation theory in is indicated, lending physical meaning to the approximations. A simple example involving a two wire line is presented and the relationship between the approximate formulation and results and the exact formulation and results substantiates the accuracy of the approximate approach.

B8/F6/G6-4 0920

PROPAGATION ALONG A COAXIAL CABLE WITH A HELICAL SHIELD

David A. Hill, ITS/NTIA
U.S. Department of Commerce
Boulder, Colorado 80303

The leaky feeder technique is now used to provide radio communication in mine tunnels and along highways and railroads (Special Issues of Radio Electronic Engr., ed. by Q.V. Davis, 45(5), 1975 and Radio Science, ed. by J.R. Wait, 11(4) 1976). Many types of leaky coaxial cables are now available, and the surface transfer impedance has been used to characterize the mean electromagnetic properties of braided cable shields. This characterization predicts the existence of two dominant modes, "monofilar" and "bifilar", which seem to predict the basic propagation mechanisms of leaky feeder systems quite successfully. However, the validity and generality of the surface transfer impedance concept are not well established, and it is desirable to perform a rigorous boundary value analysis for a specific leaky cable model in order to test the concept.

The model we choose consists of a dielectric coated conductor which is shielded by a finite number of unidirectional helical wires. The transmission line properties of such a structure have been derived by Casey (IEEE Trans. Electromag. Compat., EMC-18, 110-116, 1976) for the special case where the cable dielectric constant is that of free space. The fields inside and outside the shield are expanded in cylindrical functions, and the thin-wire boundary condition is applied at the helical wires. A modal equation for the propagation constant is obtained by setting the incident field equal to zero. In general the mode equation requires a numerical solution, but approximate expressions for the propagation constant are obtained for some special cases.

Two solutions to the modal equation are found. The bifilar mode has a propagation constant approximately equal to the wavenumber of the cable dielectric and carries most of its energy inside the cable. The monofilar mode has a propagation constant slightly greater than that of free space and carries most of its energy outside the cable. The surface transfer impedance is defined as the averaged axial electric field at the shield divided by the averaged axial shield current and is found to be different for the two modes. Numerical results are presented to illustrate the dependence of the propagation constants and the transfer impedance on the various cable parameters.

Some preliminary remarks will also be made about the counter-wound double helical model; the theory for this case has already been formulated (J.R. Wait, IEEE Trans., MTT-24, 476-480, 1976). Unfortunately, the problem is complicated in a numerical sense by the cross-coupling of the Floquet modes between the two helices.

B8/F6/G6-5 1000 TRANSIENT RESPONSE WITH THE DOUBLE DEFORMATION TECHNIQUE FOR A TWO-LAYER MEDIUM:

L. Tsang, J. A. Kong, and A. Ezzeddine, Department of Electrical Engineering and Computer Science and Research Laboratory of Electronics, Massachusetts Institute of Technology, Cambridge, MA 02139

In this paper we illustrate the technique of double deformation in the determination of transient responses for a two-layer medium due to acoustic and electromagnetic excitations. The total transient response ϕ is represented as double integrals over frequency ω and horizontal wave number k_ρ. The integration path on the ω-plane is slightly above the real axis and the integration path on the k_ρ-plane is the Sommerfeld integration path (SIP). In the double deformation technique, we first deform from the SIP to the steepest descent path (SDP) on the complex k_ρ-plane and account for all residue contributions due to the poles representing guided modes and leaky modes. We then interchange the order of integration for the double integral and deform the integration from the real frequency axis to the SDP on the complex ω-plane. Again the residues of the poles that are encountered during the second deformation are accounted for. As frequency changes, the normal mode in frequency domain may become a guided wave, a leaky wave or simply unexcited and its corresponding time domain result gives rise to noncausal response. With the double deformation approach, we can show that for time less than either the head wave or the direct wave arrival time, whichever is earlier, the result is zero and causality is observed. The transient responses are shown for a damped sinusoidal source with both acoustic and electromagnetic excitations. The double deformation technique is compared with the explicit inversion method and the Cagniard's method of integration and also illustrated with the case of a conductive two-layer medium where the latter two methods fail to apply.

B8/F6/G6-6 1020 GROUND-WAVE ATTENUATION FUNCTION FOR A CURVED, INDUCTIVE EARTH: D.A. Hill and J.R. Wait, ITS/NTIA and ERL/CIRES/NOAA, U.S. Dept. of Commerce, Boulder, CO 80303

The theory for ground-wave propagation over a spherical earth of arbitrary surface impedance has long been available, (e.g. J.R. Wait, J. Res. N.B.S., 56, 237-244, 1956) but only limited calculations have been carried out for the case of inductive surface impedance (S.H. Cho and R.J. King, IEEE Trans., GE-10, 96-105, 1972). The related flat-earth case has been more thoroughly studied, and detailed numerical results for the flat-earth attenuation function have been presented for the case of a highly inductive surface impedance (R.J. King and G.A. Schlak, Radio Science, 2 687-693, 1967). In contrast to the homogeneous earth case, the attenuation function for a highly inductive surface contains maxima and minima due to interference between the trapped surface wave and the usual ground wave. The resultant zeros in the flat-earth attenuation function have been computed by D.B. Ross (Proceedings of Conference on Environmental Effects on Antenna Performance, Vol. 1 ed. by J.R. Wait, 85-88, Boulder, Co., 1969, NTIS Doc. No. PB-183175).

For the case of a curved, inductive earth, the trapped surface wave is replaced by the Elliott mode (R.S. Elliott, IRE Trans. Ant. Prop., AP-4, 422-428, 1956 and J.R. Wait, AP-8, 445-449, 1960) and a similar interference phenomenon results. It is important to note that this well trapped (but still leaky) mode is not present when dealing with a homogeneous curved ground. In order to study the curved earth case quantitatively, we have written a computer program to obtain the curved-earth attenuation function for a vertical electric dipole source located on a spherical surface of arbitrary surface impedance. The program uses the residue series except at short distances where convergence is poor. In this case, either a power series in distance or a small curvature formula is used. The first term of the small curvature formula is simply the flat-earth attenuation function, and higher order terms involve inverse powers of the earth radius. Numerical results have been obtained for various values of frequency and surface impedance, including the highly inductive case. The results for inductive surface impedance have application to HF propagation over sea ice and MF propagation over urban areas (J.H. Causebrook, Proc. IEE, 125, 804-808, 1978.)

B8/F6/G6-7 1040 CURRENT INDUCED ON A PAIR OF WIRES ABOVE EARTH BY A VED FOR GRAZING ANGLES OF INCIDENCE: Robert G. Olsen and Abdulmagid Aburwein, Department of Electrical Engineering, Washington State University, Pullman, WA 99164

Exact expressions for the current induced on a pair of horizontal wires above earth by a vertical electric dipole (VED) have been available for some time (J. R. Wait, AEU, 1977). It is well known that the wire currents can be expanded as a continuous spectrum current plus a sum of discrete modal currents. However, it would be useful to know the conditions for which the continuous spectrum current can either be ignored or approximated by a simple expression. This is the question addressed in this work.

For simplicity it is assumed that the earth is perfectly conducting and that the wires are thin and can be characterized by a surface impedance boundary condition. As in previous work the exact induced currents are written as an inverse Fourier Transform. Each current consists of a bifilar component and monofilar component. To evaluate the inverse Fourier Transform the contour of integration (real axis) is deformed to the steepest descent path. The case for grazing incidence (distance from source to observation point (R) greater than the perependicular distance from the source to the center of the wire array (r)) is examined. It is found that two poles exist near the saddle point one on the proper Riemann sheet and one on the improper Riemann sheet. The contribution of these poles is subtracted and evaluated separately. Then an approximation to the steepest descent integration is obtained. The error for this approximation is small provided R is greater than a wavelength.

It is found that either the monofilar or the bifilar component of current can be written as a single term which is proportional to 1/R if R is on the order of r or if R is "very large." In the intermediate range the discrete modal currents dominate the solution. Transition solutions valid between these ranges will be presented and the application of this work to the lossy earth case will be discussed.

B8/F6/
G6-8
1100

EFFECT OF MODAL INDUCED CURRENTS ON A BURIED CABLE ON THE MUTUAL IMPEDANCE BETWEEN TWO HORIZONTAL LOOPS.

Adel Z. Botros, and Samir F. Mahmoud
Electronics and Communications Dept.,
Cairo University, Giza, Egypt.

Induced currents along a buried cylindrical wire parallel to the air-ground interface, are discussed. The exciting source is a vertical magnetic dipole lying on the ground surface. The dominant part of these induced currents, which are the modal currents, are determined from the roots of a modal equation which is solved numerically. Effect of these modal currents on the received voltage in another horizontal loop placed on the ground surface is evaluated. The practical case of a cable in poor contact with the surrounding medium is also considered and it is found that the modal propagation constants are appreciably affected. Numerical examples relevant to remote sensing applications are presented.

TRANSIENTS AND SEM
Thursday Morning, 8 Nov., UMC West Ballroom
Chairman: D. R. Wilton, Department of Electrical Engineering, University of Mississippi, University MS 38677

B9-1
0830

TIME DOMAIN CALCULATION OF SCATTERING CENTER RESPONSE

C.L. Bennett and H. Mieras, Sperry Research Center, Sudbury, MA 01776

The responses of scattering centers of conducting bodies have been obtained by physical optics approximations for specular points and by geometric theory of diffraction for edges usually in the frequency domain. In this paper a technique is presented for obtaining the response of scattering centers by solving a space-time integral equation in the time domain.

The target is illuminated with a "smoothed-impulse" plane wave whose width is small in comparison with target size. Surface currents are computed in the vicinity of the specular point by numerical solution of the time-domain integral equation

$$\vec{J}(\vec{r},t) = 2\hat{n} \times \vec{H}^{i}(\vec{r},t) + \frac{1}{2\pi} \int_S \hat{n} \times \left\{ \left(\frac{1}{R^2} + \frac{\partial}{Rc\partial\tau} \right) \vec{J}(\vec{r}',\tau) \times \hat{R} \right\}_{\tau = t - R/c} dS'$$

The currents are computed only over the (small) triangular region in space-time required to compute the far field response due to the scattering centers.

The technique is applicable to scatterers of arbitrary geometry and is demonstrated on a prolate spheroid (a smooth convex specular point) and a right circular cylinder (a curved edge) at various angles of incidence. This approach is found to yield good scattering center responses with minimal computer resources for arbitrary targets.

B9-2
0850

ANALYTIC PROPERTIES OF SOME SEM-DERIVED QUANTITIES:

Donald R. Wilton, Department of Electrical Engineering, University of Mississippi, University, MS, 38677

L. Wilson Pearson, Department of Electrical Engineering, University of Kentucky, Lexington, KY 40506

One interesting application of the singularity expansion method (SEM) is the possibility of developing broadband equivalent circuits to represent terminal characteristics of antennas or scatterers (C. E. Baum, Proc. IEEE, 64, 1598-1616, 1976). Since SEM analysis yields a partial fraction representation of terminal immittance quantities in which the resonant frequencies of the body appear as frequency domain poles, classical network synthesis techniques may be used to derive lumped-parameter circuits representing these terminal characteristics. It is well known that necessary and sufficient conditions for realization of such equivalent circuits as passive RLC networks are that the terminal immittances be positive-real (PR) quantities. Thus, we wish to examine whether or not SEM-derived terminal immittances are PR.

It can be shown that the dyadic kernel $\overline{\overline{\Gamma}}(\bar{r},\bar{r}';s)$ of the electric field integral equation, which we write in the form

$$\left\langle \overline{\overline{\Gamma}}(\bar{r},\bar{r}';s);\ \bar{J}(\bar{r}',s) \right\rangle = \bar{E}^{inc}(\bar{r},s),$$

satisfies a set of PR conditions analogous to those of a passive, multiport, lumped-parameter network. From this, it can also be shown that terminal immittance quantities are also PR. If all individual conjugate pole pair terms appearing in the admittance were PR, the synthesis could proceed by realizing one pole-pair at a time and connecting all resulting pole-pair circuits in parallel to obtain an equivalent network. However, counterexamples show that individual conjugate pole-pairs are not generally PR.

An alternative to pole-pair synthesis might be to group together all pole terms of the admittance corresponding to the same eigenvalue of the integral equation operator. This would appear convenient since for many problems apparently only a finite number of poles are associated with each eigenvalue. However, it may be shown that the eigenvalues only satisfy a generalized PR condition that admits the possibility of branch cuts appearing in the complex frequency plane. Such branch points do not permit us to synthesize lumped-parameter RLC "terminal eigenadmittances" even though the branch point singularities must cancel when the eigenadmittances are added to form the terminal admittance. Analogies with circuit theory suggest that the absence or presence of such branch cuts is associated with the symmetry of the object.

B9-3
0910

SINGULARITY EXTRACTION OF TIME-DOMAIN DATA WITH NON-LINEAR OPTIMIZATION

S.K. Chaudhuri and Y.L. Chow
Department of Electrical Engineering, University of Waterloo, Waterloo, Ontario, Canada. N2L 3G1

In the extraction of singularities, or poles s_m, in the complex frequency domain of a transient time domain data

$$I(t_n) = \sum_{m=1}^{N} A_m C^{s_m n\Delta t}, \quad n = 0, \ldots 2N-1, \qquad (1)$$

the Prony's method is normally used. The Prony's method involves the solution of two matrices and a solution of zeros of an N-th degree polynomial.

Eq.(1) is a set of nonlinear simultaneous equations for 2N unknowns of A_m and s_m. It can be efficiently and accurately solved by iteration with a nonlinear optimization algorithm. A number of such solutions have been cited by Chow and Chaudhuri [1979 AP-S/NRS Meeting, Seattle, WA, June 1979]. It is evident, therefore, the poles s_m in (1) can be extracted in the same way.

Two examples of such extractions are computed. The first is under ideal noiseless condition, for the six pole pairs of Van Blaricum and Mittra [IEEE, Trans. on AP 26, 174-182, 1978]. The second is under experimental condition, for the 41 pole pairs of Anderson et al. [Transient Electromagnetic Fields, Ed.L.B. Felsen, Springer-Verlag,1976, pp.121-123]. Because of the presence of noise in the second example, the match with the published poles is good but not perfect as in the first example.

Three advantages of such extraction can be observed in the examples. (i) Using an available optimization subroutine, the programming effort is smaller than the Prony's method. (ii) The optimization subroutine computes the error in the approximation to $I(t_n)$ in each iteration. Therefore when the iterations terminate, the poles extracted, their error in the approximation of $I(t_n)$ is immediately known. (iii) The Hessian matrix in the optimization subroutine is the second derivatives of the error in $I(t_n)$ with respect to the variables of optimization, namely, the pole locations and pole residues. Therefore an inspection of Hessian matrix at the end of the optimization gives an estimate in the error bounds of the pole locations and residues.

It is useful to note that in the presence of noise, the Hessian elements become smaller with respect to the error in the approximation to $I(t_n)$. Hence the error bounds become larger.

The latter two advantages may be very useful in determining the reliability of singularities extracted.

B9-4
0920

A CRITIQUE OF THE PENCIL-OF-FUNCTIONS POLE EXTRACTION METHOD IN THE SEM CONTEXT:

L.W. Pearson, J.R. Auton, Department of Electrical Engineering, University of Kentucky, Lexington, KY 40506

The so-called Pencil-of-Functions method due to Jain (V.K. Jain, IEEE Trans. Circ. & Syst., September, 1974) is examined in the context of waveforms comprising several poles, such as the transient waveforms found in many applications of the singularity expansion method. It is shown that Jain's method is poorly suited for identification of high order systems. Jain's method, in its essence, applies low-pass filters in cascade to the system input and output waveforms, thereby suppressing the high frequency content relative to the low. This phenomenon ultimately causes a numerical difficulty in the form of an ill-conditioned Gram matrix. Another difficulty arises if the recorded waveforms are truncated short of infinite time. Numerically, this is manifested in the emergence of polynomials of successively higher orders as dominant components in the successively integrated, finite data records. These polynomials can be large enough to overwhelm the waveform contributions in higher order iterates. The phenomena in question are demonstrated with numerical examples.

The two difficulties mentioned above have no solution other than a radical change in the method. In addition, a third difficulty with Jain's method, which has a simple remedy, is the use of the diagonal elements of the adjoint of the Gram matrix in the system characteristic equation. In cases where the system may be modeled exactly--i.e., no noise on the waveforms--the elements of any row of the adjoint matrix may replace the square roots of the diagonal elements in the characteristic equation with no change in the computed estimates of system parameters. However, when the system cannot be modeled exactly due to a noise component in the waveforms, the first row elements, for instance, deviate less from their uncorrupted values than the diagonal elements. The third difficulty, then, is this inaccuracy of the diagonal elements. The method's performance is much enhanced by the use of the first row elements. This point is supported by numerical results, as well.

B9-5
1000 AN ADAPTIVE FILTERING ALGORITHM FOR THE IDENTIFICATION OF SEM POLES: J.R. Auton, L.W. Pearson, Department of Electrical Engineering, University of Kentucky, Lexington, KY 40506

An adaptation of the Pencil-of-Functions concept (V.K. Jain, IEEE Trans. Circ. & Syst., September, 1974) is presented. The adaptation uses first order filters operating on the impulse response of the system undergoing identification to produce sequences used in forming a set of normal equations. The solutions of these equations yield estimates of system parameters. In contrast to the pure integrators of Jain's method, the poles of the filter transfer functions are distributed throughout the region of interest in the transform plane rather than clustered at the origin. In addition, the present method applies the filters in parallel rather than in cascade. It is shown that when the filter poles are made to converge to the system poles, phenomena occur that are meaningful in the accurate estimation of system parameters. Iterative schemes are used to attain convergence. This convergence is a stable and continuous event, and its distinctive feature is the appearance of dominant t-multiplied exponential components in the filter outputs. The most useful mode of operation determined, to date, is to hold previously identified poles fixed and to extend the identification a pole-pair at a time. This mode seems particularly attractive in the SEM context. Numerical cases are presented to demonstrate the viability of the method. The method is simple yet powerful, free of numerical difficulties, and it provides satisfactory pole estimates for systems of moderate order in the presence of high levels of noise.

B9-6
1020

PRACTICAL ISSUES OF SYNTHESIZING POLE-PAIR ADMITTANCES FOR SEM EQUIVALENT CIRCUITS, K. A. Michalski, L. Wilson Pearson, Department of Electrical Engineering, University of Kentucky, Lexington, KY 40506

The dominant resonance pole-pairs for high-Q structures have been shown to yield almost positive-real (PR) admittances in SEM derived equivalent circuits for single port structures (Streable and Pearson, 1978 Fall Radio Science Meeting). Synthesis of admittances a pole-pair at a time is attractive because it simplifies synthesis procedures and yields simple network topologies. The almost PR admittances can be padded to be PR through a negligible adjustment. In this presentation we consider the application of the various procedures available for synthesis of the biquadratic admittances associated with pole pairs. It is shown that the Bott-Duffin derived circuit constitutes the exclusive RLC form derivable. Explicit expressions are given for the elements in the resulting network. A further minor approximation yields pole-pair admittance modules which comprise four elements as shown below. This network has been shown to give very favorable results for straight-wire and wire-loop antennas (Streable and Pearson, loc. cit.). It is shown that the minimum PR character of the approximate circuits considered leads to realizations whose admittance is sensitive to change in component values. Further, some numerical data are presented which indicate the degree to which parasitic elements incubmbent in the realization influence circuit performance.

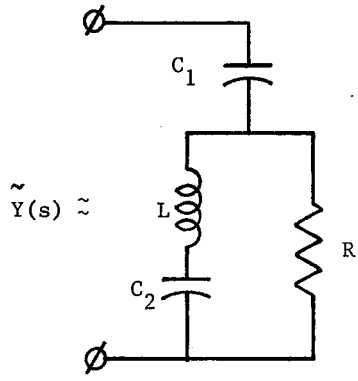

$$\tilde{Y}(s) = \frac{As^2 + Bs^2 + C}{Ds^2 + Es + F}$$

$$\sqrt{AF} - \sqrt{CD} = \sqrt{BE}$$

$$C_1 = \sqrt{\frac{AB}{EF}} \quad C_2 = \frac{M}{DF}\sqrt{\frac{A}{C}}$$

$$L = \frac{D\sqrt{DF}}{M} \quad R = \frac{D}{A}$$

$$M = B\sqrt{DF} + E\sqrt{AC}$$

B9-7
1040 THE EXPERIMENTAL TIME-DOMAIN DETERMINATION OF THE COMPLEX RESONANCES OF SIMPLE OBJECTS; Bruce Z. Hollmann and Edwin D. Ball, Naval Surface Weapons Center, Dahlgren, VA 22448

An experimental time-domain method for determining complex resonances (poles) of simple objects is described. A sub-nanosecond Gaussian pulse is generated and radiated by a long monopole antenna across a thirty-foot aluminum ground plane. The radiated pulse is reflected by an object placed on the ground plane. The return is received by a TEM horn and fed to a sampling oscilloscope which displays the waveform to be recorded. The recorded waveform is digitized. From here on, it becomes a signal processing problem. Prony's Algorithm is being studied as a means for determining the poles of the returns. Its promise and problems are discussed and suggestions for coping with the latter are given. The results of applying the technique to a hemisphere, a cone and a cylinder are given and discussed.

B9-8
1100

ANALYTICAL EXPRESSION FOR ELECTROMAGNETIC PULSE PROPAGATION OVER EARTH: David C. Chang and Hussain Haddad*, Electromagnetics Laboratory, Department of Electrical Engineering, University of Colorado, Boulder, CO 80309

In our earlier work, extensive computations were made for the time-domain electromagnetic response on the surface of a conducting earth due to a vertical current impulse. It was found that for distances greater than a few hundred meters, the contribution from waves propagating through a typical earth is heavily attenuated and is usually negligible compared with those arriving through air. Provided this is the case, we have derived in this work, analytic expressions suitable for different observation times. In the early time portion, we have shown that the z-component of the Hertzian potential can be well approximated by an error function, while in the later time, it can be represented by a complete elliptic integral of the first kind. By properly combining these two results, a unified approximation valid for all time can be made and shown to be within a few percent of the numerically computed results. We further show that our result agrees with the simpler result derived directly from the use of Sommerfeld-Norton ground wave for the very early time (typically, less than a fraction of a microsecond), but the agreement drops very rapidly after reaching the maximum. Significance of the new result in obtaining field responses both on and above the earth surface will also be discussed.

*Now with Northrop Corp. Aircraft Div., Hawthorne, CA 90250.

SCATTERING, ATTENUATION, AND POLARIZATION
Thursday Morning, 8 Nov., UMC East Ballroom
Chairman: R. H. Ott, U.S. Department of Commerce, NTIA/ITS, Boulder, CO 80303

F7-1
0830 USE OF A SATELLITE MULTIFREQUENCY RADIOMETER TO DETERMINE ATTENUATION SUFFERED BY A SATELLITE RADAR:

G.J. Dome, R.K. Moore and K. Van Sickle,
Remote Sensing Laboratory, University of Kansas, Lawrence, KS 66045

The Seasat Active Scatterometer System (SASS) is a multibeam radar designed to measure two radar backscatter signals from the sea and from them determine the wind vector. When condensed water is present in clouds and rain, the return signal is attenuated by the atmosphere and must be corrected before a wind determination can be made. The Seasat Scanning Multifrequency Microwave Radiometer (SMMR) provides the opportunity to measure the attenuation.

The antenna temperature of the radiometer observing the sea without attenuation can be calculated, for vertical polarization and at SMMR's 49° angle of incidence, if the surface temperature is known. Thus, an increase in the observed value above this value is an excess temperature caused by attenuation in the atmosphere. The amount of this excess temperature has been determined for various model cloud and rain conditions, as has the attenuation. An empirical relation was determined between excess temperature at 37 GHz, 18 GHz, and 10.69 GHz and the attenuation at 14.6 GHz (SASS frequency). An algorithm was then developed to use the 37 GHz radiometer to establish small attenuations, the 18 GHz radiometer to establish moderate attenuations, and the 10.69 GHz radiometer to establish large attenuations. This method has been tested against some of the early Seasat observations, and has been shown to be reasonably successful, within limitations posed by poor knowledge of the actual attenuation with which the results for the algorithm must be compared.

Support of NASA Langley Research Center under Grant NSG1397 is gratefully acknowledged.

F7-2
0855 MULTI-YEAR COMSTAR FADE STATISTICS AT 28.56 AND 19.04 GHz FOR WALLOPS ISLAND, VIRGINIA: J. Goldhirsh, Applied Physics Laboratory, The Johns Hopkins University, Laurel, MD 20810

Statistics compiled from measured rain fade data associated with the 28.56 GHz COMSTAR beacon signals are presented for Wallops Island, Virginia. These data cover the two year periods April 1, 1977 to March 31, 1978 and September 1, 1978 to August 31, 1979. The overall cumulative distribution as well as time of day, month of year statistics are characterized. The cumulative distribution is compared with the CCIR as well as other rain attenuation models. Simultaneous rainfall characteristics are also presented.

A derived 19.04 GHz fade cumulative distribution is also presented using an estimation technique check against simultaneous radar observations.

F7-3
0920 NOTES ON THE PREDICTION ACCURACY OF EFFECTIVE-PATH-LENGTH RAIN ATTENUATION MODELS FOR SATELLITE-TO-GROUND CIRCUITS: M. Weissberger, R. Meidenbauer, H. Hodes, R. Baker, and T. Billings, The IIT Research Institute Staff, Department of Defense, Electromagnetic Compatibility Analysis Center, Annapolis, MD 21402

This paper presents the results of a comparison between predicted and measured values of rain attenuation on satellite-to-ground circuits. The predictions are based on procedures reported by R. K. Crane (EASCON '78 Record, September, 1978), E. J. Dutton (NTIA-Report-78-10), and the International Radio Consultative Committee (Report 564-1, XIVth Plenary Assembly). A modified version of Crane's technique is also examined. These procedures are similar in that each uses an effective path length to account for the spatial inhomogeneity of rain intensity.

The measurements used in the study are from earth stations in the United States. Frequencies range from 10 - 20 GHz. Measurements are for a minimum period of one year.

The rms error of each procedure is calculated from the set of differences between measured and predicted loss values that were observed at percentages of time from 0.1 to 0.002. Using the rms errors as an indicator of accuracy, it is shown that the CCIR method is less accurate than the other methods. It is also shown that the accuracy of the Crane predictions is enhanced by assuming that the drop-size distribution is Joss-convective (cf Laws and Parsons) and that the maximum effective rain-layer altitude is the -3.5^{o} isotherm (cf 0^{o}).

F7-4
1005

SIMULATION OF EHF ATMOSPHERIC NOISE:

Jerry Hopponen, Lockheed Missiles and Space Company, P.O. Box 504, Sunnyvale, CA 94086

Atmospheric noise in the EHF band (30-300 GHz) is of interest in remote sensing applications as well as in the prediction of signal-to-noise ratios. A modular approach to computer simulation of atmospheric noise is presented, with emphasis on certain aspects of the computational methods as well as examples.

Modelling begins with a formulation for the complex refractive index of air, based on recent theoretical and experimental work, and includes the dispersive effects of molecular oxygen and water vapor. Absorption coefficients are generated for each level in a chosen model atmosphere and are then used in a surface-to-space ray tracing program. A computational procedure is given for evaluation of the noise integrals, and other numerical aspects are discussed. Noise temperature variation with season and ray elevation angle is illustrated.

F7-5
1030 SCATTERING BY A DIELECTRIC OBJECT BURIED IN A LOSSY GROUND

S.K. Chang, Schlumberger-Doll Research Center,
P.O. Box 307, Ridgefield, Connecticut 06877

The unimoment method is applied to solve the electromagnetic scattering by a dielectric object buried in a lossy ground. The calculation uses the Finite Element Method (FEM) to solve the boundary value problem involving the dielectric material. The FEM solution is terminated at a spherical surface by using a complete expansion in two-medium half spaces.

Numerical results of the scattered fields near the air ground interface will be presented. Calculations involving various frequencies and incident angles will be discussed.

F7-6 1055 GENERALIZATION OF SOMMERFELD INTEGRALS FOR MULTIPOLES IN LAYERED MEDIA

S.K. Chang, Schlumberger-Doll Research Center, P.O. Box 307, Ridgefield, Connecticut 06877

Scattering of electromagnetic waves in planar layered media is an interesting classical problem with many applications in geophysics. Recent investigation by Chang and Mei has lead to the discovery of a complete multipole expansion technique suitable for the vector wave expansions in two-medium half spaces. The vector potential of these multipoles consist of rectangular vectors $\hat{x}$, $\hat{y}$, $\hat{z}$ and the spherical waves $h_n^{(2)}(kr)\, P_n^m(\cos\theta)\, e^{jm\phi}$. The generalized Sommerfeld integrals of these multipoles were derived via a pair of recurrence formulas transforming the spherical Hankel-Legendre functions into the Fourier-Bessel integrals. This paper will advance the generalization of the Sommerfeld integrals of the multipoles into the multi-layered media. The result will conclude to a complete vector field expansion in the layered media, which in turn can be applied to solve the electromagnetic scattering problems involving objects in the layers by using various numerical techniques, such as the unimoment method.

F7-7
1120 ANISOTROPIC ELECTRICAL PROPERTIES OF COAL:
Constantine A. Balanis and Phillip W. Shepard, Department of Electrical Engineering, West Virginia University, Morgantown, WV 26506

Utilizing a two-path interferometer at microwave frequencies (≈9 GHz) the dielectric constant and conductivity of coal as a function of the direction of propagation and polarization of the electromagnetic wave within the coal were measured. Four types of eastern bituminous coal of various rank (fixed carbon content) and one type of eastern anthracite coal were studied, and the effects of the physical properties (rank and anisotropy, pyrite concentration and distribution, moisture content and other mineral matter concentration) on the conductivity and dielectric constant were investigated.

In general, moisture increases the conductivity and dielectric constant. However, preliminary results indicate that pyrite layers along the bedding planes of the bituminous coals cause a general increase in conductivity, with horizontally polarized waves showing the greatest losses. In addition, anthracites (higher rank coals) have larger values of conductivity (about a factor of 10) and permittivity (about a factor of 2 to 3) than the bituminous (lower rank) coals. Further, models of optical anisotropy seem to correlate quite well with the anisotropy of the electrical properties of anthracites.

F7-8
1140 ELECTROMAGNETIC SCATTERING FROM AN OBSTACLE IN A WAVEGUIDE:
A. Boström and P. Olsson, Institute of Theoretical Physics, S-412 96 Göteborg, Sweden

We will consider the transmission and reflection of an electromagnetic waveguide mode travelling down a waveguide of constant cross section but containing a bounded obstacle. The method used is an extension of the method introduced by Waterman (see e.g. Phys. Rev. D3, 825-839, 1971). This extension has already been given in the scalar case (A. Boström, Symposium on Recent Developments in Classical Wave Scattering, June 25-27, 1979, Columbus, Ohio; to appear in Pergamon Press). We also note the great similarities between the present problem and the case with an inhomogeneity in a half-space (G. Kristensson and S. Ström, J. Acoust. Soc. Am. 64, 917-936, 1978).

The starting point is a surface integral representation containing the free-space Green's dyadic (and not the more commonly used problem-related one). This dyadic is expanded in both cylindrical and spherical vector waves. Expanding also the incoming and surface fields we obtain the scattered field by algebraic manipulations. As an important step we have here employed the transformations between the cylindrical and spherical vector waves. We note that the effect of the obstacle is completely determined by its transition matrix.

THURSDAY AFTERNOON, 8 NOV., 1330-1700

WORKSHOP ON GUIDED WAVES
UMC Center Ballroom
Chairman: J. R. Wait, ERL/NOAA, U.S. Dept. of Commerce, Boulder, CO 80303; and D. C. Chang, Dept. of Electrical Engineering, University of Colorado, Boulder, CO 80309

FUTURE MEETINGS

URSI Commission F International Symposium on Effects of the Lower Atmosphere on Radio Propagation at Frequencies above 1 GHz, Lennoxville, Quebec, Canada, 26-30 May 1980 (contact Dr. P. A. Watson, University of Bradford, Dept. Elect. & Electronic Eng., Great Horton Road, Bradford BD7 1DP, England).

North American Radio Science Meeting and IEEE APS International Symposium, Quebec City, Quebec, Canada, 2-6 June 1980 (contact J. A. Cummins - Université Laval, Departement de Génie Electrique, Faculté des Sciences et de Génie, Cité Universitaire, Québec G1k 7P4, Canada).

URSI Commission B International Symposium on Electromagnetic Waves, Munich, Germany, 26-29 August 1980 (contact Dr. H. Hochmuth, International URSI - Symposium Postfach 70 00 73, D-8000 Munchen 70, Federal Republic of Germany).

National Radio Science Meeting, Boulder, CO, January 1981 (tentative) (contact Prof. S. W. Maley, Electrical Engineering Dept., University of Colorado, Boulder, CO 80309).

IEEE APS International Symposium and Radio Science Meeting, Los Angeles, CA, 17-19 June 1981 (contact Prof. R. S. Elliott, 7732 Boelter Hall, UCLA, Los Angeles, CA 90024).

XXth General Assembly of URSI, Washington, D.C., 10-18 August 1981 (contact Mr. R. Y. Dow, National Academy of Science, 2101 Constitution Avenue NW, Washington, D.C. 20418).

WEDNESDAY, 7 NOVEMBER

0830-1200		
B-5	Guided Waves: Optical and Millimeter	UMC West Ballroom
E-2	Non-Gaussian Noise Theory and Measurement	UMC 158
F-3	SEASAT I - Atlantic Coast Experiment	UMC East Ballroom
G-3	Recent Radio Beacon Results - II Scintillations	UMC 159
H-2	Active Experiments From the Space Shuttle - II and Waves in Plasam	UMC 157
J-4	General Session	UMC 235
1030-1200		
Commission J	Business Meeting	
1330-1700		
B-6/ F-4/ G-4	Guided Waves I: Range Dependent Modes and Hybrid Representations	UMC Forum Room
B-7	Antennas	UMC West Ballroom
E-3	Noise and Interference, Models and System Design	UMC 157
F-5	Radio Oceanography	UMC East Ballroom
G-5	Ionospheric Irregularities	UMC 159
J-5	Radio Telescopes	UMC 235
1530-1800		
VLBI	Network Users' Group	UMC 235
1700		
Commission B	Business Meeting	UMC West Ballroom
Commission E	Business Meeting	UMC 157
Commission G	Business Meeting	UMC 159
1800-2400		
Electromagnetics Society Meeting		UMC 157
2000		
USNC/URSI Executive Committee and Commission Chairmen		UMC 305

THURSDAY, 8 NOVEMBER

0830-1200		
B-8/ F-6/ G-6	Guided Waves II: Environmental Influences	UMC Forum Room
B-9	Transients and SEM	UMC West Ballroom
F-7	Scattering, Attenuation and Polarization	UMC East Ballroom
1330-1700		
Workshop on Guided Waves		UMC Center Ballroom